Volume 87, Number 8,
August 2026

ISSN 0005-1179
CODEN: AURCAT

A JOURNAL OF RUSSIAN ACADEMY OF SCIENCES

AUTOMATION AND REMOTE CONTROL

Automation and Remote Control

Vol. 87, No. 8, August 2026

http://ait.mtas.ru

Automation and Remote Control

ISSN 0005-1179

SCOPE

Automation and Remote Control is one of the first journals on control theory. The scope of the journal is control theory problems and applications. The journal publishes reviews, original articles, and short communications (deterministic, stochastic, adaptive, and robust formulations) and its applications (computer control, components and instruments, process control, social and economy control, etc.).

Automation and Remote Control is abstracted and/or indexed in *ACM Digital Library, BFI List, CLOCKSS, CNKI, CNPIEC Current Contents/Engineering, Computing and Technology, DBLP, Dimensions, EBSCO Academic Search, EBSCO Advanced Placement Source, EBSCO Applied Science & Technology Source, EBSCO Computer Science Index, EBSCO Computers & Applied Sciences Complete, EBSCO Discovery Service, EBSCO Engineering Source, EBSCO STM Source, EI Compendex, Google Scholar, INSPEC, Japanese Science and Technology Agency (JST), Journal Citation Reports/Science Edition, Mathematical Reviews, Naver, OCLC WorldCat Discovery Service, Portico, ProQuest Advanced Technologies & Aerospace Database, ProQuest-ExLibris Primo, ProQuest-ExLibris Summon, SCImago, SCOPUS, Science Citation Index, Science Citation Index Expanded (Sci-Search), TD Net Discovery Service, UGC-CARE List (India), WTI Frankfurt eG, zbMATH.*

Journal website: http://ait.mtas.ru

0005-1179/26. *Automation and Remote Control* (ISSN: 0005-1179 print version, ISSN: 1608-3032 electronic version) is published monthly by Trapeznikov Institute of Control Sciences, Russian Academy of Sciences, 65 Profsoyuznaya street, Moscow 117997, Russia.
Volume 87 (12 issues) is published in 2026.
Publisher: Trapeznikov Institute of Control Sciences, Russian Academy of Sciences.
65 Profsoyuznaya street, Moscow 117997, Russia; e-mail: redacsia@ipu.rssi.ru; http://ait.mtas.ru, http://ait-arc.ru

Contents

Automation and Remote Control
Vol. 87, No. 8, 2026

Nonlinear Systems

Control in Technical Systems

Control in Biomedical Systems

Intellectual Control Systems, Data Analysis

Obituary

ISSN 0005-1179 (print), ISSN 1608-3032 (online), Automation and Remote Control, 2026, Vol. 87, No. 8, pp. 669–687.

NONLINEAR SYSTEMS

A Hybrid–Robust Method for Estimating the Values of Linear Functionals under Essential Uncertainty and the Nonlinear Factor

Yu. G. Bulychev

JSC Concern Radioelectronic Technologies, Moscow, Russia
e-mail: profbulychev@yandex.ru

Received June 3, 2025
Revised December 22, 2025
Accepted January 27, 2026

Abstract—For secondary data processing tasks, a hybrid-robust method is developed to estimate various numerical characteristics (linear functionals) optimally under parametric uncertainty factors related to the information process, regular and irregular interferences, and the correlation function of measurement noise (including the case of nonlinear parameters). The method is fully or partially invariant with respect to these factors and yields the desired estimates without expanding the vector of estimated parameters or employing linearization procedures. A comparison with known estimation methods is presented, and the random and methodological errors, as well as the achieved computational effect, are analyzed. An illustrative example is provided.

Keywords: secondary data processing, essential uncertainty, vector linear functional, spectral coefficients, nonlinear factor, hybrid–robust method, invariance condition, constrained optimization, family of hypotheses, extended least squares method, decomposition

DOI: 10.7868/S1608303226080018

1. INTRODUCTION

When solving a wide range of secondary data processing tasks based on indirect measurements (the issues related to signal detection, discrimination, and recognition having been settled), essential uncertainty often arises. It may be associated with no reliable knowledge regarding the distribution laws of measurement errors, the presence of anomalous single and group errors, etc.; for example, see [1–32]. Such situations are often encountered, for instance, when determining the motion of aircraft from trajectory measurements in the rocket and space sphere [3].

Data processing algorithms at these stages are based on classical probabilistic methods of maximum a posteriori probability density or maximum likelihood, usually in an extended version; for example, we refer to [1–4]. In this version, all unknown uncertainty parameters are included in the expanded state vector; however, in practice, the expansion procedure leads to a sharp increase in computational costs, the well-known effect of "smearing accuracy," and problems with the convergence and stability of the resulting estimates. According to an analysis, classical probabilistic estimation methods are often unsuitable under essential uncertainty; nevertheless, they can be effectively used to create hybrid-robust algorithms or study the potential capabilities of measuring systems at the stage of mathematical modeling.

There are other estimation methods applicable under uncertainty: the extended least squares method (ELS) [3], methods for minimizing different geometric and kinematic residuals [30], the method of invariants [31], various linear and nonlinear filtering methods (e.g., Kalman filtering) [1, 3, 10, 14, 25, 26], various adaptive methods with parameter tuning [9, 26], robust methods [1, 14, 27], randomized methods [20, 21], cluster methods [21, 32], and neural network methods [28], as well as numerous heuristic methods (for example, see [5, 8, 11, 13, 29]). Under several constraints on the observation conditions, these methods overcome uncertainty factors, e.g., successfully deal with anomalous errors. However, under essential uncertainty, these methods encounter various unforeseen limitations and stringent requirements for measurement processing algorithms, which significantly narrow the scope of their application. Moreover, they often ensure convergence on average (either over an ensemble of realizations or over a single sufficiently long realization), without any guarantee for the quality of the resulting estimate for a single sample of small or medium size. Most known estimation procedures involve weight processing, and the weights are calculated a priori based on a large amount of available statistical information. If such information is absent or unreliable, one should use posterior weights and vary them from one measurement sample to another.

As a rule, the methods considered above are intended to estimate spectral coefficients of information processes or find their smoothed values. However, in measurement practice, a more general problem is highly relevant, i.e., the optimal estimation of various numerical characteristics of information processes. This concerns the vector of linear functionals (VLF), whose coordinates can be, e.g., the derivatives of various orders of information processes used to predict the motion of aircraft and perform their identification in civil and military systems.

For relatively favorable observation conditions, VLF can also be estimated using classical probabilistic methods, e.g., maximum a posteriori probability density or maximum likelihood, the ordinary least squares (OLS) method and its extended analog (ELS), as well as their various modifications. In the presence of regular-structure interferences in observations (representable as a linear span of a given system of basis functions with unknown spectral coefficients), the method of generalized invariant-unbiased estimation (GIUE) [15, 16] is applicable for the optimal estimation of VLF. This method leads to the decomposition of computations and the inversion of matrices of smaller dimensions (compared to ELS), and uses information about zero mean and a given correlation function of the measurement noise as a priori data.

If observations contain not only regular but also irregular interferences (the later have no compact mathematical models in terms of the number of degrees of freedom), the modified GIUE method can be used for the spectral analysis of the components of the input observation [17]. This modification yields good results on samples of an appropriate size when a sufficient number of reduced time grids can be created so that some of them are not associated with irregular interference. However, for a large class of applied problems dealing with medium and small samples, the application of such a method becomes a challenge. Furthermore, the modified GIUE method is oriented towards the case of an a priori known correlation matrix of the input observation noise. In practice, this noise can be semi-defined, i.e., non-centered (with an unknown mean) and characterized by a parameterized correlation function specified up to its structure. Only some uncertainty region is indicated for its parameters (both linear and nonlinear). This uncertainty regarding the characteristics of the measurement noise, as well as the parameters of regular and irregular interferences, often significantly distorts the estimation results. Therefore, a more advanced method is required to estimate VLF under uncertainty.

Below, we develop such a hybrid–robust method (HRM) considering both a priori and a posteriori data without linearization or expansion of the vector of estimated parameters. This method retains all the advantages of GIUE [15, 16] and its modification [17] in terms of decomposition, employs only elementary operations of addition, multiplication, and matrix inversion, and constructs the resulting VLF estimate by a simple operation of combining a set of conditionally optimal partial estimates corresponding to the family of alternative hypotheses. The term "decomposition" means that it is possible to estimate independently (separately) any numerical characteristic (linear functional) for each component of the input observation representable as a finite linear combination of given basis functions with unknown spectral coefficients. Such components include irregular and regular interferences.

HRM is primarily intended for measuring systems with parallel computations to ensure the required speed for real-time processing of input observations. Such computations effectively overcome the nonlinearity problem by organizing many data processing channels for the family of alternative hypotheses regarding the nonlinear uncertainty factor.

2. BASIC CONCEPTS, MODELS, AND CONSTRAINTS

Let $x_{\mathrm{IP}}(t) = x_1(t)$ and $x_{\mathrm{RI}}(t) = x_2(t)$ denote an information process and a regular interference, respectively:

$$x_i(t) = \boldsymbol{\psi}_i^{\mathrm{T}}(t)\boldsymbol{\gamma}_i, \quad i \in \{1,2\}, \quad t \in [0,T], \tag{2.1}$$

where $\boldsymbol{\psi}_i(t) = \left[\psi_{im}(t), m = \overline{1, V_i}\right]^{\mathrm{T}}$ is the vector of given basis functions, and $\boldsymbol{\gamma}_i = \left[\gamma_{im}, m = \overline{1, V_i}\right]^{\mathrm{T}}$ is the vector of unknown spectral coefficients.

We also introduce an irregular interference $z(t)$ present in measurements, in one form or another; in practice, it cannot be analytically described in compact terms and has a small number of degrees of freedom. For example, the irregular interference may contain components of the tails of infinite functional series used to describe the information process and regular interference, as well as an unknown mean of the measurement noise. Furthermore, $z(t)$ may include various measurement errors, such as anomalous (single or group) errors of both natural and intentional origin. In addition, under various observation conditions, unexpected slow and/or fast-changing components of the irregular interference may appear, the nature of which is unknown in advance. Such an interference is extremely difficult to combat, as it does not match the expected conditions of the measurement experiment; it can be characterized by the sample clogging coefficient [17].

The equation of continuous-time observations has the form

$$h(t) = x_1(t) + x_2(t) + z(t) + \xi(t), \quad t \in [0,T], \tag{2.2}$$

where $\xi(t)$ is a centered semi-defined measurement noise characterized by zero mean and a parameterized (specified up to parameters) correlation function $k(t', t'', \mathbf{q})$, where $t', t'' \in [0,T]$ and $\mathbf{q} = \left[q_r, r = \overline{1, Q}\right]^{\mathrm{T}}$ is the vector of constant parameters.

When implementing known estimation methods (OLS, ELS, and GIUE), a nominal fixed value $\mathbf{q}_0$ is conventionally chosen for $\mathbf{q}$.

In the case of a non-centered noise $\widetilde{\xi}(t)$, it is also easy to use equation (2.2) by including the non-zero mean either in the regular interference (when described by a small set of basis functions) or directly in the irregular interference (when having an extended spectral representation). Constraints are imposed on the coordinates of the vector $\mathbf{q}$ in the form of a possible uncertainty region $\alpha_r \leqslant q_r \leqslant \beta_r$, where $\alpha_r > 0$ and $\beta_r > 0$; note that $\mathbf{q}_0$ belongs to this region.

We introduce the VLF (the set of numerical characteristics) $\boldsymbol{\Omega} = \left[\boldsymbol{\Omega}_1^{\mathrm{T}}, \boldsymbol{\Omega}_2^{\mathrm{T}}\right]^{\mathrm{T}} = \left[\varsigma_j, j = \overline{1, M_1 + M_2}\right]^{\mathrm{T}}$, where

$$\boldsymbol{\Omega}_i = \boldsymbol{\Omega}_i\{x_i(t)\} = \left[\omega_{ir}\{x_i(t)\}, r = \overline{1, M_i}\right]^{\mathrm{T}} = \left[\varsigma_{ir}, r = \overline{1, M_i}\right]^{\mathrm{T}}, \quad i \in \{1,2\},$$

and ς_{ir} is the rth numerical characteristic for the component $x_i(t)$ from (2.1).

Consider the general case where different numerical characteristics (linear functionals) can be calculated separately for each component $x_1(t)$ or $x_2(t)$.

The problem is to find an optimal estimate $\mathbf{\Omega}_i^* = \mathbf{P}_i^{\mathbf{\Omega}}\mathbf{H}$ for the VLF $\mathbf{\Omega}_i$. Here, $\mathbf{P}_i^{\mathbf{\Omega}}$ is the linear estimation matrix, and $\mathbf{H}$ is the observation vector (a discrete sample for the function $h(t)$ on a time grid $\{t_1, \ldots, t_N\}$):

$$\mathbf{H} = \mathbf{X}_1 + \mathbf{X}_2 + \mathbf{Z} + \mathbf{\Xi}, \tag{2.3}$$

with $\mathbf{X}_i = \left[x_{in}, n = \overline{1, N}\right]^{\mathrm{T}}$, $x_{in} = x_i(t_n)$, $i \in \{1, 2\}$, $\mathbf{Z} = \left[z_n, n = \overline{1, N}\right]^{\mathrm{T}}$, $\mathbf{\Xi} = \left[\xi_n, n = \overline{1, N}\right]^{\mathrm{T}}$, $z_n = z(t_n)$, $\xi_n = \xi(t_n)$, and $t_n \in [0, T]$.

The irregular interference can be characterized by the clogging coefficient $\rho_{\mathbf{Z}} = 100 \times N_{\mathbf{Z}}/N$ [%], where $N_{\mathbf{Z}}$ is the number of all coordinates of the vector $\mathbf{Z}$ that can significantly affect the estimation results when using any optimal measurement processing algorithms neglecting this interference. By assumption, the sample size (2.3) at least exceeds the total number of degrees of freedom of the adopted mathematical models (i.e., $N \geqslant V_1 + V_2 + Q + N_{\mathbf{Z}}$, and often $N \gg V_1 + V_2 + Q + N_{\mathbf{Z}}$ in practice) and provides the necessary smoothing effect with respect to the noise $\mathbf{\Xi}$.

With the adopted models for the components $x_1(t)$ and $x_2(t)$, we represent the sample (2.3) as

$$\mathbf{H} = \mathbf{\Psi}_1\boldsymbol{\gamma}_1 + \mathbf{\Psi}_2\boldsymbol{\gamma}_2 + \mathbf{Z} + \mathbf{\Xi} = \mathbf{\Psi}\boldsymbol{\gamma} + \mathbf{Z} + \mathbf{\Xi}, \tag{2.4}$$

where: $\mathbf{\Psi}_i = \left[\psi_{imn}, n = \overline{1, N}, m = \overline{1, V_i}\right]$ is the basis matrix of the component $x_i(t)$, $\psi_{imn} = \psi_{im}(t_n)$; $\mathbf{\Psi} = [\mathbf{\Psi}_1; \mathbf{\Psi}_2]$ is the combined basis matrix for the two components of the observation equation (2.3); and $\boldsymbol{\gamma} = \left[\boldsymbol{\gamma}_1^{\mathrm{T}}, \boldsymbol{\gamma}_2^{\mathrm{T}}\right]^{\mathrm{T}} = \left[\gamma_j, j = \overline{1, V_1 + V_2}\right]^{\mathrm{T}}$.

The matrix $\mathbf{P}_i^{\mathbf{\Omega}} = [p_{imn}^{\mathbf{\Omega}}, m = \overline{1, M_i}, n = \overline{1, N}]$ shall satisfy a number of conditions.

The first condition (the invariance of the estimate with respect to $\mathbf{X}_j$) is

$$\mathbf{P}_i^{\mathbf{\Omega}}\mathbf{X}_j = \mathbf{P}_i^{\mathbf{\Omega}}\mathbf{\Psi}_j\boldsymbol{\gamma}_j = [\mathbf{0}]_{M_i \times 1}, \quad i \neq j. \tag{2.5}$$

The second condition (the unbiasedness of the estimate) is

$$\mathbf{P}_i^{\mathbf{\Omega}}\mathbf{X}_i = \mathbf{P}_i^{\mathbf{\Omega}}\mathbf{\Psi}_i\boldsymbol{\gamma}_i = \mathbf{\Omega}_i. \tag{2.6}$$

The third condition (the minimum trace of the correlation matrix $\mathbf{K}_i^{\mathbf{\Omega}} = \left[k_{ilp}^{\mathbf{\Omega}}, l, p = \overline{1, M_i}\right]$ of estimation errors) is

$$\operatorname{Sp}\mathbf{K}_i^{\mathbf{\Omega}} = \operatorname{Sp}\left[\mathbf{P}_i^{\mathbf{\Omega}}\mathbf{K}\left(\mathbf{P}_i^{\mathbf{\Omega}}\right)^{\mathrm{T}}\right] \to \min, \tag{2.7}$$

where $\mathbf{K} = \mathbf{K}(\mathbf{q}) = \left[k(t_n, t_m, \mathbf{q}), n, m = \overline{1, N}\right]$ stands for the correlation matrix of the noise $\mathbf{\Xi}$.

According to condition (2.5), when estimating the VLF for $x_i(t)$, the other component $x_j(t)$ is treated as an interference and vice versa. Conditions (2.6) and (2.7) are typical for any optimal linear estimation procedure [1–4].

In addition to the time grid $\{t_1, \ldots, t_N\}$, we also use a multidimensional node grid $\{\mathbf{q}_{(1)}, \ldots, \mathbf{q}_{(L)}\}$ covering the region $[\alpha_1, \beta_1] \times \ldots \times [\alpha_Q, \beta_Q]$ (e.g., uniformly) so that the cardinality L is sufficient for a qualitative description of the function $k(t', t'', \mathbf{q})$ over the entire domain of definition $[0, T] \times [0, T] \times [\alpha_1, \beta_1] \times \ldots \times [\alpha_Q, \beta_Q]$. The matrix $\mathbf{P}_i^{\mathbf{\Omega}}$ depends on $\mathbf{q}$; consequently, $\mathbf{P}_i^{\mathbf{\Omega}} = \mathbf{P}_i^{\mathbf{\Omega}}(\mathbf{q})$ and $\mathbf{\Omega}_i^* = \mathbf{\Omega}_i^*(\mathbf{q})$. Thus, an optimal value $\mathbf{q}^*$ for the parameter $\mathbf{q}$ shall be chosen according to an additional decision rule considering the presence of the component $\mathbf{Z}$ in (2.3) and the resulting set of partial estimates of the parameters $\boldsymbol{\gamma}_1$ and $\boldsymbol{\gamma}_2$ for the node family $\{\mathbf{q}_{(1)}, \ldots, \mathbf{q}_{(L)}\}$.

Taking into account (2.1)–(2.7), it is required to develop an HRM for estimating the values of the VLF $\boldsymbol{\Omega}_i$, $i \in \{1,2\}$,) under uncertainty factors regarding the vector parameters $\boldsymbol{\gamma}_1$, $\boldsymbol{\gamma}_2$, $\mathbf{Z}$, and $\mathbf{q}$. In such a general formulation, the estimation problem is nonlinear since some coordinates of the vector $\mathbf{q}$ may enter the function $k(t', t'', \mathbf{q})$ nonlinearly.

The HRM shall eliminate the above problems associated with nonlinearity and be oriented towards the elementary operations of addition, multiplication, and inversion of matrices in a linear setting. In contrast to GIUE [15, 16] and its known modification [17], a more general problem is considered here: VLF estimation is performed in addition to its spectral analysis; the measurement noise is semi-defined (there exists a parametric uncertainty regarding its correlation function due to the nonlinear factor); and, moreover, the irregular interference $\mathbf{Z}$ is present in the observation. Finally, the capability to separately estimate any coordinate (numerical characteristic) of the VLF, for both the information process and the regular interference, shall be provided.

3. FUNDAMENTAL FORMULAS

Let $\mathbf{P}_{ir}^{\boldsymbol{\Omega}} = \left[p_{irn}^{\boldsymbol{\Omega}}, n = \overline{1,N}\right]^{\mathrm{T}}$ denote the column vector representing the rth row of the matrix $\mathbf{P}_i^{\boldsymbol{\Omega}}$. This vector is used to find the estimate $\varsigma_{ir}^* = \left(\mathbf{P}_{ir}^{\boldsymbol{\Omega}}\right)^{\mathrm{T}} \mathbf{H}$ of the individual coordinate (numerical characteristic) ς_{ir} of the VLF $\boldsymbol{\Omega}_i$.

For a fixed value of $\mathbf{q}$, based on the above conditions (2.5)–(2.7), the optimal estimation vector $\mathbf{P}_{ir}^{\boldsymbol{\Omega}} = \mathbf{P}_{ir}^{\boldsymbol{\Omega}}(\mathbf{q})$ is obtained by minimizing the function

$$J\left(\mathbf{P}_{ir}^{\boldsymbol{\Omega}}, \boldsymbol{\varphi}_{ir}, \boldsymbol{\theta}_{ir}\right) = \left(\mathbf{P}_{ir}^{\boldsymbol{\Omega}}\right)^{\mathrm{T}} \mathbf{K}\mathbf{P}_{ir}^{\boldsymbol{\Omega}} + (\boldsymbol{\varphi}_{ir})^{\mathrm{T}} (\boldsymbol{\Psi}_j)^{\mathrm{T}} \mathbf{P}_{ir}^{\boldsymbol{\Omega}} + \left\{\omega_r^{\mathrm{T}}\{\boldsymbol{\psi}_i(t)\} - \left(\mathbf{P}_{ir}^{\boldsymbol{\Omega}}\right)^{\mathrm{T}} \boldsymbol{\Psi}_i\right\} \boldsymbol{\theta}_{ir}, \tag{3.1}$$

where: $[\boldsymbol{\varphi}_{ir}]_{V_j \times 1}$ and $[\boldsymbol{\theta}_{ir}]_{V_i \times 1}$ are vector Lagrange multipliers (from this point onwards, square brackets with subscripts indicate the dimensions of the corresponding matrices and vectors); $\omega_r\{\boldsymbol{\psi}_i(t)\} = \left[\omega_r\{\psi_{im}\}, m = \overline{1, M_i}\right]^{\mathrm{T}}$ is the value vector of the scalar functional $\omega_r\{\cdot\}$ on all basis functions of the component $x_i(t)$ from (2.1). (By the natural assumption, $i \neq j$.)

The function (3.1) corresponds to the equivalent conditions formulated previously:

$$\omega_r^{\mathrm{T}}\{\boldsymbol{\psi}_i(t)\} - \left(\mathbf{P}_{ir}^{\boldsymbol{\Omega}}\right)^{\mathrm{T}} \boldsymbol{\Psi}_i = [\mathbf{0}]_{1 \times V_i} \tag{3.2}$$

(the first condition),

$$\boldsymbol{\Psi}_j^{\mathrm{T}} \mathbf{P}_{ir}^{\boldsymbol{\Omega}} = [\mathbf{0}]_{V_j \times 1} \tag{3.3}$$

(the second condition), and

$$\min_{\mathbf{P}_{ir}^{\boldsymbol{\Omega}}} \left(\sigma_{ir}^{\boldsymbol{\Omega}}\right)^2 = \min_{\mathbf{P}_{ir}^{\boldsymbol{\Omega}}} \left(\mathbf{P}_{ir}^{\boldsymbol{\Omega}}\right)^{\mathrm{T}} \mathbf{K}\mathbf{P}_{ir}^{\boldsymbol{\Omega}} \tag{3.4}$$

(the third condition), where $\left(\sigma_{ir}^{\boldsymbol{\Omega}}\right)^2$ means the variance of the estimation error of the numerical characteristic ς_{ir}.

Omitting straightforward but cumbersome calculations, we obtain the following solution of the constrained optimization problem (3.1)–(3.4) (by analogy with [17]):

$$\mathbf{P}_{ir}^{\boldsymbol{\Omega}} = \boldsymbol{\Lambda}_j \mathbf{K}^{-1} \boldsymbol{\Psi}_i \left(\boldsymbol{\Psi}_i^{\mathrm{T}} \boldsymbol{\Lambda}_j \mathbf{K}^{-1} \boldsymbol{\Psi}_i\right)^{-1} \omega_r\{\boldsymbol{\psi}_i(t)\}, \tag{3.5}$$

$$\boldsymbol{\Lambda}_j = \mathbf{E} - \mathbf{K}^{-1} \boldsymbol{\Psi}_j \left[(\boldsymbol{\Psi}_j)^{\mathrm{T}} \mathbf{K}^{-1} \boldsymbol{\Psi}_j\right]^{-1} (\boldsymbol{\Psi}_j)^{\mathrm{T}}, \tag{3.6}$$

where $\mathbf{E}$ is an identity matrix of dimensions $N \times N$.

In view of (3.5), the desired matrix $\mathbf{P}_i^{\mathbf{\Omega}} = \mathbf{P}_i^{\mathbf{\Omega}}(\mathbf{q})$ for the linear estimation of the VLF is

$$\mathbf{P}_i^{\mathbf{\Omega}} = \left[\mathbf{\Lambda}_j \mathbf{K}^{-1} \mathbf{\Psi}_i \left(\mathbf{\Psi}_i^{\mathrm{T}} \mathbf{\Lambda}_j \mathbf{K}^{-1} \mathbf{\Psi}_i\right)^{-1} \mathbf{\Omega}\{\boldsymbol{\psi}_i(t)\}\right]^{\mathrm{T}}, \tag{3.7}$$

where $\mathbf{\Omega}\{\boldsymbol{\psi}_i(t)\} = \left[\omega_r\{\psi_{im}(t)\}, m = \overline{1, V_i}, r = \overline{1, M_i}\right] = \left[\varsigma_{irm}^{\boldsymbol{\psi}}, m = \overline{1, V_i}, r = \overline{1, M_i}\right]$.

We emphasize that all components in (3.5)–(3.7) depend on the parameter $\mathbf{q}$.

In the special case where $M_i = V_i$ and $\mathbf{\Omega}_i = \boldsymbol{\gamma}_i$ (i.e., the VLF consists of the spectral coefficients of the component $x_i(t)$), according to (3.7), the linear estimation matrix is given by

$$\mathbf{P}_i^{\boldsymbol{\gamma}} = \left[\mathbf{\Lambda}_j \mathbf{K}^{-1} \mathbf{\Psi}_i \left(\mathbf{\Psi}_i^{\mathrm{T}} \mathbf{\Lambda}_j \mathbf{K}^{-1} \mathbf{\Psi}_i\right)^{-1}\right]^{\mathrm{T}}. \tag{3.8}$$

For fixed values of i and $\mathbf{q}$, we construct the optimal estimate for the VLF:

$$\mathbf{\Omega}_i^*(\mathbf{q}) = \mathbf{P}_i^{\mathbf{\Omega}}(\mathbf{q})\mathbf{H}. \tag{3.9}$$

It corresponds to the following correlation matrix of estimation errors:

$$\mathbf{K}_i^{\mathbf{\Omega}}(\mathbf{q}) = \mathbf{P}_i^{\mathbf{\Omega}}(\mathbf{q})\mathbf{K}(\mathbf{q}) \left[\mathbf{P}_i^{\mathbf{\Omega}}(\mathbf{q})\right]^{\mathrm{T}}. \tag{3.10}$$

In the special case, using the matrix $\mathbf{P}_i^{\boldsymbol{\gamma}}(\mathbf{q})$, we find the optimal estimate

$$\boldsymbol{\gamma}_i^*(\mathbf{q}) = \mathbf{P}_i^{\boldsymbol{\gamma}}(\mathbf{q})\mathbf{H} \tag{3.11}$$

and the correlation matrix

$$\mathbf{K}_i^{\boldsymbol{\gamma}}(\mathbf{q}) = \mathbf{P}_i^{\boldsymbol{\gamma}}(\mathbf{q})\mathbf{K}(\mathbf{q})[\mathbf{P}_i^{\boldsymbol{\gamma}}(\mathbf{q})]^{\mathrm{T}}. \tag{3.12}$$

Note that for $\mathbf{Z} \neq \mathbf{0}$, the above estimates are biased.

For a fixed $\mathbf{q}$, taking the two estimates $\boldsymbol{\gamma}_1^*(\mathbf{q})$ and $\boldsymbol{\gamma}_2^*(\mathbf{q})$ into account, it is possible to find the residual

$$\mathbf{\Delta}(\mathbf{q}) = \mathbf{H} - \mathbf{H}^*(\mathbf{q}) = \mathbf{H} - \mathbf{\Psi}\boldsymbol{\gamma}^*(\mathbf{q}), \tag{3.13}$$

where $\boldsymbol{\gamma}^*(\mathbf{q}) = \left[[\boldsymbol{\gamma}_1^*(\mathbf{q})]^{\mathrm{T}}, [\boldsymbol{\gamma}_2^*(\mathbf{q})]^{\mathrm{T}}\right]^{\mathrm{T}} = \left[\gamma_j^*(\mathbf{q}), j = \overline{1, V_1 + V_2}\right]^{\mathrm{T}}$ is the estimate for the vector $\boldsymbol{\gamma}(\mathbf{q}) = \left[\boldsymbol{\gamma}_1^{\mathrm{T}}(\mathbf{q}), \boldsymbol{\gamma}_2^{\mathrm{T}}(\mathbf{q})\right]^{\mathrm{T}} = \left[\gamma_j(\mathbf{q}), j = \overline{1, V_1 + V_2}\right]^{\mathrm{T}}$.

The value of $\mathbf{q}$ can be chosen arbitrarily. Therefore, to overcome the nonlinear factor and partially compensate for the impact of the irregular interference $\mathbf{Z}$ on the estimation results, let us proceed as follows. First, we form a family of hypotheses $\left\{\Gamma_{(l)}\right\}_{l=1}^{L}$, each corresponding to some most preferable fixed node $\mathbf{q}_{(l)}$ from the uncertainty region $[\alpha_1, \beta_1] \times \ldots \times [\alpha_Q, \beta_Q]$. Consequently, for each $\mathbf{q}_{(l)}$, it is possible to find the partial estimate $\boldsymbol{\gamma}_{(l)}^* = \boldsymbol{\gamma}^*\left(\mathbf{q}_{(l)}\right)$ and the partial residual

$$\mathbf{\Delta}_{(l)}^* = \mathbf{\Delta}\left(\boldsymbol{\gamma}_{(l)}^*\right) = \mathbf{H} - \mathbf{H}_{(l)}^* = \mathbf{H} - \mathbf{\Psi}\boldsymbol{\gamma}_{(l)}^*.$$

In view of (2.3) and (3.11), we transform this residual to

$$\begin{aligned} \mathbf{\Delta}_{(l)}^* &= \mathbf{H} - \left(\mathbf{\Psi}_1\boldsymbol{\gamma}_{1(l)}^* + \mathbf{\Psi}_2\boldsymbol{\gamma}_{2(l)}^*\right) = \mathbf{Z} + \mathbf{\Xi} - \left(\mathbf{\Psi}_1\mathbf{P}_{1(l)} + \mathbf{\Psi}_2\mathbf{P}_{2(l)}\right)(\mathbf{Z} + \mathbf{\Xi}) \\ &= \left[\mathbf{E} - (\mathbf{\Psi}_1\mathbf{P}_{1(l)} + \mathbf{\Psi}_2\mathbf{P}_{2(l)})\right](\mathbf{Z} + \mathbf{\Xi}) = \vartheta_{(l)}(\mathbf{Z} + \mathbf{\Xi}), \end{aligned} \tag{3.14}$$

where $[\vartheta_{(l)}]_{N \times N}$ is the matrix of influence coefficients of the component $\mathbf{Z} + \mathbf{\Xi}$.

The mean of this residual is

$$M\left\{\mathbf{\Delta}^*_{(l)}\right\} = \vartheta_{(l)}\mathbf{Z}. \tag{3.15}$$

Note that for all nodes of the multidimensional grid, the linear estimation matrices $\mathbf{P}^{\mathbf{\Omega}}_{ir}(\mathbf{q}_{(l)})$ are constructed using only the a priori statistical information and the adopted mathematical models. The set of such matrices yields the families of partial estimates $\mathbf{\Omega}^*_{1(l)} = \mathbf{P}^{\mathbf{\Omega}}_{1(l)}\mathbf{H}$, $\mathbf{\Omega}^*_{2(l)} = \mathbf{P}^{\mathbf{\Omega}}_{2(l)}\mathbf{H}$, $\mathbf{\Omega}^*_{(l)} = \left[\left(\mathbf{\Omega}^*_{1(l)}\right)^{\mathrm{T}}, \left(\mathbf{\Omega}^*_{2(l)}\right)^{\mathrm{T}}\right]^{\mathrm{T}}$ and $\boldsymbol{\gamma}^*_{1(l)} = \mathbf{P}^{\boldsymbol{\gamma}}_{1(l)}\mathbf{H}$, $\boldsymbol{\gamma}^*_{2(l)} = \mathbf{P}^{\boldsymbol{\gamma}}_{2(l)}\mathbf{H}$, $\boldsymbol{\gamma}^*_{(l)} = \left[\left(\boldsymbol{\gamma}^*_{1(l)}\right)^{\mathrm{T}}, \left(\boldsymbol{\gamma}^*_{2(l)}\right)^{\mathrm{T}}\right]^{\mathrm{T}}$, where $l = \overline{1, L}$.

In turn, the resulting estimates $\boldsymbol{\gamma}^*$ and $\mathbf{\Omega}^*$ based on the partial estimates are found using HRM with some operator $\mathfrak{I}_{\mathrm{opt}}$ considering all available a priori and a posteriori information:

$$\mathfrak{I}_{\mathrm{opt}} : \left(\left\{\boldsymbol{\gamma}^*_{(l)}\right\}_{l=1}^{L}, \left\{\mathbf{\Omega}^*_{(l)}\right\}_{l=1}^{L}\right) \to \left(\boldsymbol{\gamma}^*, \mathbf{\Omega}^*\right). \tag{3.16}$$

For example, $\mathfrak{I}_{\mathrm{opt}}$ can be the minimizer of the quadratic form $F_{(l)} = \left(\mathbf{\Delta}^*_{(l)}\right)^{\mathrm{T}}\mathbf{W}_{(l)}\mathbf{\Delta}^*_{(l)}$ (*extremum search algorithm*):

$$\boldsymbol{\gamma}^* = \boldsymbol{\gamma}^*_{(l^*)}, \quad \mathbf{\Omega}^* = \mathbf{\Omega}^*_{(l^*)}, \quad l^* = \arg\min_{l} F_{(l)}, \tag{3.17}$$

where l^* is the optimal number of the node $\mathbf{q}_{(l^*)}$, $l^* \in \{1, \ldots, L\}$.

In (3.17), $\mathbf{W}_{(l)}$ denotes the normalized weight matrix

$$\mathbf{W}_{(l)} = \mathbf{W}(\mathbf{q}_{(l)}) = \left\|\mathbf{K}^{-1}(\mathbf{q}_{(l)})\right\|^{-1}\mathbf{K}^{-1}(\mathbf{q}_{(l)}), \quad \|\mathbf{W}_{(l)}\| = 1 \quad \forall l = \overline{1, L},$$

where $\|\cdot\|$ is any norm used in measurement processing.

Despite its optimality, the algorithm (3.17) has a major drawback: it requires estimates of all coordinates of the expanded vector $\boldsymbol{\gamma}^*$ necessary to form the residual $\mathbf{\Delta}^*_{(l)} = \mathbf{H} - \mathbf{\Psi}\boldsymbol{\gamma}^*_{(l)}$. Furthermore, the quadratic form considered as a function of the argument l shall have a unique global minimum. If there are several competing nodes $\mathbf{q}_{(l_1)}, \ldots, \mathbf{q}_{(l_d)}$, where $l_1, \ldots, l_d \in \{1, \ldots, L\}$ and $d \leqslant L$, with approximately equal local minima, then the following parameter (expressed as a percentage) is introduced to select such nodes:

$$\delta_{F(l)} = 100\left(F_{(l)} - F_{\min}\right)\left(F_{\max} - F_{\min}\right)^{-1},$$

where $F_{\min} = \min\limits_{l} F_{(l)}$ and $F_{\max} = \max\limits_{l} F_{(l)}$.

If we set a numerical threshold δ_{F0} (also in percentage terms), then the competing nodes are formed using the criterion $\delta_{F(l)} \leqslant \delta_{F0}$. For such nodes, it is reasonable to apply the operator $\overline{\mathfrak{I}}_{\mathrm{opt}}$ that averages the competing partial estimates instead of the operator $\mathfrak{I}_{\mathrm{opt}}$ (*averaging algorithm*):

$$\overline{\boldsymbol{\gamma}}^* = d^{-1}\sum_{k=1}^{d}\boldsymbol{\gamma}^*_{(l_k)}, \quad \overline{\mathbf{\Omega}}^* = d^{-1}\sum_{k=1}^{d}\mathbf{\Omega}^*_{(l_k)}. \tag{3.18}$$

To eliminate the main drawback of the optimal algorithm (3.17), one should use the quasi-optimal robust majority estimation operator $\overline{\overline{\mathfrak{I}}}_{\mathrm{opt}}$ [33], e.g., based on the sample median method (with a variational series for even or odd cases, the so-called *majority algorithm*).

For instance, for the vector $\boldsymbol{\gamma}$, all like-named coordinates $\gamma^*_{j(l)}, \ldots, \gamma^*_{j(L)}$ of the vectors $\left\{\boldsymbol{\gamma}^*_{(l)} = \left[\gamma^*_{j(l)}, j = \overline{1, V_1 + V_2}\right]^{\mathrm{T}}\right\}_{l=1}^{L}$ for each fixed $j \in \{1, \ldots, V_1 + V_2\}$ are arranged into the variational series

$\gamma^*_{j[1]}, \gamma^*_{j[2]}, \ldots, \gamma^*_{j[L]}$, where $\gamma^*_{j[1]} < \gamma^*_{j[2]} < \ldots < \gamma^*_{j[L]}$. For the vectors $\mathbf{\Omega}^*_{(l)} = \left[\left(\mathbf{\Omega}^*_{1(l)}\right)^{\mathrm{T}}, \left(\mathbf{\Omega}^*_{2(l)}\right)^{\mathrm{T}}\right]^{\mathrm{T}} = \left[\varsigma^*_{j(l)}, j = \overline{1, M_1 + M_2}\right]^{\mathrm{T}}$, the series $\varsigma^*_{j[1]}$, $\varsigma^*_{j[2]}, \ldots, \varsigma^*_{j[L]}$ are constructed similarly.

The optimal resulting estimate of each coordinate γ_j of the vector $\boldsymbol{\gamma} = \left[\boldsymbol{\gamma}_1^{\mathrm{T}}, \boldsymbol{\gamma}_2^{\mathrm{T}}\right]^{\mathrm{T}} = \left[\gamma_j, j = \overline{1, V_1 + V_2}\right]^{\mathrm{T}}$ and each coordinate ς_j of the vector $\mathbf{\Omega} = \left[\mathbf{\Omega}_1^{\mathrm{T}}, \mathbf{\Omega}_2^{\mathrm{T}}\right]^{\mathrm{T}} = \left[\varsigma_j, j = \overline{1, M_1 + M_2}\right]^{\mathrm{T}}$ is given by the following rule:

for even L,

$$\overline{\overline{\gamma}}{}^*_j = 2^{-1}\left(\gamma^*_{j[L/2]} + \gamma^*_{j[L/2+1]}\right), \quad \overline{\overline{\varsigma}}{}^*_j = 2^{-1}\left(\varsigma^*_{j[L/2]} + \varsigma^*_{j[L/2+1]}\right) \tag{3.19}$$

(i.e., the estimate corresponds to the average of the two central terms of the variational series);

for odd L,

$$\overline{\overline{\gamma}}{}^*_j = \gamma^*_{j[(L-1)/2-1]}, \quad \overline{\overline{\varsigma}}{}^*_j = \varsigma^*_{j[(L-1)/2-1]} \tag{3.20}$$

(i.e., the estimate coincides with the central term of the variational series).

For cases (3.19) and (3.20), the majority algorithm is based on discarding the tails of this series and is highly stable to uncertainty factors. Its implementation does not require estimating all coordinates of the vector $\boldsymbol{\gamma}$, constructing the residuals $\mathbf{\Delta}^*_{(l)}$, or minimizing the quadratic form $F_{(l)} = \left(\mathbf{\Delta}^*_{(l)}\right)^{\mathrm{T}} \mathbf{W}_{(l)} \mathbf{\Delta}^*_{(l)}$ with respect to the argument l.

The optimal resulting estimate of the VLF $\mathbf{\Omega}_i$ for the component $x_i(t)$ is found as

$$\mathbf{\Omega}^*_{i(l^*)} = \mathbf{P}^{\mathbf{\Omega}}_{i(l^*)}\mathbf{H}. \tag{3.21}$$

This estimate is associated with the following correlation matrix of estimation errors:

$$\mathbf{K}^{\mathbf{\Omega}}_{i(l^*)} = \mathbf{P}^{\mathbf{\Omega}}_{i(l^*)}\mathbf{K}_{(l^*)}\left(\mathbf{P}^{\mathbf{\Omega}}_{i(l^*)}\right)^{\mathrm{T}}. \tag{3.22}$$

It can be shown that the construction procedure of the estimate (3.21) for the VLF $\mathbf{\Omega}_i$ primarily relates to finding the optimal resulting estimate (for the vector $\boldsymbol{\gamma}$)

$$\boldsymbol{\gamma}^*_{i(l^*)} = \mathbf{P}^{\boldsymbol{\gamma}}_{i(l^*)}\mathbf{H} \tag{3.23}$$

with the correlation matrix of estimation errors

$$\mathbf{K}^{\boldsymbol{\gamma}}_{i(l^*)} = \mathbf{P}^{\boldsymbol{\gamma}}_{i(l^*)}\mathbf{K}_{(l^*)}\left(\mathbf{P}^{\boldsymbol{\gamma}}_{i(l^*)}\right)^{\mathrm{T}}. \tag{3.24}$$

This follows from the fact that

$$\mathbf{\Omega}_i = \mathbf{\Omega}\{x_i(t)\} = \mathbf{\Omega}\left\{\boldsymbol{\psi}_i^{\mathrm{T}}(t)\boldsymbol{\gamma}_i\right\} = \mathbf{\Omega}\left\{\boldsymbol{\psi}_i^{\mathrm{T}}(t)\right\}\boldsymbol{\gamma}_i. \tag{3.25}$$

In view of (3.21), we have

$$\mathbf{\Omega}^*_{i(l^*)} = \mathbf{\Omega}\left\{\boldsymbol{\psi}_i^{\mathrm{T}}(t)\right\}\boldsymbol{\gamma}^*_{i(l^*)} = \mathbf{\Omega}\left\{\boldsymbol{\psi}_i^{\mathrm{T}}(t)\right\}\mathbf{P}^{\boldsymbol{\gamma}}_{i(l^*)}\mathbf{H}. \tag{3.26}$$

Thus, for comparing different VLF estimation methods, it suffices to analyze the case where $M_i = V_i$ and $\mathbf{\Omega}_i = \boldsymbol{\gamma}_i$, i.e., to consider the problem of estimating the spectral coefficients of the component $x_i(t)$.

Note that for $\mathbf{Z} \neq \mathbf{0}$, the resulting estimates are also biased; however, due to (3.16)–(3.20), it becomes possible to minimize this bias for each fixed sample $\mathbf{H}$.

Formulas (3.1)–(3.26) are the foundation of HRM.

The next section is devoted to the applicability conditions of HRM and its comparative analysis with OLS and ELS.

4. MATHEMATICAL ASPECTS OF STUDYING THE EFFICIENCY OF THE PROPOSED METHOD

Consider the issue of a possible bias of the VLF estimate relative to the true value, caused by the irregular interference $\mathbf{Z} \neq \mathbf{0}$ and uncertainty regarding the parameter $\mathbf{q}$. Let $\widetilde{\mathbf{q}} = \mathbf{q} + \boldsymbol{\Delta}\mathbf{q}$, where $\boldsymbol{\Delta}\mathbf{q}$ will be treated as a perturbation. Let us determine its impact on the estimation result. Now, the matrix $\mathbf{P}_i^{\boldsymbol{\Omega}}(\mathbf{q})$ is replaced by

$$\mathbf{P}_i^{\boldsymbol{\Omega}}(\widetilde{\mathbf{q}}) = \mathbf{P}_i^{\boldsymbol{\Omega}}(\mathbf{q} + \boldsymbol{\Delta}\mathbf{q}) = \mathbf{P}_i^{\boldsymbol{\Omega}}(\mathbf{q}) + \boldsymbol{\Delta}\mathbf{P}_i^{\boldsymbol{\Omega}}(\widetilde{\mathbf{q}}),$$

where $\boldsymbol{\Delta}\mathbf{P}_i^{\boldsymbol{\Omega}}(\widetilde{\mathbf{q}})$ is the perturbation matrix with the condition $\boldsymbol{\Delta}\mathbf{P}_i^{\boldsymbol{\Omega}}(\mathbf{q}) = \mathbf{0}$.

The residual due to the presence of $\boldsymbol{\Delta}\mathbf{q} \neq \mathbf{0}$ is

$$\begin{aligned}\boldsymbol{\Delta\Omega}_i(\widetilde{\mathbf{q}}) = \boldsymbol{\Omega}_i^*(\widetilde{\mathbf{q}}) - \boldsymbol{\Omega}_i^*(\mathbf{q}) &= \mathbf{P}_i^{\boldsymbol{\Omega}}(\mathbf{q})\mathbf{H} + \boldsymbol{\Delta}\mathbf{P}_i^{\boldsymbol{\Omega}}(\widetilde{\mathbf{q}})\mathbf{H} - \mathbf{P}_i^{\boldsymbol{\Omega}}(\mathbf{q})\mathbf{H} \\ &= \boldsymbol{\Delta}\mathbf{P}_i^{\boldsymbol{\Omega}}(\widetilde{\mathbf{q}})\left(\mathbf{X}_i + \mathbf{X}_j + \mathbf{Z} + \boldsymbol{\Xi}\right).\end{aligned} \tag{4.1}$$

This error has the mean

$$M\left\{\boldsymbol{\Delta\Omega}_i(\widetilde{\mathbf{q}})\right\} = \boldsymbol{\Delta}\mathbf{P}_i^{\boldsymbol{\Omega}}(\widetilde{\mathbf{q}})\left(\mathbf{X}_1 + \mathbf{X}_2 + \mathbf{Z}\right). \tag{4.2}$$

Choosing any norm $\|\cdot\|$, we can utilize the inequality

$$\Delta_i^{\boldsymbol{\Omega}} \leqslant \Delta_i^{\mathbf{P}}\eta_i, \tag{4.3}$$

where $\Delta_i^{\boldsymbol{\Omega}} = \max\limits_{\widetilde{\mathbf{q}}}\left\|M\left\{\boldsymbol{\Delta\Omega}_i(\widetilde{\mathbf{q}})\right\}\right\|$, $\Delta_i^{\mathbf{P}} = \max\limits_{\widetilde{\mathbf{q}}}\left\|\boldsymbol{\Delta}\mathbf{P}_i^{\boldsymbol{\Omega}}(\widetilde{\mathbf{q}})\right\|$, and $\eta_i = \max\limits_{\boldsymbol{\gamma}_1,\boldsymbol{\gamma}_2,\mathbf{Z}}\left\|\boldsymbol{\Psi}_1\boldsymbol{\gamma}_1 + \boldsymbol{\Psi}_2\boldsymbol{\gamma}_2 + \mathbf{Z}\right\|$.

When calculating $\Delta_i^{\boldsymbol{\Omega}}$ and $\Delta_i^{\mathbf{P}}$, the maximum is found over the entire uncertainty region $[\alpha_1, \beta_1] \times \ldots \times [\alpha_Q, \beta_Q]$; and when calculating η_i, over the region of possible values of the vectors $\boldsymbol{\gamma}_1$, $\boldsymbol{\gamma}_2$, and $\mathbf{Z}$.

Consider three estimates as follows: $\boldsymbol{\gamma}_{\mathrm{OLS1}}^*$ is the separate estimate for $\boldsymbol{\gamma}_1$ based on OLS (with neglecting the regular and irregular interferences); $\boldsymbol{\gamma}_{\mathrm{ELS}}^*$ is the combined estimate for $\boldsymbol{\gamma} = \left[\boldsymbol{\gamma}_1^{\mathrm{T}}, \boldsymbol{\gamma}_2^{\mathrm{T}}\right]^{\mathrm{T}}$ based on ELS (with neglecting the irregular interference), and $\boldsymbol{\gamma}_{\mathrm{HRM}i}^*$ is the separate estimate for $\boldsymbol{\gamma}_i$ based on the developed HRM. (For brevity, the parameter $\mathbf{q}$ is omitted below.) Resting on [3], we will comprehensively assess these methods in terms of their correctness in measurement experiment design in the absence and presence of the regular and irregular interferences.

For OLS, which involves no expansion, let us determine the impact of the combined interference $\mathbf{Y}_2 = \mathbf{X}_2 + \mathbf{Z} = \boldsymbol{\Psi}_2\boldsymbol{\gamma}_2 + \mathbf{Z}$ on the estimate $\boldsymbol{\gamma}_{\mathrm{OLS1}}^*$ of the vector $\boldsymbol{\gamma}_1$ of the spectral coefficients of the information process. The expectation operator $M\{\cdot\}$ can be used to show that

$$M\left\{\boldsymbol{\gamma}_{\mathrm{OLS1}}^*\right\} = \boldsymbol{\gamma}_1 + \mathbf{C}_1^{-1}\boldsymbol{\Psi}_1^{\mathrm{T}}\mathbf{K}^{-1}\mathbf{Y}_2 = \boldsymbol{\gamma}_1 + \mathbf{C}_1^{-1}\boldsymbol{\Psi}_1^{\mathrm{T}}\mathbf{K}^{-1}\left(\boldsymbol{\Psi}_2\boldsymbol{\gamma}_2 + \mathbf{Z}\right), \tag{4.4}$$

where $\mathbf{C}_1 = \boldsymbol{\Psi}_1^{\mathrm{T}}\mathbf{K}^{-1}\boldsymbol{\Psi}_1$.

The second term in (4.4) corresponds to the bias of the estimate $\boldsymbol{\gamma}_{\mathrm{OLS1}}^*$ relative to the true value $\boldsymbol{\gamma}_1$ when neglecting the contribution of the combined interference $\mathbf{Y}_2$. The scatter of $\boldsymbol{\gamma}_{\mathrm{OLS1}}^*$ relative to $\boldsymbol{\gamma}_1$ (without considering $\mathbf{Y}_2$) is given by

$$\begin{aligned}\widetilde{\mathbf{K}}_{\mathrm{OLS1}}^{\boldsymbol{\gamma}} = M\left\{\left(\boldsymbol{\gamma}_{\mathrm{OLS1}}^* - \boldsymbol{\gamma}_1\right)\left(\boldsymbol{\gamma}_{\mathrm{OLS1}}^* - \boldsymbol{\gamma}_1\right)^{\mathrm{T}}\right\} &= \mathbf{C}_1^{-1} + \mathbf{B}_1\mathbf{Y}_2\mathbf{Y}_2^{\mathrm{T}}\mathbf{B}_1^{\mathrm{T}} \\ &= \mathbf{C}_1^{-1} + \mathbf{B}_1(\boldsymbol{\Psi}_2\boldsymbol{\gamma}_2 + \mathbf{Z})(\boldsymbol{\Psi}_2\boldsymbol{\gamma}_2 + \mathbf{Z})^{\mathrm{T}}\mathbf{B}_1^{\mathrm{T}},\end{aligned} \tag{4.5}$$

where $\mathbf{B}_1 = \mathbf{C}_1^{-1}\boldsymbol{\Psi}_1^{\mathrm{T}}\mathbf{K}^{-1}$.

In turn, the scatter of the estimate $\boldsymbol{\gamma}_{\mathrm{OLS1}}^*$ relative to the mean (4.4) (for OLS with neglecting $\mathbf{Y}_2$) is calculated as follows:

$$\mathbf{K}_{\mathrm{OLS1}}^{\boldsymbol{\gamma}} = M\left\{\left(\boldsymbol{\gamma}_{\mathrm{OLS1}}^* - M\left\{\boldsymbol{\gamma}_{\mathrm{OLS1}}^*\right\}\right)\left(\boldsymbol{\gamma}_{\mathrm{OLS1}}^* - M\left\{\boldsymbol{\gamma}_{\mathrm{OLS1}}^*\right\}\right)^{\mathrm{T}}\right\} = \mathbf{C}_1^{-1}. \tag{4.6}$$

In (4.6), $\mathbf{K}^{\boldsymbol{\gamma}}_{\mathrm{OLS1}}$ denotes the correlation matrix of estimation errors for the spectral coefficients of the information process.

Next, we employ ELS to generate the combined estimate $\boldsymbol{\gamma}^*_{\mathrm{ELS}}$ for the vector $\boldsymbol{\gamma} = \left[\boldsymbol{\gamma}_1^{\mathrm{T}}, \boldsymbol{\gamma}_2^{\mathrm{T}}\right]^{\mathrm{T}}$ of the spectral coefficients of the information process and regular interference (with neglecting the irregular interference $\mathbf{Z}$):

$$\boldsymbol{\gamma}^*_{\mathrm{ELS}} = \mathbf{C}^{-1}\boldsymbol{\Psi}^{\mathrm{T}}\mathbf{K}^{-1}\mathbf{H}, \tag{4.7}$$

where $\mathbf{C} = \boldsymbol{\Psi}^{\mathrm{T}}\mathbf{K}^{-1}\boldsymbol{\Psi}$.

By analogy with (4.4), the mean of such an estimate is

$$M\left\{\boldsymbol{\gamma}^*_{\mathrm{ELS}}\right\} = \boldsymbol{\gamma} + \mathbf{C}^{-1}\boldsymbol{\Psi}^{\mathrm{T}}\mathbf{K}^{-1}\mathbf{Z}, \tag{4.8}$$

where the second term characterizes its bias due to the presence of the irregular interference.

In this case, the correlation matrix of ELS estimation errors has the form

$$\mathbf{K}^{\boldsymbol{\gamma}}_{\mathrm{ELS}} = \mathbf{C}^{-1} = \left(\boldsymbol{\Psi}^{\mathrm{T}}\mathbf{K}^{-1}\boldsymbol{\Psi}\right)^{-1}; \tag{4.9}$$

similar to (4.5), the scatter matrix of the estimate $\boldsymbol{\gamma}^*_{\mathrm{ELS}}$ relative to the true value $\boldsymbol{\gamma}$ is found as

$$\widetilde{\mathbf{K}}^{\boldsymbol{\gamma}}_{\mathrm{ELS}} = \mathbf{C}^{-1} + \mathbf{B}\mathbf{Z}\mathbf{Z}^{\mathrm{T}}\mathbf{B}^{\mathrm{T}}, \tag{4.10}$$

where $\mathbf{B} = \mathbf{C}^{-1}\boldsymbol{\Psi}^{\mathrm{T}}\mathbf{K}^{-1}$.

Since ELS and HRM are linear optimal estimates, they inherit the same potential capabilities in terms of accuracy. The matrix $\widetilde{\mathbf{K}}^{\boldsymbol{\gamma}}_{\mathrm{ELS}}$ contains four blocks, i.e.,

$$\widetilde{\mathbf{K}}^{\boldsymbol{\gamma}}_{\mathrm{ELS}} = \begin{bmatrix} \mathbf{S}_{11} & \mathbf{S}_{12} \\ \mathbf{S}_{21} & \mathbf{S}_{22} \end{bmatrix}, \tag{4.11}$$

and the conditions $\mathbf{S}_{11} = \mathbf{K}^{\boldsymbol{\gamma}}_1 = \mathbf{P}^{\boldsymbol{\gamma}}_1\mathbf{K}\left[\mathbf{P}^{\boldsymbol{\gamma}}_1\right]^{\mathrm{T}}$ and $\mathbf{S}_{22} = \mathbf{K}^{\boldsymbol{\gamma}}_2 = \mathbf{P}^{\boldsymbol{\gamma}}_2\mathbf{K}\left[\mathbf{P}^{\boldsymbol{\gamma}}_2\right]^{\mathrm{T}}$ hold accordingly.

Now, let the combined interference $\mathbf{Y}_2 = \mathbf{X}_2 + \mathbf{Z}$ (the sum of the regular and irregular interferences) admit the finite-analytic representation $\mathbf{Y}_2 = \boldsymbol{\Psi}_{\mathrm{RI+II}}\boldsymbol{\gamma}_{\mathrm{RI+II}}$, where $\boldsymbol{\Psi}_{\mathrm{RI+II}}$ is a given basis matrix of the regular and irregular interferences, and $\boldsymbol{\gamma}_{\mathrm{RI+II}}$ is the vector of unknown spectral coefficients. When the vectors $\boldsymbol{\gamma}_1$ and $\boldsymbol{\gamma}_{\mathrm{RI+II}}$ are estimated simultaneously by ELS, one can find the correlation matrix of joint estimation errors:

$$\mathbf{K}^{\boldsymbol{\gamma}}_{\mathrm{ELS1}} = \mathbf{C}_1^{-1} + \mathbf{B}_1\boldsymbol{\Psi}_{\mathrm{RI+II}}\mathbf{D}_1\left(\mathbf{B}_1\boldsymbol{\Psi}_{\mathrm{RI+II}}\right)^{\mathrm{T}}, \tag{4.12}$$

where

$$\mathbf{D}_1 = \left(\boldsymbol{\Psi}^{\mathrm{T}}_{\mathrm{RI+II}}\mathbf{K}^{-1}\boldsymbol{\Psi}_{\mathrm{RI+II}} - \boldsymbol{\Psi}^{\mathrm{T}}_{\mathrm{RI+II}}\mathbf{K}^{-1}\boldsymbol{\Psi}_1\mathbf{C}_1^{-1}\boldsymbol{\Psi}_1^{\mathrm{T}}\mathbf{K}^{-1}\boldsymbol{\Psi}_{\mathrm{RI+II}}\right)^{-1}.$$

For practice, the following question is of interest: is it necessary to expand the vector of estimated parameters considering the combined interference $\mathbf{Y}_2 = \mathbf{X}_2 + \mathbf{Z}$? Let the traces $\widetilde{\chi} = Sp\left[\mathbf{B}_1\mathbf{Y}_2\mathbf{Y}_2^{\mathrm{T}}\mathbf{B}_1^{\mathrm{T}}\right]$ and $\chi = Sp\left[\mathbf{B}_1\boldsymbol{\Psi}_{\mathrm{RI+II}}\mathbf{D}_1\left(\mathbf{B}_1\boldsymbol{\Psi}_{\mathrm{RI+II}}\right)^{\mathrm{T}}\right]$ of the second matrix terms in (4.10) and (4.12), respectively, be formed. Since the unknown vector parameter $\mathbf{Y}_2$ figures in $\widetilde{\chi}$, we can replace the trace $\widetilde{\chi}$ with its estimate $\widetilde{\chi}^* = Sp\left[\mathbf{B}_1\boldsymbol{\Psi}_{\mathrm{RI+II}}\boldsymbol{\gamma}^*_{\mathrm{RI+II}}\left(\boldsymbol{\Psi}_{\mathrm{RI+II}}\boldsymbol{\gamma}^*_{\mathrm{RI+II}}\right)^{\mathrm{T}}\mathbf{B}_1^{\mathrm{T}}\right]$. The next step is to verify the condition

$$\widetilde{\chi}^* > \chi. \tag{4.13}$$

If this condition fails, then the impact of the combined interference $\mathbf{Y}_2 = \mathbf{X}_2 + \mathbf{Z}$ on the estimate $\boldsymbol{\gamma}_1^*$ of the vector $\boldsymbol{\gamma}_1$ can be considered sufficiently small, and the vector of estimated parameters should not be expanded. Otherwise, it is necessary to apply ELS and, for HRM, ensure the invariance condition with respect to $\mathbf{Y}_2 = \mathbf{X}_2 + \mathbf{Z}$ considering the combined basis matrix $\boldsymbol{\Psi}_{\mathrm{RI+II}}$.

Formulas (4.1)–(4.13) can be used in practice to compare the three methods and settle many issues related to measurement experiment design.

According to a direct analysis of the expressions (3.5) and (3.6), HRM involves the inversion of matrices of dimensions $V_1 \times V_1$ and $V_2 \times V_2$ whereas ELS the inversion of a matrix of dimensions $(V_1 + V_2) \times (V_1 + V_2)$. Consequently, HRM-based estimation is preferable from the computational stability viewpoint: smaller matrices are inverted. Also, the computational process gets decomposed: the VLF is estimated for each component $x_i(t)$ independently (separately) in a dedicated measurement processing channel.

Formulas (4.1)–(4.13) can be used to tune the necessary HRM parameters minimizing the resulting VLF estimation error in each particular case. Necessary and sufficient conditions for the existence of a unique solution of the estimation problem with HRM require nonsingularity and some rank constraints for several matrices, by analogy with [15–17]. In practice, the given conditions are fulfilled by rationally choosing the functional bases and the number of degrees of freedom in the adopted models as well as by specifying appropriate observation conditions. Such issues are associated with computational experiment design and are not considered below: they require separate research in each particular case.

5. THE RECOGNITION ALGORITHM IN THE PRESENCE OF REGULAR AND IRREGULAR INTERFERENCES

Step 1. For each node $\mathbf{q}_{(l)}$, construct the basis matrices $\boldsymbol{\Psi}_{i(l)} = \boldsymbol{\Psi}_i(\mathbf{q}_{(l)})$ and $\boldsymbol{\Psi}_{j(l)} = \boldsymbol{\Psi}_j(\mathbf{q}_{(l)})$, where $i \neq j$.

Step 2. For each node $\mathbf{q}_{(l)}$, use (3.6) to find the matrix $\boldsymbol{\Lambda}_{j(l)} = \boldsymbol{\Lambda}_j\left(\mathbf{q}_{(l)}\right)$.

Step 3. For each node $\mathbf{q}_{(l)}$, use (3.8) to find the weight estimation matrix $\mathbf{P}_{i(l)}^{\boldsymbol{\gamma}} = \mathbf{P}_i^{\boldsymbol{\gamma}}\left(\mathbf{q}_{(l)}\right)$.

Step 4. For each node $\mathbf{q}_{(l)}$, use (3.11) to find the optimal estimate $\boldsymbol{\gamma}_{i(l)}^* = \boldsymbol{\gamma}_i^*\left(\mathbf{q}_{(l)}\right)$.

Step 5. For each node $\mathbf{q}_{(l)}$, use (3.13) to form the residual $\boldsymbol{\Delta}_{(l)} = \boldsymbol{\Delta}\left(\mathbf{q}_{(l)}\right)$.

Step 6. For the case where the function $\boldsymbol{\Delta}_{(l)}$ of the argument l has a minimum point, apply the extremum search algorithm (3.17) to find the optimal number l^* of the node $\mathbf{q}_{(l^*)}$ where this minimum is achieved and the resulting estimate $\boldsymbol{\gamma}^* = \boldsymbol{\gamma}_{(l^*)}^*$.

Step 7. This step is needed in the absence of an explicit minimum point. Then the resulting estimate $\boldsymbol{\gamma}^*$ is obtained by any other method, e.g., the averaging algorithm (3.18) or the majority algorithm (3.19), (3.20).

Step 8. Use (3.21) to compute the optimal resulting estimate $\boldsymbol{\Omega}_{i(l^*)}^*$ of the VLF $\boldsymbol{\Omega}_i$ for the component $x_i(t)$.

Step 9. Use (3.22) and (3.24) to find the correlation matrices $\mathbf{K}_{i(l^*)}^{\boldsymbol{\Omega}} = \mathbf{K}_i^{\boldsymbol{\Omega}}\left(\mathbf{q}_{(l^*)}\right)$ and $\mathbf{K}_{i(l^*)}^{\boldsymbol{\gamma}} = \mathbf{K}_i^{\boldsymbol{\gamma}}\left(\mathbf{q}_{(l^*)}\right)$.

6. SOME GENERALIZATIONS AND PRACTICAL RECOMMENDATIONS

It is possible to interpret HRM for broader conditions by setting $\mathfrak{I}_{\mathrm{opt}}$ as an operator that maximizes the corresponding conditional probability density (e.g., the posterior one or a likelihood function) depending on the parametrically defined correlation matrix $\mathbf{K}(\mathbf{q})$. For instance, for

Gaussian measurement noise, $\mathfrak{I}_{\text{opt}}$ can be taken as the operator maximizing the likelihood function

$$p\left(\mathbf{H}/\boldsymbol{\gamma}^*_{(l)}\right) = (2\pi)^{-N/2}\left(\det \mathbf{K}(\mathbf{q}_{(l)})\right)^{-1/2}\exp\left\{\left(\boldsymbol{\Delta}^*_{(l)}\right)^{\mathrm{T}}(\mathbf{q}_{(l)})\boldsymbol{\Delta}^*_{(l)}\right\}$$

with respect to the parameter l.

In contrast to algorithm (3.17), there is no need to construct the normalized weight matrix $\mathbf{W}_{(l)}$: the required normalization is performed naturally due to the properties of any probability density.

HRM for VLF estimation can be extended to observation models of a more general form. For example, it is possible to consider in (2.1) the basis functions $\psi_{jm}\left(t, \boldsymbol{\mu}_{jm}\right)$ that depend nonlinearly on a vector parameter $\boldsymbol{\mu}_{jm}$. In this case, one shall specify a common uncertainty region for all nonlinear parameters of the estimation problem and choose an appropriate cardinality L of the numerical grid to cover this region with a sufficient accuracy; for example, see [16]. The dimensions of all models (the information process and regular interference) shall be consistent with the sample size N in (2.3).

Obviously, such an approach to VLF estimation shall agree with the computing resources used, which directly depend on the number of alternative hypotheses under consideration. To reduce the requirements for these resources, it is reasonable to minimize the number of nonlinear parameters (i.e., the number of hypotheses) and increase the dimension of the vector of linear parameters. But even in this case, one should seek for a rational tradeoff to exclude possible paradoxes associated with practical VLF estimation. Such questions are the scope of the general theory of measurement experiment design; for example, see [3].

It is possible to combine HRM with the estimation method [17], oriented to form a family of reduced grids corresponding to all possible configurations of irregular interferences at the original grid nodes $\{t_1, \ldots, t_N\}$. Under a sufficiently large size of this grid, such a combination can significantly decrease the impact of regular and irregular interferences on the estimation results. For HRM, this will further increase the family of alternative hypotheses under consideration, and the resulting estimate will correspond to the optimal reduced grid for which the residual is minimal. A criterion and an algorithm for finding such a grid were presented in [17]; also, various options for forming a family of reduced grids, consistent with the available computing resources, were considered.

The normalized weight matrix can be specified as $\mathbf{W}(q)$, where the scalar argument $q \in \{0, 1, 2, \ldots\}$ corresponds to different observation options. Among them, one can provide options considering the properties of the measurement noise and, moreover, irregular interferences. For example, by appropriately selecting the diagonal elements of the matrix $\mathbf{W}(q)$, it is often possible to partially compensate for the irregular interference (via its rejection in the time domain) and smooth the noise.

Hopefully, with current progress in the field of parallel computing (especially based on new principles [34, 35]), HRM will not become an obstacle for advanced real-time systems. However, such an approach remains infeasible for many existing systems, where large samples and numerous alternative hypotheses may require a huge number of parallel data processing channels and significant computational costs. Some useful formulas to justify the computational costs for implementing HRM were provided in [15–17].

7. TEST EXAMPLES

Consider simple but application-relevant examples that are typical, for instance, for altimeters of certain aircraft and are related to smoothing trajectory measurements of small volume [3]. In model (2.2), $x_1(t) = \gamma_1 = \text{const}$ can be treated as the altitude of a loitering aircraft (the parameter γ_1 is a scalar linear functional), and $x_2(t) = \gamma_2 t^2$ with $\gamma_2 = \text{const}$ can be treated as a slowly varying power function representing a regular interference. The latter is often due to imperfections in the aircraft's control system or interferences of various origins on the side lobes of the altimeter antenna pattern.

For each fixed measurement sample, we introduce the relative energy coefficient $\varepsilon_E = \varepsilon_E(\mathbf{H}) = E_1\left(E_2 + E_{\mathbf{Z}} + E_{\mathbf{\Xi}}\right)^{-1} = \mathbf{X}_1^{\mathrm{T}}\mathbf{X}_1\left(\mathbf{X}_2^{\mathrm{T}}\mathbf{X}_2 + \mathbf{Z}^{\mathrm{T}}\mathbf{Z} + \mathbf{\Xi}^{\mathrm{T}}\mathbf{\Xi}\right)^{-1}$, which will be used in the comparative assessment of the developed method.

Example 1. This example is intended only to demonstrate the algorithmic features of HRM and assess its potential capabilities. The uncertainty regarding a nonstationary uncorrelated measurement noise is characterized by the matrix $\mathbf{K} = \mathbf{K}(q) = \operatorname{diag}\left[2\exp\{-q(n-1)\},\ n = \overline{1,N}\,\right]$, where $q > 0$, $\alpha \leqslant q \leqslant \beta$, $\alpha > 0$, and $\beta > 0$. The spectral analysis problem is solved: find the estimate γ_1^* of the coefficient γ_1 (for the information process) and the estimate γ_2^* of the coefficient γ_2 (for the regular interference). For the sake of simplicity, all problem parameters are appropriately scaled to dimensionless quantities.

To demonstrate HRM and perform its comparative analysis, we took a small sample ($N = 5$), with $[0, T] = [0, 5]$, $t_n = n \cdot \Delta t$, $n = \overline{1,5}$, and $\Delta t = 1$.

In (2.3), let $V_1 = 1$, $\boldsymbol{\gamma}_1 = [\gamma_{11}]$, $\boldsymbol{\psi}_1(t) = [\psi_{11}(t)]$, $\psi_{11}(t) \equiv 1$, $\gamma_{11} = \gamma_1$, $V_2 = 1$, $\boldsymbol{\gamma}_2 = [\gamma_{21}]$, $\boldsymbol{\psi}_2(t) = [\psi_{21}(t)]$, $\psi_{21}(t) = t^2$, $\gamma_{21} = \gamma_2$, $\boldsymbol{\gamma} = [\gamma_{11}, \gamma_{21}]^{\mathrm{T}} = [\gamma_1, \gamma_2]^{\mathrm{T}}$, $M_1 = 1$, $\mathbf{\Omega}\{x_1(t)\} = [\omega_1\{x_1(t)\}] = [\varsigma_{11}] = [\gamma_1]$, $M_2 = 1$, $\mathbf{\Omega}\{x_2(t)\} = [\omega_1\{x_2(t)\}] = [\varsigma_{21}] = [\gamma_2]$, $Q = 1$, $\mathbf{q} = [q_1]^{\mathrm{T}}$, $q_1 = q$, $q > 0$, $\alpha_1 = \alpha$, and $\beta_1 = \beta$.

Let the true values of the parameters for the observation equation (2.3) be $\gamma_1 = 10$, $\gamma_2 = 10^{-1}$, $\alpha = 0$, $\beta = 9 \times 10^{-1}$, $L = 6$, $q_{(1)} = 0$, $q_{(2)} = 10^{-1}$, $q_{(3)} = 3 \times 10^{-1}$, $q_{(4)} = 5 \times 10^{-1}$, $q_{(5)} = 7 \times 10^{-1}$, $q_{(6)} = 9 \times 10^{-1}$. In other words, the parameter q belongs to the one-dimensional uncertainty region $[0, 5]$ with six nodes uniformly located nodes. In this example, $\mathbf{\Psi}_1^{\mathrm{T}} = [1; 1; 1; 1; 1]$ and $\mathbf{\Psi}_2^{\mathrm{T}} = [1; 4; 9; 16; 25]$.

First, using (3.8), we found the coefficient vectors $\mathbf{P}_{1(l)}^{\boldsymbol{\gamma}}$ necessary for constructing the linear estimate $\gamma_{1(l)}^*$ of the coefficient γ_1, invariant with respect to the regular interference:

$$\mathbf{P}_{1(1)}^{\boldsymbol{\gamma}} = [0.4941; 0.4059; 0.2588; 0.0529; -0.2118]^{\mathrm{T}},$$

$$\mathbf{P}_{1(2)}^{\boldsymbol{\gamma}} = [0.4495; 0.4118; 0.2985; 0.0876; -0.2474]^{\mathrm{T}},$$

$$\mathbf{P}_{1(3)}^{\boldsymbol{\gamma}} = [0.3620; 0.4107; 0.3790; 0.1802; -0.3320]^{\mathrm{T}},$$

$$\mathbf{P}_{1(4)}^{\boldsymbol{\gamma}} = [0.2803; 0.3923; 0.4547; 0.3066; -0.4339]^{\mathrm{T}},$$

$$\mathbf{P}_{1(5)}^{\boldsymbol{\gamma}} = [0.2082; 0.3584; 0.5175; 0.4666; -0.5510]^{\mathrm{T}},$$

$$\mathbf{P}_{1(6)}^{\boldsymbol{\gamma}} = [0.1482; 0.3133; 0.5605; 0.6550; -0.6771]^{\mathrm{T}}.$$

We verified the unbiasedness condition $\mathbf{P}_{1(l)}^{\boldsymbol{\gamma}}\mathbf{X}_1 = \gamma_1$, where $\mathbf{X}_1 = [10; 10; 10; 10; 10]^{\mathrm{T}}$, and the invariance condition $\mathbf{P}_{1(l)}^{\boldsymbol{\gamma}}\mathbf{X}_2 = 0$, where $\mathbf{X}_2 = [0.1; 0.4; 0.9; 1.6; 2.5]^{\mathrm{T}}$, for all $l = \overline{1,6}$. The matrices $\mathbf{\Lambda}_{2(l)}$ for $\mathbf{\Lambda}_2$ (3.6) were constructed when finding the vectors. For instance, for $l = 1$,

$$\mathbf{\Lambda}_{2(1)} = \begin{bmatrix} 0.9990 & -0.0041 & -0.0092 & -0.0163 & -0.0255 \\ -0.0041 & 0.9837 & -0.0368 & -0.0654 & -0.1021 \\ -0.0092 & -0.0368 & 0.9173 & -0.1471 & -0.2298 \\ -0.0163 & -0.0654 & -0.1471 & 0.7385 & -0.4086 \\ -0.0255 & -0.1021 & -0.2298 & -0.4086 & 0.3616 \end{bmatrix}.$$

Next, using (3.12), we computed the estimation error variances for the coefficient γ_1 :

$$\sigma^2_{1(1)} = 1.0471, \quad \sigma^2_{1(2)} = 0.9503, \quad \sigma^2_{1(3)} = 0.7625,$$
$$\sigma^2_{1(4)} = 0.5888, \quad \sigma^2_{1(5)} = 0.4364, \quad \sigma^2_{1(6)} = 0.3103.$$

Clearly, for the uncertainty region in the parameter q, the spread of the estimation error variances changes by a factor of 3.37. Therefore, for HRM, the estimation accuracy of γ_1 significantly depends on the chosen hypothesis of the family $\left\{\Gamma_{(l)}\right\}_{l=1}^{6}$.

With the vectors $\mathbf{P}^{\boldsymbol{\gamma}}_{1(l)}$ replaced by the ones $\overline{\mathbf{P}}^{\boldsymbol{\gamma}}_{1(l)}$ neglecting the regular interference $\mathbf{X}_2$ (which is typical for OLS), we obtained the following biases of the estimate γ_1^* :

$$\left(\overline{\mathbf{P}}^{\gamma}_{1(1)}\right)^{\mathrm{T}}\mathbf{X}_2 = 1.1000, \quad \left(\overline{\mathbf{P}}^{\gamma}_{1(2)}\right)^{\mathrm{T}}\mathbf{X}_2 = 1.2207, \quad \left(\overline{\mathbf{P}}^{\gamma}_{1(3)}\right)^{\mathrm{T}}\mathbf{X}_2 = 1.4591,$$
$$\left(\overline{\mathbf{P}}^{\gamma}_{1(4)}\right)^{\mathrm{T}}\mathbf{X}_2 = 1.6733, \quad \left(\overline{\mathbf{P}}^{\gamma}_{1(5)}\right)^{\mathrm{T}}\mathbf{X}_2 = 1.8540, \quad \left(\overline{\mathbf{P}}^{\gamma}_{1(6)}\right)^{\mathrm{T}}\mathbf{X}_2 = 2.8015.$$

Thus, with the regular interference being neglected, an error of up to 28% arises when estimating the coefficient γ_1 by OLS.

The estimates $\gamma^*_{2(l)}$ for γ_2 are also needed to implement the optimal algorithm (3.17). The corresponding weight vectors were computed as

$$\mathbf{P}^{\boldsymbol{\gamma}}_{2(1)} = [-0.0267; -0.0187; -0.0053; 0.0134; 0.0374]^{\mathrm{T}},$$
$$\mathbf{P}^{\boldsymbol{\gamma}}_{2(2)} = [-0.0235; -0.0191; -0.0082; 0.0107; 0.0401]^{\mathrm{T}},$$
$$\mathbf{P}^{\boldsymbol{\gamma}}_{2(3)} = [-0.0179; -0.0189; -0.0134; 0.0046; 0.0456]^{\mathrm{T}},$$
$$\mathbf{P}^{\boldsymbol{\gamma}}_{2(4)} = [-0.0133; -0.0177; -0.0177; -0.0028; 0.0515]^{\mathrm{T}},$$
$$\mathbf{P}^{\boldsymbol{\gamma}}_{2(5)} = [-0.0095; -0.0159; -0.0210; -0.0113; 0.0577]^{\mathrm{T}},$$
$$\mathbf{P}^{\boldsymbol{\gamma}}_{2(6)} = [-0.0066; -0.0137; -0.0231; -0.0206; 0.0639]^{\mathrm{T}}.$$

When finding these vectors, we constructed the matrices $\boldsymbol{\Lambda}_{1(l)}$ for $\boldsymbol{\Lambda}_1$ (3.6). For instance, for $l = 3$,

$$\boldsymbol{\Lambda}_{1(3)} = \begin{bmatrix} 0.8995 & -0.1005 & -0.1005 & -0.1005 & -0.1005 \\ -0.1356 & 0.8644 & -0.1356 & -0.1356 & -0.1356 \\ -0.1831 & -0.1831 & 0.8169 & -0.1831 & -0.1831 \\ -0.2472 & -0.2472 & -0.2472 & 0.7528 & -0.2472 \\ -0.3336 & -0.3336 & -0.3336 & -0.3336 & -0.6664 \end{bmatrix}.$$

Next, using (3.12), we computed the estimation error variances for the parameter $\gamma_2 \times 10^{-3}$:

$$\sigma^2_{2(1)} = 5.3476, \quad \sigma^2_{2(2)} = 4.2002, \quad \sigma^2_{2(3)} = 2.6396,$$
$$\sigma^2_{2(4)} = 1.6881, \quad \sigma^2_{2(5)} = 1.0861, \quad \sigma^2_{2(6)} = 0.6955.$$

In this case, the spread of the estimation error variances changes by a factor of 7.69.

According to the above data, the implementation of both HRM and well-known methods (OLS, ELS, and GIUE) with only one pre-fixed (nominal) value $q_0 \in [\alpha, \beta]$ can lead to a considerable spread of the estimates. Therefore, it is possible to significantly improve the estimation quality by HRM, which chooses an optimal node in the uncertainty region $[\alpha, \beta]$.

With no need for matrix inversion in this example, in the case of ELS, the combined vector estimate $\gamma^*_{\text{ELS}} = [\gamma^*_{\text{ELS1}}, \gamma^*_{\text{ELS2}}]^{\text{T}}$ was found for all hypotheses $\Gamma_{(l)}$; this required inverting the matrices $\mathbf{C}_{(l)} = \mathbf{\Psi}^{\text{T}}\mathbf{W}_{(l)}\mathbf{\Psi}$, where

$$\mathbf{\Psi}^{\text{T}} = \begin{bmatrix} 1 & 1 & 1 & 1 & 1 \\ 1 & 4 & 9 & 16 & 25 \end{bmatrix}.$$

For the family of all these matrices, we found their condition numbers $\nu_{(l)} = \nu(\mathbf{C}_{(l)})$ (in the Euclidean norm): $\nu_{(1)} = 515.7839$, $\nu_{(2)} = 666.9735$, $\nu_{(3)} = 1101.7277$, $\nu_{(4)} = 1778.5476$, $\nu_{(5)} = 2789.8688$, $\nu_{(6)} = 4239.6586$. Obviously, even for the simplest low-dimensional test example and a small sample, we are dealing with ill-conditioned matrices and, hence, with an additional computational error to find the desired estimates. This fact is characteristic of most estimation problems with a power basis [27–29].

Example 2. Let the matrix $\mathbf{K} = \mathbf{K}(q) = \operatorname{diag}\big[[1 + q(n-1)]^{-2},\ n = \overline{1,5}\,\big]$ correspond to the case of uncorrelated nonstationary measurements of a small volume. In this case, $\mathbf{W}_{(l)} = \operatorname{diag}\big[w_{nn}(q_{(l)}),\ n = \overline{1,5}\,\big]$, where $w_{nn}(q_{(l)}) = [1 + q(n-1)]^2 \left(\sum\limits_{n=1}^{5} [(1 + q(n-1))]^2\right)^{-1}$, which holds for the norm $\|\mathbf{W}_{(l)}\| = \sum\limits_{n=1}^{n} w_{nn(l)}$ with $w_{nn(l)} > 0$. We set $[0, T] = [0, 4]$, $t_n = (n-1)\Delta t$, $n = \overline{1,5}$, $\Delta t = 1$, $\alpha = -0.25$, $\beta = 1$, $L = 6$, $q_{(1)} = -0.2$, $q_{(2)} = -0.125$, $q_{(3)} = 0$, $q_{(4)} = 0.3$, $q_{(5)} = 0.7$, and $q_{(6)} = 1$. For each node in the uncertainty region, Table 1 presents the estimation results of the coefficient γ_1 by HRM for the family of characteristic samples $\{\mathbf{H}_k\}_{k=1}^{5}$ corresponding to different variants of irregular interference occurrence (for particular values of the energy parameter $\{\varepsilon_{Ek}\}_{k=1}^{5}$ and a threshold $\delta_{F0} = 15\%$).

Table 1

$\varepsilon_{E1} = 5.44$, $\mathbf{H}_1 = [9.5; 11.5; 12.3; 14.1; 18.2]^{\text{T}}$					
$\gamma^*_{1(1)} = 11.92$	$\gamma^*_{1(2)} = 10.11$	$\gamma^*_{1(3)} = 10.12$	$\gamma^*_{1(4)} = 10.11$	$\gamma^*_{1(5)} = 10.09$	$\gamma^*_{1(6)} = 10.09$
$F_{(1)} = 3.74$	$F_{(2)} = 0.37$	$F_{(3)} = 0.29$	$F_{(4)} = 0.21$	$F_{(5)} = 0.16$	$F_{(6)} = 0.15$
$\delta_{F(1)} = 100$	$\delta_{F(2)} = 6.13$	$\delta_{F(3)} = 3.90$	$\delta_{F(4)} = 1.67$	$\delta_{F(5)} = 0.28$	$\delta_{F(6)} = 0$
$\varepsilon_{E2} = 7.30$, $\mathbf{H}_2 = [9; 11.5; 10; 17.5; 13]^{\text{T}}$					
$\gamma^*_{1(1)} = 11.92$	$\gamma^*_{1(2)} = 10.11$	$\gamma^*_{1(3)} = 10.12$	$\gamma^*_{1(4)} = 10.11$	$\gamma^*_{1(5)} = 10.09$	$\gamma^*_{1(6)} = 10.09$
$F_{(1)} = 2.37$	$F_{(2)} = 4.30$	$F_{(3)} = 7.36$	$F_{(4)} = 10.33$	$F_{(5)} = 11.59$	$F_{(6)} = 13.77$
$\delta_{F(1)} = 0$	$\delta_{F(2)} = 17$	$\delta_{F(3)} = 43.88$	$\delta_{F(4)} = 69.82$	$\delta_{F(5)} = 80.88$	$\delta_{F(6)} = 100$
$\varepsilon_{E3} = 3.28$, $\mathbf{H}_3 = [17; 16.5; 13; 14; 16]^{\text{T}}$					
$\gamma^*_{1(1)} = 14.88$	$\gamma^*_{1(2)} = 13.91$	$\gamma^*_{1(3)} = 12.30$	$\gamma^*_{1(4)} = 10.47$	$\gamma^*_{1(5)} = 9.87$	$\gamma^*_{1(6)} = 9.67$
$F_{(1)} = 7.77$	$F_{(2)} = 11.31$	$F_{(3)} = 12.76$	$F_{(4)} = 9.09$	$F_{(5)} = 6.46$	$F_{(6)} = 5.46$
$\delta_{F(1)} = 31.64$	$\delta_{F(2)} = 80.19$	$\delta_{F(3)} = 100$	$\delta_{F(4)} = 49.72$	$\delta_{F(5)} = 13.66$	$\delta_{F(6)} = 0$
$\varepsilon_{E4} = 2.83$, $\mathbf{H}_4 = [9; 18.5; 7; 15.5; 18]^{\text{T}}$					
$\gamma^*_{1(1)} = 11.04$	$\gamma^*_{1(2)} = 10.92$	$\gamma^*_{1(3)} = 10.60$	$\gamma^*_{1(4)} = 10.10$	$\gamma^*_{1(5)} = 10.06$	$\gamma^*_{1(6)} = 10.04$
$F_{(1)} = 21.78$	$F_{(2)} = 21.01$	$F_{(3)} = 17.84$	$F_{(4)} = 12.73$	$F_{(5)} = 9.99$	$F_{(6)} = 9.08$
$\delta_{F(1)} = 100$	$\delta_{F(2)} = 93.97$	$\delta_{F(3)} = 69.98$	$\delta_{F(4)} = 28.74$	$\delta_{F(5)} = 7.18$	$\delta_{F(6)} = 0$
$\varepsilon_{E5} = 6.89$, $\mathbf{H}_5 = [17; 11.5; 11; 14.8; 10]^{\text{T}}$					
$\gamma^*_{1(1)} = 13.02$	$\gamma^*_{1(2)} = 11.81$	$\gamma^*_{1(3)} = 9.8$	$\gamma^*_{1(4)} = 7.52$	$\gamma^*_{1(5)} = 6.68$	$\gamma^*_{1(6)} = 6.39$
$F_{(1)} = 13.97$	$F_{(2)} = 18.95$	$F_{(3)} = 22.96$	$F_{(4)} = 20.24$	$F_{(5)} = 18.18$	$F_{(6)} = 17.24$
$\delta_{F(1)} = 0$	$\delta_{F(2)} = 55.39$	$\delta_{F(3)} = 100$	$\delta_{F(4)} = 71.74$	$\delta_{F(5)} = 46.82$	$\delta_{F(6)} = 36.37$

Next, Table 2 provides the estimation results of the coefficient by HRM with algorithms (3.17), (3.18), and (3.20), where Δ_1, $\overline{\Delta}_1$, and $\overline{\overline{\Delta}}_1$ are the absolute estimation errors.

Table 2

$\mathbf{H}_1$	$\mathbf{H}_2$	$\mathbf{H}_3$	$\mathbf{H}_4$	$\mathbf{H}_5$
$\gamma^*_{1(1)} = 10.09$	$\gamma^*_{1(1)} = 9.64$	$\gamma^*_{1(1)} = 9.67$	$\gamma^*_{1(1)} = 10.04$	$\gamma^*_{1(1)} = 13.02$
$\Delta_1 = 0.09$	$\Delta_1 = 0.36$	$\Delta_1 = 0.33$	$\Delta_1 = 0.04$	$\Delta_1 = 3.02$
$\overline{\gamma}^*_{1(1)} = 10.1$	$\overline{\gamma}^*_{1(1)} = 9.64$	$\overline{\gamma}^*_{1(1)} = 9.77$	$\overline{\gamma}^*_{1(1)} = 10.05$	$\overline{\gamma}^*_{1(1)} = 13.02$
$\overline{\Delta}_1 = 0.1$	$\overline{\Delta}_1 = 0.36$	$\overline{\Delta}_1 = 0.23$	$\overline{\Delta}_1 = 0.05$	$\overline{\Delta}_1 = 3.02$
$\overline{\overline{\gamma}}^*_{1(1)} = 10.11$	$\overline{\overline{\gamma}}^*_{1(1)} = 9.64$	$\overline{\overline{\gamma}}^*_{1(1)} = 9.77$	$\overline{\overline{\gamma}}^*_{1(1)} = 10.05$	$\overline{\overline{\gamma}}^*_{1(1)} = 13.02$
$\overline{\overline{\Delta}}_1 = 0.11$	$\overline{\overline{\Delta}}_1 = 0.36$	$\overline{\overline{\Delta}}_1 = 0.23$	$\overline{\overline{\Delta}}_1 = 0.05$	$\overline{\overline{\Delta}}_1 = 3.02$

The data in this table clearly show the possibility of reliable information process estimation in the presence of regular and irregular interferences in the input observation.

Finally, Table 3 presents the estimation results by OLS and ELS with the nominal value $q_0 = q_{(3)} = 0$ used in the processing algorithms, where δ_1 is the relative error expressed as a percentage.

Table 3

$\varepsilon_{E1} = 5.44$, $\mathbf{H}_1 = \left[9.5; 11.5; 12.3; 14.1; 18.2\right]^{\mathrm{T}}$				
OLS	$\gamma^*_{1(1)} = 13.12$	$F = 8.63$	$\Delta_1 = 3.12$	$\delta_1 = 31.2$
ELS	$\gamma^*_{1(1)} = 10.12$	$F = 0.29$	$\Delta_1 = 0.12$	$\delta_1 = 1.2$
$\varepsilon_{E2} = 7.30$, $\mathbf{H}_2 = \left[9; 11.5; 10; 17.5; 13\right]^{\mathrm{T}}$				
OLS	$\gamma^*_{1(1)} = 12.2$	$F = 8.86$	$\Delta_1 = 2.2$	$\delta_1 = 22$
ELS	$\gamma^*_{1(1)} = 9.2$	$F = 7.36$	$\Delta_1 = 0.8$	$\delta_1 = 8$
$\varepsilon_{E3} = 3.28$, $\mathbf{H}_3 = \left[17; 16.5; 13; 14; 16\right]^{\mathrm{T}}$				
OLS	$\gamma^*_{1(1)} = 15.31$	$F = 2.36$	$\Delta_1 = 5.3$	$\delta_1 = 53$
ELS	$\gamma^*_{1(1)} = 12.3$	$F = 12.76$	$\Delta_1 = 2.3$	$\delta_1 = 18.7$
$\varepsilon_{E4} = 2.83$, $\mathbf{H}_4 = \left[9; 18.5; 7; 15.5; 18\right]^{\mathrm{T}}$				
OLS	$\gamma^*_{1(1)} = 13.6$	$F = 22.34$	$\Delta_1 = 3.6$	$\delta_1 = 36$
ELS	$\gamma^*_{1(1)} = 10.6$	$F = 17.84$	$\Delta_1 = 0.6$	$\delta_1 = 6$
$\varepsilon_{E5} = 6.89$, $\mathbf{H}_5 = \left[17; 11.5; 11; 14.8; 10\right]^{\mathrm{T}}$				
OLS	$\gamma^*_{1(1)} = 12.8$	$F = 6.66$	$\Delta_1 = 2.8$	$\delta_1 = 28$
ELS	$\gamma^*_{1(1)} = 9.8$	$F = 22.96$	$\Delta_1 = 0.2$	$\delta_1 = 2$

We also considered the case of correlated nonstationary measurements of large volume ($N = 41$) with the matrix $\mathbf{K} = \mathbf{K}(q)$ composed of the diagonal elements $k_{nn}(q) = \left[1 + q\Delta t(n-1)\right]^{-2}$, $n = \overline{1, 41}$, where $\Delta t = 0.1$, and the off-diagonal elements $k_{nm} = \exp\{-|n-m|\Delta t\}$, $n, m = \overline{1, 41}$, $n \neq m$. Using a random number generator, one thousand input observation samples were generated, with each sample containing regular and irregular interferences. The parameters q and ε_E were specified as random variables with the uniform distribution on the intervals from -0.2 to 1 and from 1.7 to 2.5, respectively. The number of anomalous outliers in each realization corresponded to $\rho_{\mathbf{Z}} = 30\%$. The entire observation interval was divided into three equal-size segments (initial, middle, and final). In each experiment, the irregular interference was concentrated on one of the segments (with a uniform distribution law). Based on the simulation results, the coefficient γ_1 was estimated with the following averaged (over all samples) absolute errors: for OLS, $\Delta_1 = 4.78$; for ELS and GIUE, $\Delta_1 = 2.11$; for HRM, $\Delta_1 = 0.32$.

ELS and GIUE coincide in accuracy since a small-dimensional case is considered. The gain from GIUE, due to the decomposition of the estimation algorithm, manifests itself only for large-dimensional problems.

Thus, even for one degree of freedom (the parameter q is scalar) in uncertainty description, it is possible to significantly improve the estimation accuracy of information processes with regular and irregular interferences. Obviously, when solving more complex applied problems, one should choose a multidimensional uncertainty region and an appropriate number of nodes $\mathbf{q}_{(l)}$, $l = \overline{1, L}$.

8. CONCLUSIONS

Under essential uncertainty, HRM allows studying in detail any component of the observation equation using VLF while ensuring the invariance condition of the estimation result with respect to a regular interference and minimizing (within the adopted criterion) the impact of an irregular interference on the estimation results. It is possible to organize several parallel computation channels for VLF in the entire uncertainty region of the correlation function parameters of the semi-defined measurement noise. Within a single channel, all advantages of linear estimation are preserved without expanding the vector of estimated parameters. Analytical formulas have been derived to assess the potential capabilities of HRM and the conditions for its most effective application.

HRM can be modified for other known problems, e.g., estimation from a growing-volume sample, signal detection/recognition/resolution, and the linear or nonlinear filtering of signal parameters. This method is well suited for multichannel information-measuring systems designed to operate in real time. All computational procedures in each channel reduce to simple mathematical operations on vectors and matrices; and HRM can be combined with conventional approaches to applications-relevant problems of optimal and quasi-optimal measurement processing.

REFERENCES

1. Repin, V.G. and Tartakovskii, G.P., *Statisticheskii sintez pri apriornoi neopredelennosti i adaptatsiya informatsionnykh sistem* (Statistical Synthesis under A Priori Uncertainty and Adaptation of Information Systems), Moscow: Sovetskoe Radio, 1977.

2. Bogdanovich, V.A. and Vostretsov, A.G., *Teoriya ustoychivogo obnaruzheniya, razlicheniya i otsenivaniya signalov* (Theory of Stable Detection, Discrimination and Estimation of Signals), Moscow: Fizmatlit, 2004.

3. Zhdanyuk, B.F., *Osnovy statisticheskoi obrabotki traektornykh izmerenii* (Foundations of Statistical Processing of Trajectory Measurements), Moscow: Sovetskoe Radio, 1978.

4. Fomin, A.F., Novoselov, O.N., and Plyushchev, A.V., *Otbrakovka anomal'nykh rezul'tatov izmerenii* (Rejection of Abnormal Measurement Results), Moscow: Energoatomizdat, 1985.

5. Hajiyev, Ch.M., Abnormal Measurement Rejection for Multidimensional Dynamic Systems, *Avtometriya*, 2003, vol. 39, no. 4, pp. 33–39.

6. Bulychev, Yu.G., Vasil'ev, V.V., Dzhugan, R.V., et al., *Informatsionno-izmeritel'noe obespechenie naturnykh ispytanii slozhnykh tekhnicheskikh kompleksov* (Information and Measurement Support for Live Testing of Complex Technical Systems), Manin, A.P. and Vasil'ev, V.V., Eds., Moscow: Mashinostroenie-Polet, 2016.

7. Denisov, V.P., Dubinin, D.V., and Mescheryakov, A.A., Rejection of Abnormally Large Direction-Finding Errors in the Process of Resolving the Measurement Ambiguities in Phase Direction-Finders Implementing the Maximum-Likelihood Method, *Journal of Communications Technology and Electronics*, 2016, vol. 61, no. 10, pp. 1095–1100.

8. Shen, K., Shakhtarin, B.I., Neusypin, K.A., and Nguyen, D.T., Algorithms for Correction of the Navigation Information Using a Satellite Radio Navigation System under Anomalous Measurement Conditions, *Journal of Communications Technology and Electronics*, 2019, vol. 64, no. 1, pp. 29–34.

9. Ivanov, A.V., Shishkin, V.Y., Boikov, D.V., et al., Adaptive Algorithms for Information Processing in Navigation Complexes of Mobile Ground Objects, *Journal of Communications Technology and Electronics*, 2021, vol. 66, no. 8, pp. 926–937.

10. Kalianov, A.A., Lukin, O.V., and Tsyganova, I.V., The Algorithm of Adaptive Filtering of Motion Parameters, *Automation of Control Processes*, 2023, no. 1(71), pp. 75–87.

11. Gu, T., Tu, Y., Tang, D., and Luo, T., A Robust Moving Total Least-Squares Fitting Method for Measurement Data, *IEEE Transact. Instrument. Measurement.*, 2020, vol. 69, no. 10, pp. 7566–7573.

12. Gu, T., Luo, Z., Guo, T., and Luo, T., A New Reconstruction Method for Measurement Data with Multiple Outliers, *IEEE Transact. Instrument. Measurement*, 2022, vol. 71, art. no. 1005709, pp. 1–9.

13. Ji, C., Song, C., Li, S., et. al., An Online Combined Compensation Method of Geomagnetic Measurement Error, *IEEE Sensor. J.*, 2022, vol. 22, no. 14, pp. 14026–14037.

14. Gao, G., Gao, B., Gao, S., et. al., Hypothesis Test-Constrained Robust Kalman Filter for INS/GNSS Integration with Abnormal Measurement, *IEEE Transact. Vehicular Tech.*, 2023, vol. 72, no. 2, pp. 1662–1673.

15. Bulychev, Yu.G. and Eliseev, A.V., Computational Scheme for Invariantly Unbiased Estimation of Linear Operators in a Given Class, *Comput. Math. Math. Phys.*, 2008, vol. 48, no. 4, pp. 549–560.

16. Bulychev, Yu.G., Signal Recognition without State Space Expansion Based on Observations Containing a Singular Interference: The Case of Nonlinear Parameters of Basis Functions, *Autom. Remote Control*, 2024, vol. 85, no. 2, pp. 160–176.

17. Bulychev, Yu.G., A Decomposition–Autocompensation Method for Signal Recognition Based on the Principles of Continuity, Invariance, Multiplication, and Ranking with Regular and Irregular Interferences, *Autom. Remote Control*, 2025, vol. 86, no. 4, pp. 315–329.

18. Sutti, C., Local and Global Optimization by Parallel Algorithms for MIMD Systems, *Ann. Oper. Res.*, 1984, vol. 1, pp. 151–164.

19. Price, W.L., Global Optimization Algorithms for a CAD Workstation, *J. Optim. Theory Appl.*, 1987, vol. 55, pp. 133–146.

20. Granichin, O.N. and Polyak, B.T., *Randomizirovannye algoritmy otsenivaniya i optimizatsii pri pochti proizvol'nykh pomekhakh* (Randomized Algorithms for Estimation and Optimization under Almost Arbitrary Noise), Moscow: Nauka, 2003.

21. Granichin, O.N., Shalymov, D.S., Avros, R., et al., A Randomized Algorithm for Estimating the Number of Clusters, *Autom. Remote Control*, 2011, vol. 72, no. 4, pp. 754–765.

22. Kupriyanov, A.I., Petrenko, P.B., and Sychev, M.P., *Teoreticheskie osnovy radioelektronnoi razvedki* (Theoretical Foundations of Electronic Reconnaissance), Moscow: Bauman Moscow State Technical University, 2010.

23. Verba, V.S. and Tatarskii, B.G., *Osnovy teorii radiolokatsionnykh sistem i kompleksov* (Fundamentals of the Theory of Radar Systems and Complexes), Moscow: Tekhnosfera, 2024.

24. Zekavat, S. and Buehrer, R., *Handbook of Position Location: Theory, Practice and Advances*, 2nd ed., Hoboken: Wiley-IEEE Press, 2019.

25. Wang, X., Wang, A., Wang, D., et al., A Modified Sage-Husa Adaptive Kalman Filter for State Estimation of Electric Vehicle Servo Control System, *Energy Reports*, 2022, vol. 8, no. 5, pp. 20–27.

26. Kalianov, A.A., Lukin, O.V., and Tsyganova, I.V., The Algorithm of Adaptive Filtering of Motion Parameters, *Automation of Control Processes*, 2023, no. 1(71), pp. 75–87.

27. Peng, L., Wenhui, W., Junda, Q., et al., Robust Generalized Labeled Multi-Bernoulli Filter and Smoother for Multiple Target Tracking Using Variational Bayesian, *KSII Transactions on Internet and Information Systems*, 2022, vol. 16, no. 3, pp. 908–928.

28. Tatuzov, A.L., *Neironnye seti v zadachakh radiolokatsii* (Neural Networks in Radiolocation Problems), Moscow: Radiotekhnika, 2009.

29. Stepanov, O.A. and Mostafa, M., Integrated Processing Algorithms for Correction of Navigation System Using Nonlinear Measurements, *Izv. Tula State University*, 2016, no. 6, pp. 89–102.

30. Bulychev, Yu.G., Bulychev, V.Yu., Ivakina, S.S., et al., Substantiation of Methods for Optimal Estimation of Target Motion Parameters in Triangulation Location Systems, *J. Comput. Syst. Sci. Int.*, 2015, vol. 54, no. 4, pp. 593–608.

31. Bulychev, V.Y., Bulychev, Y.G., Ivakina, S.S., et al., Classification of Passive Location Invariants and Their Use, *J. Comput. Syst. Sci. Int.*, 2015, vol. 54, no. 6, pp. 905–915.

32. Bulychev, Yu.G. and Chepel', E.N., Optimization of the Cluster-Variant Method of Constructing a Multi-Position Direction Finding System for Conditions of a Priori Uncertainty, *Autom. Remote Control*, 2023, vol. 84, no. 4, pp. 460–473.

33. Gil'bo, E.P. and Chelpanov, I.B., *Obrabotka signalov na osnove uporyadochennogo vybora* (Signal Processing Based on Ordered Selection), Moscow: Sovetskoe Radio, 1977.

34. Ezhova, N.A. and Sokolinsky, L.B., Survey of Parallel Computation Models, *Bull. South Ural State Univ. Ser. Comput. Math. Software Eng.*, 2019, vol. 8, no. 3, pp. 58–91.

35. Ivanov, A.I. and Shpilevaya, S.G., On Quantum Parallel Computing, *Vestn. Kant Baltic Univ. Ser. Phys., Math., Eng.*, 2021, no. 2, pp. 95–99.

This paper was recommended for publication by A.A. Galyaev, a member of the Editorial Board

ISSN 0005-1179 (print), ISSN 1608-3032 (online), Automation and Remote Control, 2026, Vol. 87, No. 8, pp. 688–698.

NONLINEAR SYSTEMS

Identification of Unknown Inputs in Nonlinear Systems Based on Interval Methods

A. N. Zhirabok[*,**,a], **A. V. Zuev**[*,**,b], **V. F. Filaretov**[***,c], **I. V. Gornostaev**[**,d], **D. V. Kvasov**[**,e], **and D. D. Danilov**[**,f]

[*] *Far Eastern Federal University, Vladivostok, Russia*
[**] *Institute of Marine Technology Problems, Far Eastern Branch, Russian Academy of Sciences, Vladivostok, Russia*
[***] *Institute of Automation and Control Processes, Far Eastern Branch, Russian Academy of Sciences, Vladivostok, Russia*
e-mail: [a] *zhirabok@mail.ru*, [b] *alvzuev@yandex.ru*, [c] *filaretov@inbox.ru*, [d] *gornostaev_iv@mail.ru*, [e] *kvasov.dv@dvfu.ru*, [f] *danilov.dd@dvfu.ru*

Received September 9, 2025
Revised December 17, 2025
Accepted December 29, 2025

Abstract—This paper considers the problem of estimating (identifying) the magnitude of unknown inputs in engineering systems described by nonlinear dynamic models with measurement noises, which is necessary to compensate for the effect of such inputs. The solution of the problem is based on minimal-order interval observers, and their explicit relations are obtained. Such an observer and a differentiator are used to derive relations for an interval estimate of the magnitude of unknown inputs. The theoretical results are illustrated by a practical example of estimating the magnitude of unknown inputs on an electric drive of a manipulator robot. The simulations in MATLAB demonstrate the correctness of the theoretical results. The above relations can be used to design fault-tolerant systems.

Keywords: nonlinear systems, unknown inputs, identification, observers, interval methods

DOI: 10.7868/S1608303226080028

1. INTRODUCTION

During operation, engineering systems can be subjected to various unknown inputs. Different methods are used to compensate for them, and most of the methods employ information about the magnitudes of such inputs. Direct measurement of input magnitudes often encounters significant difficulties. In these cases, the problem can be solved based on known mathematical models of the systems and standard sensors, which provide the required information after appropriate processing.

There are various ways to process this information; approaches based on sliding mode observers are very popular, and the corresponding design methods were considered in [1–4] for different classes of systems. As a rule, certain constraints are imposed on the original system to construct sliding mode observers. In particular, it is required that the system be minimum phase or detectable, and a matching condition must hold. Furthermore, such observers are sensitive to perturbations.

An interesting method was proposed in [4]: the so-called interval observers are used to generate interval estimates of the desired functions. The design problem of such observers has been actively researched over the past 20 years; solutions for various classes of systems and examples of practical applications can be found in [5–9]. Note that in [4], the solution of the estimation problem was obtained by imposing the minimum-phase condition on the original linear system. Moreover, the author of [4] neglected measurement noises, which are always present in real systems.

In this paper, we pose and solve the following problem: using interval observers, it is required to estimate the magnitudes of unknown inputs in nonlinear continuous-time dynamic systems with measurement noises and without the minimum-phase condition. A similar problem was addressed in [9] for discrete-time nonlinear systems; the solution for continuous-time systems is significantly different. By analogy with [9], the solution provided below involves a reduced-order model of the original system. This approach simplifies the interval observer design, reduces the interval width, and allows one to account for measurement noises. In this case, the minimum-phase requirement is not used, and the transformations are limited to reducing the model to canonical form.

The objective of this work is to construct interval estimators for the magnitudes of unknown inputs in engineering systems described by nonlinear dynamic models with measurement noises.

Consider systems described by a nonlinear model of the form

$$\begin{aligned}\dot{x}(t) &= Fx(t) + Gu(t) + C\Psi(x(t), u(t)) + L\rho(t),\\ y(t) &= Hx(t) + w(t)\end{aligned} \tag{1.1}$$

with the following notation: $x(t) \in \mathbb{R}^n$, $u(t) \in \mathbb{R}^m$, and $y(t) \in \mathbb{R}^l$ are the state, control, and output vectors, respectively; F, G, C, H, and L are constant matrices of dimensions $n \times n$, $n \times m$, $n \times q$, $l \times n$, and $n \times 1$, respectively; $w(t) \in \mathbb{R}^l$ is measurement noises, $\rho(t) \in \mathbb{R}$ is an unknown time-varying function describing system inputs. By assumption, $w(t)$ and $\rho(t)$ are bounded functions: $\underline{w} \leqslant w(t) \leqslant \overline{w}$ and $\underline{\rho} \leqslant \rho(t) \leqslant \overline{\rho}$ for all $t \geqslant 0$, where $\underline{w}$, $\overline{w}$, $\underline{\rho}$, and $\overline{\rho}$ are known. For vectors, the inequality sign $\leqslant$ is understood elementwise. Also, the initial state $x(0)$ is assumed to satisfy $\underline{x}(0) \leqslant x(0) \leqslant \overline{x}(0)$ for some $\underline{x}(0)$ and $\overline{x}(0)$. The nonlinear term $\Psi(x, u)$ has the form

$$\Psi(x, u) = \begin{pmatrix} \varphi_1(A_1 x, u) \\ \dots \\ \varphi_q(A_q x, u) \end{pmatrix},$$

where $A_1, \dots, A_q$ are known constant row matrices, and $\varphi_1, \dots, \varphi_q$ are arbitrary nonlinear functions.

It is required to construct an interval observer for estimating the function $\rho(t)$. The bounds $\underline{\rho}$ and $\overline{\rho}$ are treated as preliminary and will be refined during the problem solution. Similar to [3, 9], this problem is solved based on an input-insensitive reduced-order model of the original system. Such a model has a smaller dimension than the original system, which decreases computational complexity. By analogy with [4], we assume the matching condition $\operatorname{rank}(HL) = \operatorname{rank}(L)$: roughly speaking, the function $\rho(t)$ enters the equations for the state vector components that are measured by the system's sensors.

First, the linear case is considered: $C = 0$.

2. BUILDING THE REDUCED-ORDER MODEL

2.1. General Relations

The reduced-order model mentioned above has the form

$$\begin{aligned}\dot{x}_*(t) &= F_* x_*(t) + G_* u(t) + J_* Hx(t) + L_* \rho(t),\\ y_*(t) &= H_* x_*(t),\end{aligned} \tag{2.1}$$

where $x_*(t) \in \mathbb{R}^k$ is the state vector; $y_*(t) \in \mathbb{R}$ is the output; and F_*, G_*, J_*, and L_* are matrices of compatible dimensions to be determined. The term $J_* Hx(t)$ is introduced instead of the expected $J_* y(t)$ to account for measurement noises; it will appear as $J_* y(t)$ in the interval observer.

To design an interval observer, the matrix F_* is required to be stable and Metzler, i.e., have nonnegative off-diagonal elements. Therefore, F_* is specified in the diagonal Jordan form

$$F_* = \begin{pmatrix} \lambda_1 & 0 & 0 & \dots & 0 \\ 0 & \lambda_2 & 0 & \dots & 0 \\ \dots & \dots & \dots & \dots & \dots \\ 0 & 0 & 0 & \dots & \lambda_k \end{pmatrix},$$

which possesses these properties if the eigenvalues $\lambda_1, \dots, \lambda_k$ are chosen negative.

As is known [10], an observable system (2.1) can always be written with

$$F_* = \begin{pmatrix} 0 & 1 & 0 & \dots & 0 \\ 0 & 0 & 1 & \dots & 0 \\ \dots & \dots & \dots & \dots & 0 \\ 0 & 0 & 0 & \dots & 0 \end{pmatrix}$$

(the identification canonical form). Otherwise, it can be reduced to another system with an observable subsystem [10], and the latter's matrix can be written in the identification canonical form. One can always pass to the Jordan form from the identification form by introducing feedback with an appropriate gain matrix [11].

To build the reduced-order model, we assume the existence of a matrix Φ such that $x_*(t) = \Phi x(t)$ for all $t \geqslant 0$. According to [9], this matrix and those describing the model satisfy the equations

$$\Phi F = F_* \Phi + J_* H, \quad \Phi G = G_*, \quad \Phi L = L_*.$$

For the adopted form of F_*, the first equation above splits into k independent equations:

$$\Phi_i F = \lambda_i \Phi_i + J_{*i} H, \quad i = 1, \dots, k. \tag{2.2}$$

Each of them can be written as

$$(\Phi_i \quad -J_{*i}) \begin{pmatrix} F - \lambda_i I_n \\ H \end{pmatrix} = 0, \quad i = 1, \dots, k, \tag{2.3}$$

where I_n denotes an identity matrix of dimensions $n \times n$. To build the reduced-order model, an appropriate value $\lambda_i < 0$ is chosen so that the matrix Φ_i determined from (2.3) satisfies the two requirements

$$\Phi_i L = L_* \neq 0, \quad R_i H = \Phi_i \tag{2.4}$$

for some matrix R_i, with $H_* = 1$. To account for the second requirement, let us replace Φ_i in (2.2) with $R_i H$,

$$R_i H F = \lambda R_i H + J_{*i} H,$$

and rewrite the resulting equation as

$$(R_i \quad -J_{*i}) \begin{pmatrix} HF - \lambda_i H \\ H \end{pmatrix} = 0, \quad i = 1, \dots, k.$$

By analogy with the solution of (2.3), a value $\lambda_i < 0$ is chosen so that the matrix R_i determined from the above equation satisfies the condition $L_* = R_i H L \neq 0$. If this condition holds, $G_* = R_i H G$ is determined, and the linear model is successfully built. Otherwise, the problem has no solution by the current method.

2.2. Use of Virtual Sensors

The mutual independence of equations (2.2) restricts the solvability of the problem. Indeed, consider an example of an electric drive described by the equations

$$\begin{aligned}\dot{x}_1(t) &= k_1 x_2(t),\\ \dot{x}_2(t) &= k_2 x_2(t) + k_3 x_3(t) + k_7 \operatorname{sgn}(x_2(t)),\\ \dot{x}_3(t) &= k_4 x_2(t) + k_5 x_3(t) + k_6 u(t) + \rho(t).\end{aligned} \tag{2.5}$$

Here, the coefficients k_1–k_7 represent the parameters of the electric drive; and the unknown input $\rho(t)$ is due to changes in the armature winding resistance during overheating. The model under consideration is described by the matrices

$$F = \begin{pmatrix} 0 & k_1 & 0 \\ 0 & k_2 & k_3 \\ 0 & k_4 & k_5 \end{pmatrix}, \quad G = \begin{pmatrix} 0 \\ 0 \\ k_6 \end{pmatrix}, \quad C = \begin{pmatrix} 0 \\ k_7 \\ 0 \end{pmatrix}, \quad L = \begin{pmatrix} 0 \\ 0 \\ 1 \end{pmatrix}.$$

By assumption, $y(t) = x_3(t) + w(t)$, i.e., $H = (\,0 \;\; 0 \;\; 1\,)$. It is required to estimate the function $\rho(t)$.

Equation (2.3) takes the form

$$(\Phi \quad -J_*)\begin{pmatrix} -\lambda & k_1 & 0 \\ 0 & k_2-\lambda & k_3 \\ 0 & k_4 & k_5-\lambda \\ 0 & 0 & 1 \end{pmatrix} = 0.$$

Since $k_2 < 0$, it has a unique solution $\lambda = k_2$ with the matrix $\Phi_1 = (0 \;\; 1 \;\; 0)$, which violates conditions (2.4). One recipe is to use a so-called virtual sensor, i.e., an observer estimating the unmeasured component of the state vector of the original system. In the case under study, the reduced-order model for constructing such a sensor is a special case of the general model (2.1) described by the equation

$$\dot{x}_{*1}(t) = k_2 x_{*1}(t) + k_3 Hx(t) + k_7 \operatorname{sgn}(x_{*1}(t)),$$

where $x_{*1}(t) = \Phi_1 x(t)$. Note that since the measurement $y(t)$ is noisy, the readings of this sensor will include noises as well; this aspect will be considered below by interval methods. Taking the state $x_{*1}(t)$ as the readings of such a sensor $y_v(t) = H_v x(t)$ with $H_v = (0 \;\; 1 \;\; 0)$, we extend equation (2.2):

$$\Phi_i F = \lambda_i \Phi_i + J_{*i} H + J_{*v} H_v, \quad i = 1, \ldots, k;$$

in the case under consideration, it takes the form

$$(\Phi \quad -J_* \quad -J_{*v})\begin{pmatrix} -\lambda & k_1 & 0 \\ 0 & k_2-\lambda & k_3 \\ 0 & k_4 & k_5-\lambda \\ 0 & 0 & 1 \\ 0 & 1 & 0 \end{pmatrix} = 0.$$

Now it has another solution $\lambda = k_5 < 0$ with the matrices $\Phi_2 = (0 \;\; 0 \;\; 1)$ and $(J_* \;\; J_{*v}) = (0 \;\; 1)$; the first satisfies conditions (2.3) with $R = 1$ and $L_* = 1$. The model with the virtual sensor is described by the equations

$$\begin{aligned}\dot{x}_{*1}(t) &= k_2 x_{*1}(t) + k_3 Hx(t) + k_7 \operatorname{sgn}(x_{*1}(t)),\\ \dot{x}_{*2}(t) &= k_5 x_{*2}(t) + k_4 x_{*1}(t) + k_6 u(t) + \rho(t),\\ y_*(t) &= x_{*2}(t) = y(t).\end{aligned} \tag{2.6}$$

In general, there can be several virtual sensors.

2.3. Obtaining the Interval Estimate

We begin with the case where a virtual sensor is not required. Then, for the chosen value λ, model (2.1) becomes one-dimensional:

$$\begin{aligned}\dot{x}_*(t) &= \lambda x_*(t) + G_* u(t) + J_* H x(t) + L_* \rho(t),\\ y_*(t) &= x_*(t).\end{aligned} \tag{2.7}$$

Obviously, if the measurement noises are absent or can be neglected, then, taking the equalities $y_*(t) = x_*(t) = Ry(t)$ and $J_* H x(t) = J_* y(t)$ into account, the input $\rho(t)$ can be estimated as

$$\hat{\rho}(t) = L_*^{-1}(\dot{y}_*(t) - (\lambda y_*(t) + G_* u(t) + J_* y(t))). \tag{2.8}$$

To compute the derivative $\dot{y}_*(t)$, we apply the differentiator proposed in [12]:

$$\begin{aligned}\dot{z}_1(t) &= z_0(t),\\ z_0(t) &= z_2(t) - \alpha_1 |z_1(t) - y_*(t)|^{1/2} \operatorname{sgn}(z_1(t) - y_*(t)),\\ \dot{z}_2(t) &= -\alpha_2 \operatorname{sgn}(z_1(t) - y_*(t)),\end{aligned}$$

where α_1 and α_2 are positive constants chosen according to the recommendations in [12]. As shown therein, $z_2(t)$ provides an exact estimate of $\dot{y}_*(t)$ in finite time under no unknown inputs in $y_*(t)$. If the function $y_*(t)$ is subjected to noises of intensity $w_y(t)$, then $|\dot{y}_*(t) - z_2(t)| \leqslant |w_y(t)|^{1/2}$.

If the function $\rho(t)$ represents a vector, the described approach should be applied to each of its components. By analogy with [4], the estimate $\hat{\rho}(t)$ can be used to estimate the full state vector $x(t)$ of the original system based on the equation

$$\dot{\hat{x}}(t) = F\hat{x}(t) + Gu(t) + L\hat{\rho}(t) + K(y(t) - H\hat{x}(t)),$$

where the gain K is chosen to ensure the stability of the matrix $F - KH$.

Note that for linear systems, a similar problem was considered in [4]; in contrast to the simple relations (2.7) and (2.8), it was solved using complex analytical transformations of the original system and interval observers, which are unnecessary here.

If the original system is nonlinear, then an additional term $\Psi_{**}(y_*, y, u)$ is incorporated into (2.7) (see the details below), and the estimate (2.8) takes the form

$$\hat{\rho}(t) = L_*^{-1}(\dot{y}_*(t) - (\lambda y_*(t) + G_* u(t) + J_* y(t) + \Psi_{**}(y_*, y, u))). \tag{2.9}$$

With a virtual sensor described by the equation

$$\begin{aligned}\dot{x}_v(t) &= \lambda_v x_v(t) + G_v u(t) + J_v y(t),\\ y_v(t) &= x_v(t)\end{aligned} \tag{2.10}$$

(by assumption, without $\rho(t)$), the expression (2.8) gets complicated:

$$\hat{\rho}(t) = L_*^{-1}(\dot{y}_*(t) - (\lambda y_*(t) + G_* u(t) + J_* y(t) + J_{*v} y_v(t))). \tag{2.11}$$

The presence of measurement noise makes the estimates (2.8) and (2.9) approximate. In this case, the use of an interval observer allows finding guaranteed limits (bounds) of the estimate, by analogy with confidence intervals in mathematical statistics. By assumption, the lower $\underline{\rho}$ and upper $\overline{\rho}$ bounds of the function $\rho(t)$ introduced previously are a first approximation, which will be refined later.

3. INTERVAL OBSERVER AND ITS USE

We begin with the case where a virtual sensor is not required. By analogy with [5, 9], the interval observer based on model (2.1) takes the form

$$\begin{aligned} \dot{\underline{y}}_*(t) &= \lambda \underline{y}_*(t) + G_* u(t) + J_* y(t) + J_*^- \underline{w} - J_*^+ \overline{w} + L_*^+ \underline{\rho} - L_*^- \overline{\rho}, \\ \dot{\overline{y}}_*(t) &= \lambda \overline{y}_*(t) + G_* u(t) + J_* y(t) + J_*^- \overline{w} - J_*^+ \underline{w} + L_*^+ \overline{\rho} - L_*^- \underline{\rho}, \end{aligned} \tag{3.1}$$

where $Q^+ = \max\{0, Q\}$ and $Q^- = Q^+ - Q$ for an arbitrary matrix Q; obviously, Q^+ and Q^- are nonnegative.

Similar to [5, 9], it can be shown that the condition $\overline{x}(0) \geqslant x(0) \geqslant \underline{x}(0)$ implies $\overline{y}_*(t) \geqslant y_*(t) \geqslant \underline{y}_*(t)$ for all $t \geqslant 0$. By analogy with [4], in this case, there exists a variable $0 \leqslant \beta(t) \leqslant 1$ such that

$$y_*(t) = \underline{y}_*(t) + \beta(t)(\overline{y}_*(t) - \underline{y}_*(t)) = \overline{y}_*(t) + (\beta(t) - 1)(\overline{y}_*(t) - \underline{y}_*(t)) \tag{3.2}$$

for all $t \geqslant 0$. Replacing $y_*(t)$ with $Ry(t)$ yields

$$\beta(t) = \frac{Ry(t) - \underline{y}_*(t)}{\overline{y}_*(t) - \underline{y}_*(t)}, \tag{3.3}$$

where all variables can be determined. By assumption, the function $\beta(t)$ is differentiable.

Theorem 1. *The refined upper $\overline{\overline{\rho}}(t)$ and lower $\underline{\underline{\rho}}(t)$ bounds for $\rho(t)$ are given by*

$$\overline{\overline{\rho}}(t) = L_*^{-1}(\dot{\beta}(t)(\overline{y}_*(t) - \underline{y}_*(t)) + L_*^+ \underline{\rho} - L_*^- \overline{\rho} + \beta(t)(|L_*|(\overline{\rho} - \underline{\rho}) + |J_*|(\overline{w} - \underline{w}))) \tag{3.4}$$

and

$$\underline{\underline{\rho}}(t) = L_*^{-1}(\dot{\beta}(t)(\overline{y}_*(t) - \underline{y}_*(t)) + L_*^+ \overline{\rho} - L_*^- \underline{\rho} + (\beta(t) - 1)(|L_*|(\overline{\rho} - \underline{\rho}) + |J_*|(\overline{w} - \underline{w}))), \tag{3.5}$$

respectively.

Proof. We compute $\dot{y}_*(t)$ based on the first part of equality (3.2) and equation (3.1):

$$\begin{aligned} \dot{y}_*(t) &= \dot{\underline{y}}_*(t) + \dot{\beta}(t)(\overline{y}_*(t) - \underline{y}_*(t)) + \beta(t)\frac{d}{dt}(\overline{y}_*(t) - \underline{y}_*(t)) \\ &= \lambda \underline{y}_*(t) + G_* u(t) + J_* y(t) + J_*^- \underline{w} - J_*^+ \overline{w} + L_*^+ \underline{\rho} - L_*^- \overline{\rho} \\ &\quad + \dot{\beta}(t)(\overline{y}_*(t) - \underline{y}_*(t)) + \lambda \beta(t)(\overline{y}_*(t) - \underline{y}_*(t)) \\ &\quad + \beta(t)(|L_*|(\overline{\rho} - \underline{\rho}) + |J_*|(\overline{w} - \underline{w})), \end{aligned}$$

where the matrix $|Q| = Q^+ + Q^-$ is composed of the absolute values of the elements of the matrix Q. Let the variable $\dot{y}_*(t)$ in this expression be replaced by the right-hand side of equality (2.7):

$$\begin{aligned} &\lambda y_*(t) + G_* u(t) + J_* H x(t) + L_* \rho(t) \\ &= \lambda \underline{y}_*(t) + G_* u(t) + J_* y(t) + J_*^- \underline{w} - J_*^+ \overline{w} + L_*^+ \underline{\rho} - L_*^- \overline{\rho} \\ &\quad + \dot{\beta}(t)(\overline{y}_*(t) - \underline{y}_*(t)) + \lambda \beta(t)(\overline{y}_*(t) - \underline{y}_*(t)) \\ &\quad + \beta(t)(|L_*|(\overline{\rho} - \underline{\rho}) + |J_*|(\overline{w} - \underline{w})). \end{aligned}$$

After straightforward transformations, we have

$$\begin{aligned} L_* \rho(t) &= \lambda(\underline{y}_*(t) - y_*(t)) + J_* w(t) + J_*^- \underline{w} - J_*^+ \overline{w} + L_*^+ \underline{\rho} - L_*^- \overline{\rho} \\ &\quad + \dot{\beta}(t)(\overline{y}_*(t) - \underline{y}_*(t)) + \lambda \beta(t)(\overline{y}_*(t) - \underline{y}_*(t)) \\ &\quad + \beta(t)(|L_*|(\overline{\rho} - \underline{\rho}) + |J_*|(\overline{w} - \underline{w})) \\ &= \dot{\beta}(t)(\overline{y}_*(t) - \underline{y}_*(t)) + \beta(t)(|L_*|(\overline{\rho} - \underline{\rho}) + |J_*|(\overline{w} - \underline{w})) \\ &\quad + J_* w(t) + J_*^- \underline{w} - J_*^+ \overline{w} + L_*^+ \underline{\rho} - L_*^- \overline{\rho}. \end{aligned}$$

Since

$$J_*w(t) + J_*^-\underline{w} - J_*^+\overline{w} = J_*^+w(t) - J_*^-w(t) + J_*^-\underline{w} - J_*^+\overline{w}$$
$$= J_*^+(w(t) - \overline{w}) + J_*^-(\underline{w} - w(t)) \leqslant 0,$$

the bound (3.4) is obtained by removing the term $J_*w(t) + J_*^-\underline{w} - J_*^+\overline{w}$ from the last expression.

Similar operations with the second part of equality (3.2) give

$$\begin{aligned}\dot{y}_*(t) &= \dot{\overline{y}}_*(t) + \dot{\beta}(t)(\overline{y}_*(t) - \underline{y}_*(t)) + (\beta(t) - 1)\tfrac{d}{dt}(\overline{y}_*(t) - \underline{y}_*(t))\\ &= \lambda\overline{y}_*(t) + G_*u(t) + J_*y(t) + J_*^-\overline{w} - J_*^+\underline{w} + L_*^+\overline{\rho} - L_*^-\underline{\rho}\\ &\quad + \dot{\beta}(t)(\overline{y}_*(t) - \underline{y}_*(t)) + \lambda\beta(t)(\overline{y}_*(t) - \underline{y}_*(t))\\ &\quad - \lambda(\overline{y}_*(t) - \underline{y}_*(t)) + (\beta(t) - 1)(|L_*|(\overline{\rho} - \underline{\rho}) + |J_*|(\overline{w} - \underline{w}));\end{aligned}$$

the replacement of $\dot{y}_*(t)$ and analogous transformations lead to

$$\begin{aligned}L_*\rho(t) &= \dot{\beta}(t)(\overline{y}_*(t) - \underline{y}_*(t)) + (\beta(t) - 1)(|L_*|(\overline{\rho} - \underline{\rho}) + |J_*|(\overline{w} - \underline{w}))\\ &\quad + J_*w(t) + J_*^-\overline{w} - J_*^+\underline{w} + L_*^+\overline{\rho} - L_*^-\underline{\rho}.\end{aligned}$$

Since $J_*w(t) + J_*^-\overline{w} - J_*^+\underline{w} \geqslant 0$, we remove this term to obtain the bound (3.5). Clearly,

$$\underline{\underline{\rho}}(t) \leqslant \rho(t) \leqslant \overline{\overline{\rho}}(t),$$

and the proof of Theorem 1 is complete.

To compute the derivative $\dot{\beta}(t)$, the above differentiator can be used:

$$\begin{aligned}\dot{z}_1(t) &= z_0(t),\\ z_0(t) &= z_2(t) - \gamma_1|z_1(t) - \beta(t)|^{1/2}\,\mathrm{sgn}(z_1(t) - \beta(t)),\\ \dot{z}_2(t) &= -\gamma_2\,\mathrm{sgn}(z_1(t) - \beta(t)),\end{aligned} \tag{3.6}$$

where γ_1 and γ_2 are positive constants; the variable $z_2(t)$ provides the exact estimate of the function $\dot{\beta}(t)$ in finite time under no unknown inputs in $\beta(t)$.

If a virtual sensor (2.10) is required, it must be implemented in interval form as well:

$$\begin{aligned}\dot{\underline{x}}_v(t) &= \lambda_v\underline{x}_v(t) + G_vu(t) + J_vy(t) + J_v^-\underline{w} - J_v^+\overline{w},\\ \dot{\overline{x}}_v(t) &= \lambda_v\overline{x}_v(t) + G_vu(t) + J_vy(t) + J_v^-\overline{w} - J_v^+\underline{w},\\ \underline{y}_v(t) &= \underline{x}_v(t),\\ \overline{y}_v(t) &= \overline{x}_v(t).\end{aligned}$$

The interval observer (3.1) is supplemented with the corresponding elements:

$$\begin{aligned}\dot{\underline{y}}_*(t) &= \lambda\underline{y}_*(t) + G_*u(t) + J_*y(t) + J_*^-\underline{w} - J_*^+\overline{w} + L_*^+\underline{\rho} - L_*^-\overline{\rho} + J_{*v}^+\underline{y}_v(t) - J_{*v}^-\overline{y}_v(t),\\ \dot{\overline{y}}_*(t) &= \lambda\overline{y}_*(t) + G_*u(t) + J_*y(t) + J_*^-\overline{w} - J_*^+\underline{w} + L_*^+\overline{\rho} - L_*^-\underline{\rho} + J_{*v}^+\overline{y}_v(t) - J_{*v}^-\underline{y}_v(t),\end{aligned}$$

and the upper bound $\overline{\overline{\rho}}(t)$ is refined to

$$\begin{aligned}\overline{\overline{\rho}}(t) &= L_*^{-1}(\dot{\beta}(t)(\overline{y}_*(t) - \underline{y}_*(t)) + L_*^+\underline{\rho} - L_*^-\overline{\rho}\\ &\quad + \beta(t)(|L_*|(\overline{\rho} - \underline{\rho}) + |J_*|(\overline{w} - \underline{w}) + |J_{*v}|(\overline{y}_v(t) - \underline{y}_v(t)))).\end{aligned}$$

The lower bound is refined by analogy.

4. NONLINEAR SYSTEMS

In the nonlinear case, the reduced-order model is built using the linear model obtained previously: for the matrix Φ, it is necessary to verify the possibility of transforming the argument of the nonlinear term $\Psi(x, u)$ based on the following operations [3]. For simplicity, we restrict the considerations to the case of no virtual sensor; if such a sensor is needed and contains a nonlinear component, the model can be built by analogy.

The matrix $C_* = \Phi C$ is computed, and the serial numbers $j_i, \ldots, j_s$ of its nonzero columns are determined. Next, it is necessary to check the condition

$$\operatorname{rank}\begin{pmatrix}\Phi\\ H\end{pmatrix} = \operatorname{rank}\begin{pmatrix}\Phi\\ H\\ A_j\end{pmatrix}, \quad j = j_i, \ldots, j_s. \tag{4.1}$$

If this condition holds, then the nonlinear component is sought in the form

$$\Psi_*(y_*, Hx, u) = \begin{pmatrix}\varphi_{j_1}(A_{*j_1}\xi, u)\\ \ldots\\ \varphi_{j_s}(A_{*j_s}\xi, u)\end{pmatrix},$$

where $\xi = \begin{pmatrix} y_* \\ Hx \end{pmatrix}$, the matrices $A_{*j_1}, \ldots, A_{*j_s}$ are determined from the linear equations

$$A_j = A_{*j}\begin{pmatrix}\Phi\\ H\end{pmatrix}, \quad j = j_i, \ldots, j_s,$$

and the component $C_*\Psi_*(y_*, Hx, u)$ is added to the linear model (2.1). If condition (4.1) fails, it is necessary to find another solution of equation (2.3) and repeat the above procedure with a new matrix Φ of the same or increased dimension k. If (4.1) does not hold for all k, a virtual sensor should be added to satisfy condition (4.1).

The nonlinear model is described by the equation

$$\begin{aligned}&\dot{x}_*(t) = x_*(t) + J_*Hx(t) + G_*u(t) + C_*\Psi_*(y_*(t), Hx(t), u(t)) + L_*\rho(t),\\ &y_*(t) = x_*(t).\end{aligned}$$

If measurement noises are absent or negligible, then the estimate is given by the expression (2.9). Otherwise, an interval observer is designed under the following assumption for $\Psi_{**}(y_*, Hx, u) = C_*\Psi_*(y_*, Hx, u)$.

Assumption. If $\underline{w} \leqslant w(t) \leqslant \overline{w}$ for $\underline{w}$, $\overline{w} \in \mathbb{R}^l$, then

$$\underline{\Psi}_{**}(y_*, \underline{y}, \overline{y}, u) \leqslant \Psi_{**}(y_*, Hx, u) \leqslant \overline{\Psi}_{**}(y_*, \underline{y}, \overline{y}, u) \tag{4.2}$$

for some functions $\underline{\Psi}_{**}(y_*, \underline{y}, \overline{y}, u)$ and $\overline{\Psi}_{**}(y_*, \underline{y}, \overline{y}, u)$ and all u, where $\underline{y} = y - \overline{w}$ and $\overline{y} = y - \underline{w}$. The assumption itself is valid for arbitrary functions, but according to [13, 14], the procedure for computing the bounds $\underline{\Psi}_{**}(y_*, \underline{y}, \overline{y}, u)$ and $\overline{\Psi}_{**}(y_*, \underline{y}, \overline{y}, u)$ is known only for a continuous function $\Psi_{**}(y_*, Hx, u)$; it involves methods of interval arithmetic. In special cases, however, condition (4.2) can be established heuristically; see an illustrative example below.

The interval observer takes the form

$$\begin{aligned}\dot{\underline{y}}_*(t) &= \lambda\underline{y}_*(t) + G_{*i}u(t) + J_*y(t) + J_*^-\underline{w} - J_*^+\overline{w}\\ &\quad + L_*^+\underline{\rho} - L_*^-\overline{\rho} + \underline{\Psi}_{**}(y_*(t), \underline{y}(t), \overline{y}(t), u(t)),\\ \dot{\overline{y}}_*(t) &= \lambda\overline{y}_*(t) + G_{*i}u(t) + J_*y(t) + J_*^-\overline{w} - J_*^+\underline{w}\\ &\quad + L_*^+\overline{\rho} - L_{*i}^-\underline{\rho} + \overline{\Psi}_{**}(y_*(t), \underline{y}(t), \overline{y}(t), u(t)).\end{aligned}$$

Theorem 2. *The refined upper* $\overline{\overline{\rho}}(t)$ *and lower* $\underline{\underline{\rho}}(t)$ *bounds without using a virtual sensor are given by*

$$\begin{aligned}
\overline{\overline{\rho}}(t) &= L_*^{-1}\Big(\dot{\beta}(t)(\overline{y}_*(t) - \underline{y}_*(t)) + L_*^{+}\underline{\rho} - L_*^{-}\overline{\rho} \\
&\quad + \beta(t)(|L_*|(\overline{\rho} - \underline{\rho}) + |J_*|(\overline{w} - \underline{w}) + \overline{\Psi}_{**}(y_*(t), \underline{y}(t), \overline{y}(t), u(t)) \\
&\quad - \underline{\Psi}_{**}(y_*(t), \underline{y}(t), \overline{y}(t), u(t)))\Big), \\
\underline{\underline{\rho}}(t) &= L_*^{-1}\Big(\dot{\beta}(t)(\overline{y}_*(t) - \underline{y}_*(t)) + L_*^{+}\overline{\rho} - L_*^{-}\underline{\rho} + (\beta(t) - 1)(|L_*|(\overline{\rho} - \underline{\rho}) \\
&\quad + |J_*|(\overline{w} - \underline{w}) + \overline{\Psi}_{**}(y_*(t), \underline{y}(t), \overline{y}(t), u(t)) \\
&\quad - \underline{\Psi}_{**}(y_*(t), \underline{y}(t), \overline{y}(t), u(t)))\Big).
\end{aligned} \tag{4.3}$$

Proof. In view of the nonlinear term, the estimate (3.4) takes the form

$$\begin{aligned}
\overline{\overline{\rho}}(t) = {} & L_*^{-1}(\dot{\beta}(t)(\overline{y}_*(t) - \underline{y}_*(t)) + L_*^{+}\underline{\rho} - L_*^{-}\overline{\rho} + \beta(t)(|L_*|(\overline{\rho} - \underline{\rho}) + |J_*|(\overline{w} - \underline{w}) \\
& + \overline{\Psi}_{**}(y_*(t), \underline{y}(t), \overline{y}(t), u(t)) - \underline{\Psi}_{**}(y_*(t), \underline{y}(t), \overline{y}(t), u(t)))) \\
& + \underline{\Psi}_{**}(y_*(t), \underline{y}(t), \overline{y}(t), u(t)) - \Psi_{**}(y_*, Hx, u).
\end{aligned}$$

Due to (4.2), the difference $\underline{\Psi}_{**}(y_*(t), \underline{y}(t), \overline{y}(t), u(t)) - \Psi_{**}(y_*, Hx, u)$ is negative; then, by removing it from the last expression, we obtain the first of formulas (4.3). Similarly, the estimate (3.5) takes the form

$$\begin{aligned}
\underline{\underline{\rho}}(t) = {} & L_*^{-1}(\dot{\beta}(t)(\overline{y}_*(t) - \underline{y}_*(t)) + L_*^{+}\overline{\rho} - L_*^{-}\underline{\rho} + (\beta(t) - 1)(|L_*|(\overline{\rho} - \underline{\rho}) + |J_*|(\overline{w} - \underline{w}) \\
& + \overline{\Psi}_{**}(y_*(t), \underline{y}(t), \overline{y}(t), u(t)) - \underline{\Psi}_{**}(y_*(t), \underline{y}(t), \overline{y}(t), u(t)))) \\
& + \overline{\Psi}_{**}(y_*(t), \underline{y}(t), \overline{y}(t), u(t)) - \Psi_{**}(y_*, Hx, u).
\end{aligned}$$

According to (4.2), $\overline{\Psi}_{**}(y_*(t), \underline{y}(t), \overline{y}(t), u(t)) - \Psi_{**}(y_*, Hx, u) \geqslant 0$, and, by removing this difference, we obtain the second formula in (4.3). The proof of Theorem 2 is complete.

The nonlinearity entering the virtual sensor can be considered by analogy, i.e., using a corresponding assumption of the form (4.2).

5. EXAMPLE

We continue the analysis of system (2.5), for which model (2.6) has been constructed in the form

$$\begin{aligned}
\dot{x}_{*1}(t) &= k_2 x_{*1}(t) + k_3 Hx(t) + k_7 \operatorname{sgn}(x_{*1}(t)), \\
\dot{x}_{*2}(t) &= k_5 x_{*2}(t) + k_4 x_{*1}(t) + k_6 u(t) + \rho(t), \\
y_*(t) &= x_{*2}(t) = y(t).
\end{aligned} \tag{5.1}$$

Since $k_4 < 0$, $k_3 > 0$, and $k_7 < 0$, we have $k_3^+ = k_3$, $k_3^- = 0$, $k_4^+ = 0$, $k_4^- = |k_4|$, $k_7^+ = 0$, $k_7^- = |k_7|$, and $L_* = 1$.

In the absence of measurement noises, the exact estimate of the input $\rho(t)$ is given by the expression (2.11):

$$\hat{\rho}(t) = \dot{y}(t) - (k_5 y(t) + k_6 u(t) + k_4 x_{*1}(t)),$$

and the virtual sensor is given by the first equation in (5.1) with $Hx(t) = y(t)$. In the presence of noises, it is necessary to construct the interval observer (3.1); together with the virtual sensor, it takes the form

$$\begin{aligned}
\dot{\underline{x}}_{*1}(t) &= k_2 \underline{x}_{*1}(t) + k_3 y(t) - k_3 \overline{w} - |k_7| \operatorname{sgn}(\overline{x}_{*1}(t)), \\
\dot{\overline{x}}_{*1}(t) &= k_2 \overline{x}_{*1}(t) + k_3 y(t) - k_3 \underline{w} - |k_7| \operatorname{sgn}(\underline{x}_{*1}(t)), \\
\dot{\underline{y}}_*(t) &= k_5 \underline{y}_*(t) + k_6 u(t) - |k_4| \overline{x}_{*1}(t) + \underline{\rho}, \\
\dot{\overline{y}}_*(t) &= k_5 \overline{y}_*(t) + k_6 u(t) - |k_4| \underline{x}_{*1}(t) + \overline{\rho}.
\end{aligned} \tag{5.2}$$

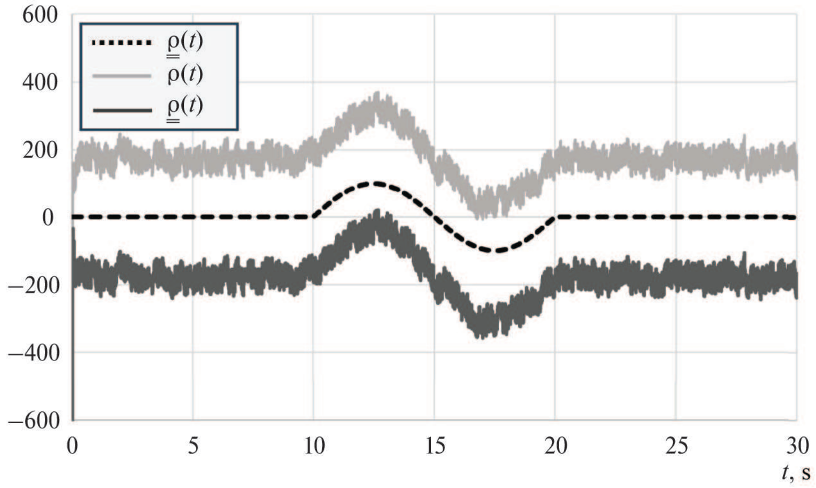

Fig. 1. The unknown input and its lower and upper bounds as functions of time.

Let us introduce the error $\underline{e}_1(t) = x_{*1}(t) - \underline{x}_{*1}(t)$. Obviously, $\underline{x}(0) \leqslant x(0) \leqslant \overline{x}(0)$ and $x_{*1}(t) = \Phi x(t)$ imply $\underline{x}_{*1}(0) \leqslant x_{*1}(0) \leqslant \overline{x}_{*1}(0)$ and $\underline{e}_1(0) \geqslant 0$. Further, if $\underline{x}_{*1}(t) \leqslant x_{*1}(t) \leqslant \overline{x}_{*1}(t)$, then $\operatorname{sgn}(\underline{x}_{*1}(t)) \leqslant \operatorname{sgn}(x_{*1}(t)) \leqslant \operatorname{sgn}(\overline{x}_{*1}(t))$, and since $k_7 < 0$, we have

$$-|k_7| \operatorname{sgn}(\underline{x}_{*1}(t)) \geqslant k_7 \operatorname{sgn}(x_{*1}(t)) \geqslant -|k_7| \operatorname{sgn}(\overline{x}_{*1}(t)).$$

In other words, $k_7 \operatorname{sgn}(x_{*1}(t))$ satisfies an assumption of the form (4.2) with the functions

$$\underline{\Psi}_{**}(\underline{x}_{*1}, \overline{x}_{*1}) = -|k_7| \operatorname{sgn}(\overline{x}_{*1}), \quad \overline{\Psi}_{**}(\underline{x}_{*1}, \overline{x}_{*1}) = -|k_7| \operatorname{sgn}(\underline{x}_{*1}).$$

The error $\underline{e}_1(t)$ satisfies the equation

$$\dot{\underline{e}}_1(t) = k_2 \underline{e}_1(t) - k_3 w(t) + k_3 \overline{w} + k_7 \operatorname{sgn}(x_{*1}(t)) + |k_7| \operatorname{sgn}(\overline{x}_{*1}(t)).$$

In view of $k_2 < 0$, $\underline{e}_1(0) \geqslant 0$, and $-k_3 w(t) + k_3 \overline{w} + k_7 \operatorname{sgn}(x_{*1}(t)) + k_7 \operatorname{sgn}(x_{*1}(t)) \geqslant 0$, according to [13], by induction we obtain $\underline{e}_1(t) \geqslant 0$, i.e., $x_{*1}(t) \geqslant \underline{x}_{*1}(t)$ for all $t \geqslant 0$. Similar operations can be used to prove the inequality $\overline{x}_{*1}(t) \geqslant x_{*1}(t)$ for all $t \geqslant 0$.

By analogy, based on the above relations and the third and fourth equations in (5.2), it can be shown that $\overline{y}_*(t) \geqslant y_*(t) \geqslant \underline{y}_*(t)$ for all $t \geqslant 0$; and the function $\beta(t)$ can be determined in the form (3.3).

The refined lower $\underline{\underline{\rho}}$ and upper $\overline{\overline{\rho}}$ bounds for $\rho(t)$ take the form

$$\begin{aligned}
\overline{\overline{\rho}} &= \dot{\beta}(t)(\overline{y}_*(t) - \underline{y}_*(t)) + \underline{\rho} + \beta(t)(\overline{\rho} - \underline{\rho} + |k_3|(\overline{w} - \underline{w}) \\
&\quad + |k_4|(\overline{x}_{*1}(t) - \underline{x}_{*1}(t)) - |k_7|(\operatorname{sgn}(\underline{x}_{*1}) - \operatorname{sgn}(\overline{x}_{*1}))), \\
\underline{\underline{\rho}} &= \dot{\beta}(t)(\overline{y}_*(t) - \underline{y}_*(t)) + \overline{\rho} + (\beta(t) - 1)(\overline{\rho} - \underline{\rho} + |k_3|(\overline{w} - \underline{w}) \\
&\quad + |k_4|(\overline{x}_{*1}(t) - \underline{x}_{*1}(t)) - |k_7|(\operatorname{sgn}(\underline{x}_{*1}) - \operatorname{sgn}(\overline{x}_{*1}))).
\end{aligned}$$

The derivative $\dot{\beta}(t)$ is computed by formula (3.6) with $Ry = y$.

The following model parameters were used for simulation: $k_1 = 0.01$, $k_2 = -10$, $k_3 = 100$, $k_4 = -25$, $k_5 = -100$, $k_6 = 1000$, and $k_7 = -0.02$; the measurement noise was represented by a random variable with the uniform distribution on the interval $[-0.3, 0.3]$, i.e., $\underline{w} = -0.3$ and $\overline{w} = 0.3$; the unknown input was specified as $\rho(t) = 100 \sin(\pi t/5)$ for $10 \leqslant t \leqslant 20$, and $\rho(t) = 0$ otherwise, hence $\underline{\rho} = -100$ and $\overline{\rho} = 100$. The simulation results with $u(t) = 2\sin(t/5) + 2$ are shown in the figure. Due to the presence of measurement noises, as well as the large value of the coefficient k_3, the refined bounds $\underline{\underline{\rho}}$ and $\overline{\overline{\rho}}$ are strongly noisy; and their average values are explained by the accepted preliminary values of the bounds $\underline{\rho}$ and $\overline{\rho}$.

6. CONCLUSIONS

In this paper, we have estimated (identified) the magnitudes of unknown inputs in systems described by nonlinear models with measurement noises. In contrast to known solution methods using sliding mode observers, the approach developed above expands the class of systems for which the identification procedure can be performed. The reason is that the design method for sliding mode observers restricts the systems for which unknown inputs need to be identified. Note also that unknown inputs can be interpreted as faults in system dynamics; therefore, the proposed methods are applicable to design fault-tolerant systems by compensating for the estimated fault effect by a control system.

FUNDING

This work was supported by the Russian Science Foundation, project no. 25-19-00590 (https://rscf.ru/project/25-19-00590/).

REFERENCES

1. Edwards, C., Spurgeon, S., and Patton, R., Sliding Mode Observers for Fault Detection and Isolation, *Automatica*, 2000, vol. 36, pp. 541–553.

2. Fridman, L., Levant, A., and Davila, J., Observation of Linear Systems with Unknown Inputs via High Order Sliding-Modes, *Int. J. Syst. Sci.*, 2007, vol. 38, pp. 773–791.

3. Zhirabok, A.N., Zuev, A.V., Sergiyenko, O., and Shumsky, A.E., Identification of Faults in Nonlinear Dynamical Systems and Their Sensors Based on Sliding Mode Observers, *Autom. Remote Control*, 2022, vol. 83, no. 2, pp. 214–236.

4. Zhu, F., Fu, Y., and Dinh, T., Asymptotic Convergence Unknown Input Observer Design via Interval Observer, *Automatica*, 2023, vol. 147, art. no. 110744.

5. Efimov, D.V. and Raissi, T., Design of Interval Observers for Uncertain Dynamical Systems, *Autom. Remote Control*, 2016, vol. 77, no. 2, pp. 191–225.

6. Khan, A., Xie, W., Zhang, L., and Liu, L., Design and Applications of Interval Observers for Uncertain Dynamical Systems, *IET Circuits Devices Syst.*, 2020, vol. 14, no. 6, pp. 721–740.

7. Chebotarev, S.G. and Kremlev, A.S., Synthesis of Interval Observer for Linear System with Variable Parameters, *Journal of Instrument Engineering*, 2013, vol. 56, no. 4, pp. 42–46.

8. Zhirabok, A.N., Zuev, A.V., and Kim, Chkhun Ir, Method to Design Interval Observers for Linear Time-Invariant Systems, *J. Comput. Syst. Sci. Int.*, 2022, vol. 61, no. 5, pp. 485–495.

9. Zhirabok, A.N. and Zuev, A.V., Interval Observers for Estimating Unknown Inputs in Discrete Time-Invariant Dynamic Systems, *Autom. Remote Control*, 2024, vol. 85, no. 8, pp. 747–760.

10. Kwakernaak, H. and Sivan, R., *Linear Optimal Control Systems*, New York: Wiley, 1972.

11. Zhirabok, A.N., Zuev, A.V., Filaretov, V.F., et al., Interval Observers for Continuous-Time Systems with Parametric Uncertainties, *Autom. Remote Control*, 2023, vol. 84, no. 11, pp. 1275–1286.

12. Levant, A., Higher-Order Sliding Modes, Differentiation and Output-Feedback Control, *Int. J. Control*, 2003, vol. 76, nos. 9-10, pp. 924–941.

13. Chebotarev, S., Efimov, D., Raissi, T., and Zolghadri, A., Interval Observers for Continuous-Time LPV Systems with $\mathcal{L}_1/\mathcal{L}_2$ Performance, *Automatica*, 2015, vol. 58, pp. 82–89.

14. Efimov, D., Raissi, T., Chebotarev, S., and Zolghadri, A., Interval State Observer for Nonlinear Time-Varying Systems, *Automatica*, 2013, vol. 49, pp. 200–206.

This paper was recommended for publication by N.N. Bakhtadze, a member of the Editorial Board

ISSN 0005-1179 (print), ISSN 1608-3032 (online), Automation and Remote Control, 2026, Vol. 87, No. 8, pp. 699–712.

NONLINEAR SYSTEMS

Symmetric Multifrequency Oscillations of a Lagrangian System and Their Stabilization

V. N. Tkhai

Trapeznikov Institute of Control Sciences, Russian Academy of Sciences, Moscow, Russia
e-mail: tkhai@ipu.ru

Received August 24, 2025
Revised January 12, 2026
Accepted January 19, 2026

Abstract—This paper considers a Lagrangian system subjected to positional forces. By assumption, the frequencies of small oscillations for an equilibrium are incommensurable. The existence of multifrequency symmetric oscillations in the neighborhood of the equilibrium and their extension to global families of such oscillations is established; the families fill the entire domain of the phase space adjacent to the equilibrium. A nonlocal continuation of the above families in the system parameter is proved. In the conservative case, an autonomous control is found, and a symmetric multifrequency oscillation is stabilized in the large. In this case, feedback on potential energy is constructed.

Keywords: Lagrangian system, positional forces, reversibility, symmetric multifrequency oscillation, birth, global family, nonlocal continuation in parameter, conservative system, feedback, adaptive scheme, stabilization

DOI: 10.7868/S1608303226080038

1. INTRODUCTION

Multifrequency oscillations are an important research area in nonlinear dynamics; see [1–4], other books, and numerous papers. Oscillations are studied using universal asymptotic methods and perturbation theory. The latter includes L.S. Pontryagin's theorem [5] on oscillation control by constructing a limit cycle. An example of a qualitatively reorganized phase portrait under a small perturbation can be found in the relaxation regimes (without a driving force) of a regenerative receiver, as investigated by B. Van der Pol [6]. In 1929, A.A. Andronov discovered that the physical embodiment of Poincaré curves is the stable self-oscillations, constructed by him and independently by Van der Pol. In 1881, A. Poincaré introduced the concept of a limit cycle for a system in the plane [7, Chap. VI]. The theory of self-oscillations was further developed within Andronov's school [8].

A qualitative reorganization is observed in the general case of a corrected conservative system [9]. In the constructed autonomous control system, the feedback is implemented by tracking potential energy at the current trajectory point.

In this paper, the idea from [9] is utilized to stabilize symmetric multifrequency oscillations. To stabilize an oscillation with a given energy level h^*, an adaptive scheme [10] was applied in [9]; according to this scheme, the gain $K(h^*)$ is chosen depending on the value of h^*. The computation of $K(h^*)$ in [9] is based on the known global family Σ_1 of single-frequency symmetric oscillations, constructed for all admissible energy levels h. The family Σ_1 is obtained by a global extension of the symmetric local Lyapunov family, whose existence is given by an analog [11, 12] of Lyapunov's center theorem [13] for reversible mechanical systems. For a symmetric multifrequency oscillation, the global family Σ is constructed below.

In this paper, we introduce the concept of a symmetric multifrequency oscillation of a Lagrangian system with n degrees of freedom, subjected to positional forces; prove a theorem on the birth of k-frequency oscillations ($1 \leqslant k \leqslant n$); provide their continuation in the phase space to the global family Σ_k ($1 \leqslant k \leqslant n$) of such oscillations; prove a nonlocal extension of Σ_k in the system parameter; and address other related issues. As a result, a global theory is developed to solve the stabilization problem in the large.

According to Lyapunov [13], the stability problem for a chosen solution can always be reduced to the study of the zero (trivial) solution. However, for a solution of an autonomous system, including a multifrequency oscillation, this leads to a special case in stability theory. For a periodic solution of an autonomous system, the Andronov–Vitt stability theorem [14] is applied.

In an autonomous system, a solution constitutes a family parameterized by β, i.e., the shift of the initial point along the trajectory. Therefore, two stabilization problems are distinguished here: stabilization of the entire family of solutions and stabilization of a chosen solution from this family. Usually, the second problem is solved using controls with an explicit dependence on time. Such formulations of control problems for single-frequency oscillations were given in [15–21].

When stabilizing the entire family of solutions, it is necessary that the controlled system trajectories be attracted to the family; this requires preserving the autonomy of the original system and using autonomous control. Here, known concepts are utilized: stability with respect to part of the variables [22], characterizing the deviation of trajectories of a family from other trajectories, orbital stability and orbital asymptotic stability, and attraction [23]. In the Andronov–Vitt theorem [14], attraction is ensured by the roots of the characteristic equation lying in the left half-plane.

Due to the action of control, the closed-loop system no longer admits the original solution. Therefore, in the controlled system, a solution close to the original one is stabilized. The closed-loop system is made close to the original system by using a control law with a small gain. This approach is characteristic of perturbation theory; it was pioneered by Pontryagin [5]. Attraction to the family (solution) is provided by dissipation, i.e., a velocity-linear force acting at each trajectory point. Simultaneously, the control law ensures the isolation of the stabilized oscillation. A textbook example of such stabilization is the Van der Pol equation [6]. Further studies on the application of Van der Pol-type dissipation were reviewed in [9]; also, see the bibliography in the paper. Only single-frequency oscillations were considered.

2. SYMMETRIC MULTIFREQUENCY OSCILLATIONS OF A LAGRANGIAN SYSTEM SUBJECTED TO POSITIONAL FORCES

Consider a smooth system governed by Lagrange's equations of the second kind and subjected to positional forces Q_s :

$$\frac{d}{dt}\frac{\partial T}{\partial \dot{q}_s} - \frac{\partial T}{\partial q_s} = Q_s(q_1, \ldots, q_n), \quad s = 1, \ldots, n. \tag{1}$$

The force $Q = (Q_1, \ldots, Q_n)$ is generally the sum of a potential force and a nonconservative positional force. The kinetic energy T is represented as a positive definite quadratic form of velocities; equations (1) describe the dynamics in an inertial frame. System (1) is invariant with respect to the transformation $(q, \dot{q}, t) \to (q, -\dot{q}, -t)$ and belongs to the class of reversible mechanical systems. The phase space of system (1) is symmetric with respect to the fixed set $M = \{q, \dot{q} : \dot{q} = 0\}$. An equilibrium of system (1) lies on M. Symmetric motions intersect the set M: at the intersection point, the velocity satisfies $\dot{q} = 0$. Nonsymmetric motions are realized in pairs; they are symmetric to each other with respect to M, and the directions of motion in a pair are mutually opposite. A symmetric motion intersecting the set M twice constitutes a single-frequency symmetric oscillation.

Let $q = (q_1, \ldots, q_n) = 0$ for the equilibrium. In system (1), the roots of the characteristic equation are split into pairs $\pm\lambda_s$. System (1) is studied under the assumption that all λ_s are pure imaginary, and the numbers $|\lambda_s| > 0$ are incommensurable. Then all motions in the linearized system near the equilibrium are described by quasi-periodic functions with k frequencies, $1 \leqslant k \leqslant n$. They represent symmetric oscillations (SOs). For $k = 1$, we have a single-frequency oscillation; for $k > 1$, a multifrequency oscillation arises.

An SO starts at a point $q^0 = (q_1^0, \ldots, q_n^0) \in M$ at $t = 0$ and is described by a function $q(q^0, t)$, in which an arbitrary shift β of the initial point along the trajectory is set to zero. At the time instant t_s, the SO along the coordinate q_s will have the next zero velocity $\dot{q}_s$. In the case under study, the numbers t_s are supposed to be incommensurable. Therefore, at the time instants $t = t_s$ the velocities $\dot{q}_s$ on the SO satisfy the equalities

$$\dot{q}_s(q_1^0, \ldots, q_n^0, t) = 0, \quad t = t_s; \quad s = 1, \ldots, n. \tag{2}$$

The left-hand sides of equalities (2) contain the velocities $\dot{q}_s$ for the solution of system (1) as functions of the initial point q^0 and time t. Equalities (2) mean that for each variable q_s, there is a closed curve in the phase space. Conditions (2) are necessary and sufficient for the existence of an SO of system (1). They can hold in (2) for k velocities $\dot{q}_s$, where $s = 1, \ldots, k$ and $k \leqslant n$. For $k = n$, system (1) admits an SO with the maximum possible number of frequencies; in the case $k < n$, at the initial point q^0 the accelerations satisfy $\ddot{q}_{k+1} = \ldots = \ddot{q}_n = 0$ and $t_{k+1} = \ldots = t_n$, so the system has an SO with $k < n$ frequencies: if $k = 1$, we have a single-frequency SO. Each coordinate q_s is given by a $2t_s$-periodic function of time t; therefore, the SO is described by a quasi-periodic function $(q(q^0, t), \dot{q}(q^0, t))$ with k frequencies. For $k = 1$, the function is periodic. For $k = n$, the phase-space trajectory belongs to the direct product of n closed curves, i.e., a symmetric n-torus; for $k < n$, we obtain symmetric k-tori.

In equalities (2), a separate time t_s is associated with each variable q_s. The *unified time* γ for all variables of the SO is introduced by the formula $t_s = \nu_s\gamma$. In time γ, all velocities vanish simultaneously: a multifrequency SO can be studied as an *imaginary* symmetric periodic motion with a separate time for each variable. Equalities (2) are written for fixed numbers $t_s = t_s^*$. If $t_s^* = \nu_s\gamma^*$, the number γ^* hence means the time instant when the trajectory intersects the fixed set M, as in the case of a single-frequency SO of period $2\gamma^*$. Therefore, the introduction of the unified time γ leads to the concept of a *common period* for all variables of a multifrequency SO. It equals $2\gamma^*$, and this number identifies the SO under consideration in the family. The number γ^* is denoted by τ and is called the SO parameter. It characterizes the transition from one SO to another and depends on the initial point q^0 for the SO.

The concepts of unified time and common period allow constructing a theory of multifrequency SOs similar to that of symmetric periodic motions. The latter motion represents an SO with $k = 1$; the half-period on it serves as the parameter τ.

Equalities (2) are written as

$$\dot{q}_s(q_1^0, \ldots, q_n^0, \nu_s\tau) = 0, \quad s = 1, \ldots, n. \tag{3}$$

The incommensurability condition of the numbers in the set $\{t_s^*\}$ translates to the set $\nu = \{\nu_1, \ldots, \nu_n\}$: ν is called the *basis* (of frequencies) of an SO. When passing from one SO to another, the point $q^0 \in M$ changes. Equalities (2) are treated as a system of equations for finding the numbers $t_s = \nu_s\tau$. In equalities (3) with the parameter τ, the initial point q^0 is determined, while the basis ν will have to be obtained up to a factor $\delta(q^0)$ and thus remains preserved. Since the n equalities (3) relate the $n + 1$ variables $q_1^0, \ldots, q_n^0, \tau$, they lead to a family of SOs of dimension n with the parameter τ. In the case of $k < n$ equalities in (3), the dimension of the SO family equals k.

When extending the SO family in the parameter τ, one changes the projection of the SO onto the fixed set M; on the interval $\Delta\tau$, the projection leads to the domain q^0 of initial points for the local SO family. This set is also obtained by proportionally changing the elements of the basis ν while preserving the incommensurability of all numbers ν_s in the basis. And the basis, defined up to a factor δ, remains invariable. This provides another local extension method for the SO. Note that both methods yield the same result.

3. THE BIRTH OF SYMMETRIC OSCILLATIONS FROM THE EQUILIBRIUM

Consider a k-frequency SO with an initial point $q^0 \in M$. It satisfies equalities (3), which relate the variables q^0 and τ. At the point q^0, the Jacobi matrix is computed:

$$\mathrm{J}(\mathrm{q}^0, \tau) = \left\| \frac{\partial \dot{q}_s(q^0, \tau)}{\partial q_j^0} \right\|. \tag{4}$$

Definition 1. A symmetric k-frequency oscillation $(1 \leqslant k \leqslant n)$ that satisfies the condition $\operatorname{rank} \mathrm{J}(\mathrm{q}^0, \tau) = n$ is said to be nondegenerate.

For a nondegenerate SO, the following local continuation properties hold.

1°. A nondegenerate SO locally continues in the parameter τ.

Let (3) be valid. For this nondegenerate SO, we form the equations in the deviations Δq^0 and $\Delta\tau$ in the linear approximation to obtain the linear system

$$\frac{\partial \dot{q}_s(q^0, \tau)}{\partial q_1^0} \Delta q_1^0 + \ldots \frac{\partial \dot{q}_s(q^0, \tau)}{\partial q_n^0} \Delta q_n^0 + \frac{\partial \dot{q}_s(q^0, \tau)}{\partial \tau} \Delta\tau = 0, \quad s = 1, \ldots, n. \tag{5}$$

In this system of equations, the principal matrix coincides with $\mathrm{J}(\mathrm{q}^0, \tau)$, and the right-hand side is represented by the acceleration vector with a minus sign, computed on M. For a nondegenerate SO, the inequality $\det \mathrm{J}(\mathrm{q}^0, \tau) \neq 0$ holds: the acceleration vector vanishes only at the equilibrium. Therefore, the system is consistent, and the SO locally extends in $\Delta\tau$, both toward increasing and decreasing $\Delta\tau$. The factor $\delta(q^0)$ is also incremented simultaneously.

2°. A nondegenerate SO locally continues in the system parameter μ.

For a system with the parameter μ, system (5) contains this parameter and, in addition, a term with the increment $\Delta\mu$. For a nondegenerate SO, the Jacobi matrix is nonsingular; therefore, the extension is carried out in τ and μ. Restricting the analysis only to the increment in μ, we obtain property 2°.

In the neighborhood of the equilibrium, system (1) is written as

$$\ddot{q}_s + \sum_{j=1}^{n} a_{sj} q_j + \tilde{Q}_s(q, \dot{q}) = 0, \quad \tilde{Q}_s(q, \dot{q}) = \tilde{Q}_s(q, -\dot{q}), \quad s = 1, \ldots, n, \tag{6}$$

where $||a_{sj}||$ is a constant matrix, and $\tilde{Q}_s$ are nonlinear functions.

The following result is true.

Theorem 1 (on the birth of SOs). *The neighborhood of the equilibrium of system* (6) *with incommensurable frequencies ν_s, $s = 1, \ldots, n$, of the linear system is filled with families of nondegenerate k-frequency SOs, $1 \leqslant k \leqslant n$. They are parameterized by the distance to the equilibrium.*

Proof. Let us perform the change of variables $(q, \dot{q}) \to (\varepsilon\xi, \varepsilon\dot{\xi})$. Then, a quasilinear system is obtained in the variables ξ_s, and its linear approximation coincides with that of system (6).

For $\varepsilon = 0$, the resulting system admits a k-frequency nondegenerate SO, $1 \leqslant k \leqslant n$. For this system, $\mathrm{J}(0, 0) = -||a_{sj}||_1^n$, $\operatorname{rank} \mathrm{J}(0, 0) = n$, and the basis for k-frequency oscillations contains k

numbers from the set $\nu(0) = \{\nu_s(0)\}$, $\nu_s(0) = |\lambda_s|$. Moreover, the system containing a k-frequency SO is described by k variables, and the SO basis includes k numbers. For the whole system, SOs of the linear system continue in the parameter ε: the quasilinear system possesses families of nondegenerate SOs in ε with all frequencies: $1 \leqslant k \leqslant n$. When considering the SOs with all possible frequencies k, $1 \leqslant k \leqslant n$, the neighborhood of the equilibrium of system (6) is completely filled with families of nondegenerate SOs parameterized by the distance ε to the equilibrium. The proof of Theorem 1 is complete.

Remark 1. For $k = 1$, we obtain [11, 12] the reversible analog of Lyapunov's center theorem [13].

Remark 2. Under the hypotheses of Theorem 1, the equilibrium of the system is stable.

4. THE GLOBAL FAMILY OF NONDEGENERATE SYMMETRIC OSCILLATIONS IN THE PHASE SPACE

A nondegenerate SO possesses the local continuation property in the family parameter τ. Theorem 2 below formulates a result on the global extension of SOs in the parameter τ.

Definition 2. A family of nondegenerate SOs parameterized by τ is called a global family of SOs if the parameter τ takes all possible values for this family.

Theorem 2 (on the global family of SOs in the phase space). *Let a Lagrangian system subjected to positional forces admit a nondegenerate k-frequency SO, $1 \leqslant k \leqslant n$. Then the SO always extends in the family parameter τ to a global family Σ_k of nondegenerate SOs, and the parameter τ changes monotonically on this family. Also, the condition* $\operatorname{rank} J(q^0, \tau) = n$ *holds on the global family, being violated on its boundary.*

Proof. During the local extension of a nondegenerate k-frequency SO in the parameter τ, its initial point $q^0(\tau)$ will be a function of τ. And the domain $\Upsilon_k(q^0, \tau)$ of points with the condition $\operatorname{rank} J(q^0, \tau) = n$ is formed on the fixed set M. We apply the local continuation property of a nondegenerate SO to the points of $\Upsilon_k(q^0, \tau)$. Then two situations arise. In the first situation, no new points appear in the domain $\Upsilon_k(q^0, \tau)$. Then the global family Σ_k is successfully constructed. In the second situation, the domain $\Upsilon_k(q^0, \tau)$ has been increased, which is accompanied by a monotonic change of the parameter τ. Again, two situations arise here.

As a result, at some iteration, the global family Σ_k is successfully constructed, or the construction process continues with an infinite approach to the boundary of the initial domain $\Upsilon_{\sigma k}(q^0, \tau)$ for the global family Σ_k. At each point of this domain, we have $\operatorname{rank} J(q^0, \tau) = n$. The monotonic change of SOs of the family Σ_k in the parameter τ follows from the construction procedure. The proof of Theorem 2 is complete.

Remark 3. The proof of Theorem 2 is valid for k-frequency SOs, $1 \leqslant k \leqslant n$. For a single-frequency oscillation ($k = 1$), the result was described in [24].

Remark 4. For the analytic system (6) with incommensurable numbers $\nu_1, \ldots, \nu_n$, a rigorous transformation to a system with k-dimensional manifolds ($1 \leqslant k \leqslant n$) was constructed in [25], including its convergence conditions [25, Theorem 2]. System (6) possesses reversibility; as a result, the phase space contains n manifolds, and a single-frequency SO is realized on each manifold.

5. THE GLOBAL EXTENSION OF A NONDEGENERATE SYMMETRIC OSCILLATION IN THE PARAMETER SPACE OF THE SYSTEM

A nondegenerate SO possesses the local continuation property in the system parameter μ. Thus, in perturbation theory, a nondegenerate perturbed SO always exists together with an SO of system (1). The boundary of existence of a nondegenerate SO in the parameter μ is an open issue in perturbation theory. In applications, the boundary is usually found by direct computation.

Theorem 3 formulates a result on the global extensibility of a nondegenerate SO in the parameter μ. The parameter $\mu = (\mu_1, \ldots, \mu_m)$ is generally a vector.

Theorem 3. *Let a Lagrangian system with the parameter μ, subjected to positional forces, admit an SO with the parameter μ, nondegenerate for $\mu = \mu^*$. Then this SO globally extends to the entire domain of μ. On the global family of nondegenerate SOs in the parameter μ, the condition* $\operatorname{rank} J(q^0, \tau) = n$ *holds. The basis ν is preserved on this family. On the boundaries of the global family, the condition* $\operatorname{rank} J(q^0, \tau) = n$ *is violated.*

Proof. An SO with the parameter μ, nondegenerate at $\mu = \mu^*$, possesses property 2°. It is applied for the global extension in μ exactly as property 1° for the global extension of a nondegenerate SO in the parameter τ. The extension in μ is carried out until exhausting the entire domain of μ with $\det \mathrm{J}(\mathrm{q}^0(\mu), \tau) \neq 0$.

Remark 5. Theorem 3 concerns the parameter μ on which the SO depends. Another possible situation is demonstrated in Example 2 below.

Theorems 2 and 3 applied to a nondegenerate SO yield the following conclusion.

General postulate. If a Lagrangian system subjected to positional forces admits a nondegenerate SO, then it globally extends in the parametric phase space.

Remark 6. This paper employs Pontryagin's approach [26] to autonomous ordinary differential equations: parameters and phase variables are treated equally.

6. THE OSCILLATION DOMAIN AND STABILIZATION OF THE SYMMETRIC OSCILLATIONS OF SYSTEM (6)

Consider system (6) with incommensurable frequencies $\nu_1, \ldots, \nu_n$ in the linear system. In the neighborhood of the equilibrium, k-frequency SOs ($1 \leqslant k \leqslant n$) are born (see Theorem 1); they fill the entire neighborhood of the equilibrium. The continuation of SOs in the parameter τ (Theorem 2) leads in the phase space to an oscillation domain Ω, adjacent to the equilibrium and filled with global families of k-frequency SOs, $1 \leqslant k \leqslant n$. They are denoted by Σ_k: the number of the families equals the binomial coefficient C_n^k (in combinatorics, the number of ways to choose k out of n objects). The family Σ_k fills the integral manifold $\tilde{\Sigma}_k$. Each SO in the family Σ_k is identified by the value of the parameter τ.

In this paper, we develop the approach of [9], originally proposed for a single-frequency SO, for multifrequency SOs. In the stabilization problem of an SO for system (6), an autonomous controlled system, ε-close to (6), is constructed; in this system, an isolated oscillation (IO) is separated. In the perturbed system, the manifold $\tilde{\Sigma}_k$ is associated with the manifold $\tilde{\Sigma}_k(\varepsilon)$: $\tilde{\Sigma}_k = \tilde{\Sigma}_k(0)$. When separating the IO, we simultaneously ensure its orbital asymptotic stabilization. A local attraction problem is usually posed: trajectories from the neighborhood of the IO are attracted to it. However, due to the structure of the domain Ω, it is possible to pose the problem of attracting all trajectories from $\tilde{\Sigma}_k(\varepsilon)$, as well as from the neighborhood of $\tilde{\Sigma}_k(\varepsilon)$ [9]. This is the case, e.g., in the Van der Pol equation [6] ($k = 1$). In a conservative system with one degree of freedom, all trajectories from the oscillation domain are attracted [9].

In a conservative system, the kinetic energy on the set M is zero. When passing from one SO of the family to another, the potential energy $\Pi(q)$ computed on M changes. One can therefore take the value of the function $\Pi(q)$ on M or the constant h of the total mechanical energy E as the SO parameter instead of τ. Due to the monotonic change of the parameter τ on the global family, the energy h changes monotonically as well. By specifying the value h, we obtain all SOs with this energy level. On the graph of the function $\Pi(q)$, the value $h = 0$ corresponds to the equilibrium; for $h > 0$, the born k-frequency SOs extend to the global families Σ_k unboundedly together with the energy h.

In a conservative system, the SOs in the family Σ_k are parameterized by the constant h and form integral k-dimensional manifolds $\tilde{\Sigma}_k$, $1 \leqslant k \leqslant n$. Hence, the SOs of all dimensions k correspond to a given value of h. For this reason, a control law independent of the number of frequencies in the SO is designed. For the energy level $h = h^*$, attraction to the IO on $\tilde{\Sigma}_k(\varepsilon)$ with all numbers k: $1 \leqslant k \leqslant n$ is investigated accordingly.

In the case $k = 1$, the family Σ_1 is described by a system with one degree of freedom. Therefore, the stabilization problem naturally decomposes as follows [9]: first, the attraction problem on $\tilde{\Sigma}_1(\varepsilon)$ is solved; and in the system of order $(n-1)$, local attraction to the trivial solution (the IO on $\tilde{\Sigma}_1(\varepsilon)$) is ensured, for which $h = h^*$.

For SOs with $k > 1$ frequencies, $\tilde{\Sigma}_k$ has dimension k. Local attraction to the trivial solution is ensured in the system of order $(n-k)$. Regardless of the number of frequencies k, the trivial solution in the problem is associated with the IO corresponding to the energy level $h = h^*$ in the controlled system.

In a conservative system with n degrees of freedom, the controlled system with k frequencies has C_n^k stabilizable IOs. The sum over all k gives the number of all stabilizable IOs.

7. STABILIZATION OF THE SYMMETRIC OSCILLATIONS OF A CONSERVATIVE SYSTEM

Consider the controlled (corrected) system

$$\frac{d}{dt}\frac{\partial L}{\partial \dot{q}_s} - \frac{\partial L}{\partial q_s} = \varepsilon[1 - K\Pi_\varphi]\frac{\partial T}{\partial \dot{q}_s}, \quad L = T - \Pi, \quad s = 1, \ldots, n, \tag{7}$$

given by Lagrange's equations of the second kind. Here, T and Π are the kinetic and potential energies, respectively. (When computed on the SO family, the latter is denoted by Π_φ.) By assumption, for $\varepsilon = 0$, system (7) admits the set Σ_σ containing all global families of SOs born from the equilibrium with incommensurable frequencies $\nu_1, \ldots, \nu_n$. We choose $0 < \varepsilon < \varepsilon_0$, where ε_0 is some finite number for Σ_σ; h^* is the energy level corresponding to the separated oscillation: the equilibrium is associated with the value $h = 0$. In system (7), the coefficient K is set equal to the value $K(h^*)$ of the function $K(h)$ for the stabilized oscillation. The dependence $K(h)$ itself will be defined below.

The control system (7) was applied in [9] for the adaptive stabilization scheme of a symmetric periodic motion ($k = 1$). The control law on the right-hand side of equality (7) is universal for stabilizing SOs with $k = 1$. It is represented by a nonlinear force linear in velocity. For $\varepsilon = 0$, system (7) belongs to the class of reversible mechanical systems. The feedback is implemented by tracking the value of the potential energy $\Pi(q)$ at the current point of the closed-loop system trajectory.

In the stabilization problem, one should understand that a unique family Σ_k is realized in the set of global families Σ_σ in the system with $\varepsilon = 0$. Moreover, a unique SO is realized on the family Σ_k, which corresponds to the parameter τ (the energy h in the conservative system). Therefore, we pose the problem of stabilizing a unique SO corresponding to the separated energy level $h = h^*$. For this SO, the variables are $q_{k+1} = \ldots = q_n = 0$.

The following computations are valid for all global families Σ_k with k frequencies, $1 \leqslant k \leqslant n$, regardless of the number of frequencies k of the oscillations.

For system (7) with $\varepsilon = 0$, we determine the total mechanical energy

$$E \equiv T(q, \dot{q}) + \Pi(q). \tag{8}$$

It takes a constant value h on the solutions of the conservative system. System (7) satisfies the equality

$$\frac{dE}{dt} = \varepsilon[1 - K(h^*)\Pi_\varphi]T(q, \dot{q}). \tag{9}$$

For $\varepsilon = 0$, we have $E = h(\text{const}) > 0$. On the SO, the coordinate is $q = \varphi$. The SOs form a global family Σ_k belonging to the invariant integral manifold $\tilde{\Sigma}_k$. We stabilize the SO with the parameter $\tau = \tau^*$ $(h = h^*)$.

The energy E is the sum of two terms: $E = E_\varphi + E_\varepsilon$, where E_φ is computed on the solutions in $\tilde{\Sigma}_k(\varepsilon)$, and E_ε on the solutions in the neighborhood of $\tilde{\Sigma}_k(\varepsilon)$. The law for E_ε involves the kinetic energy of motion in the ε-neighborhood of $\tilde{\Sigma}_k(\varepsilon)$. It is a quadratic form of the velocities $\dot{q}_{k+1}, \ldots, \dot{q}_n$. Thus, the motion in the neighborhood of $\tilde{\Sigma}_k(\varepsilon)$ is tracked by the potential energy of the SO on Σ_k.

For $\varepsilon > 0$, we write the expressions

$$\Pi(q) = \Pi(\varphi) + h\varepsilon\rho(\varepsilon, h, q), \quad T = E - \Pi(q) = h - \Pi(\varphi) + h\varepsilon\sigma(\varepsilon, h, q)$$

$(\Pi(\varphi) = \Pi_\varphi)$ with functions ρ and σ of order 1. As a result, the right-hand side of equality (9) has the principal term

$$f = \varepsilon[(1 - K(h^*)\Pi_\varphi)](h - \Pi(\varphi)),$$

which is computed on the SO; it does not contain t explicitly.

For SOs, the *unified* time γ has been introduced for all variables q_s (Section 2). And the multifrequency SO in the function E is treated here as a single-frequency SO with a *common period* equal to 2τ. The time γ is determined up to a factor. In the unified time, the rate of change of the variable q_s acquires its individual factor ν_s such that the numbers in the set $\{\nu_s\}$ are incommensurable. Finally, the potential energy in the function f is computed on the SO $q = \varphi$: f also changes as a function of γ.

In the unified time γ, the rate of change of the energy is proportional to its rate in the time t. Therefore, the increment $\Delta E_\varphi(\varepsilon, h)$ of the energy in γ is computed from the right-hand side of (9) as an integral over the period 2τ in the variable γ :

$$\Delta E_\varphi(\varepsilon, h) = \varepsilon 2\tau(h)[I(h) + \varepsilon h\Phi(\varepsilon, h)]. \tag{10}$$

This formula is valid on the entire global family Σ_k. The family Σ_k consists of SOs, and each value h is associated with only one SO. If $\Delta E_\varphi(\varepsilon, h^*) = 0$ at the point $h = h^*$, then the value h^* corresponds to a k-frequency oscillation. The oscillation will be nonsymmetric since $\varepsilon = 0$ for a symmetric one. For the isolated root h^*, the oscillation will be isolated. Thus, we obtain an isolated oscillation (IO), representing a cycle in the case $k = 1$. The IO is a one-parameter family in the shift of the initial point for the oscillation.

The function $I(h)$ has the form

$$I(h) \equiv \int_0^{2\tau^*} [1 - K(h^*)\Pi_\varphi](h - \Pi(\varphi))d\gamma \tag{11}$$

and gives the amplitude (bifurcation) equation $I(h) = 0$ for the multifrequency SO. As in the case of symmetric periodic motion in [9], a simple root h^* of equation (11) leads at the point $h = h^*$ of the family of k-frequency SOs to a bifurcation and the birth of a k-frequency IO.

In the integral (11), the function $\Pi(\varphi)$ on the SO family is computed through the coordinate $q = \varphi(h, \gamma)$, given in the unified time γ for the SO. By replacing the variable γ in the integral (11) with $\tilde{\gamma} = (\tau^*/\tau(h))\gamma$, where $\tau^* = \tau(h^*)$ for the stabilized oscillation with the energy level h^*, we make the coordinate q directly dependent on $\tilde{\gamma}$.

In the case $k = 1$, the family of nonlinear oscillations is reduced to an isochronous family in [9].

The potential energy on the SO changes as a function of $\tilde{\gamma}$; therefore, in view of the equality $\Pi(\varphi(h,0)) = h$, it can be written as $\Pi(\varphi(h,\tilde{\gamma})) = hz(\tilde{\gamma})$, $0 \leqslant z \leqslant 1$. Consequently, the integral (11) becomes

$$I(h) \equiv 2h \int_0^1 (1 - K(h^*)hz(\tilde{\gamma}))(1 - z(\tilde{\gamma}))d\tilde{\gamma}, \tag{12}$$

being represented as a quadratic function without a constant term:

$$I(h) = 2h(\alpha - \beta h), \quad \alpha = \int_0^1 (1 - z)d\tilde{\gamma}, \quad \beta = -K(h^*) \int_0^1 z(1 - z)d\tilde{\gamma}. \tag{13}$$

Due to the expression (13), the equation $I(h) = 0$ clearly admits a unique nonzero root $h^* = \alpha/\beta$. The root h^* corresponds to the multifrequency IO of the controlled system (7). This oscillation is ε-close to the SO with the energy level $h = h^*$; however, the oscillation is not symmetric.

Note that each number $K(h^*)$ is uniquely associated with the root $h = h^*$ and vice versa. Thus, the following function is defined:

$$K(h) = \frac{b}{h}, \quad b = \text{const}, \ b > 0.$$

The kinetic energy on the fixed set M is zero; therefore, the potential energies of the systems under study on the SO are distinguished by the constant b.

The root of the equation $I(h) = 0$ is computed for the one-parameter (in h) family Σ_k of trajectories in the ε-corrected system. The root h^* corresponds to a fixed point of the mapping defined on the manifold $\tilde{\Sigma}_k(\varepsilon)$, and its isolation indicates that the existence of the root is derived via the linear (principal) terms in ε. Hence, $\Delta E_\varphi(\varepsilon, h^*) = 0$, and we arrive at the equality $\Phi(\varepsilon, h^*) = 0$.

Lemma 1. *The equation*

$$I(h) + \varepsilon h \Phi(\varepsilon, h) = 0 \tag{14}$$

has a unique root for $0 < \varepsilon < \varepsilon_0$, where ε_0 is a number independent of h^*.

Proof. The number ε_0 is found using exactly the same procedure as the one described for a single-frequency oscillation in [9, Lemma 1].

Next, it is necessary to study the corrected system (7) for $0 < \varepsilon < \varepsilon_0$. Consider the integral manifold $\tilde{\Sigma}_k$ containing the global family of k-frequency SOs, $1 \leqslant k \leqslant n$. It is obtained by the continuation, in the parameter h, of the small oscillations with incommensurable frequencies.

Theorem 4. *Let a conservative system be governed by Lagrange's equations of the second kind and admit the equilibrium with incommensurable frequencies of small oscillations. Then the system has an integral manifold $\tilde{\Sigma}_\sigma$ containing the set Σ_σ of global families Σ_k of k-frequency oscillations that fill the manifolds $\tilde{\Sigma}_k$, $1 \leqslant k \leqslant n$. For the corrected system* (7)*, there always exists a number $\varepsilon_0 > 0$ such that for $0 < \varepsilon < \varepsilon_0$, system* (7) *possesses k-frequency IOs, $1 \leqslant k \leqslant n$, ε-close to the oscillation of the conservative system with the energy level $h = h^*$. The number of k-frequency IOs is C_n^k. Each IO attracts trajectories from $\tilde{\Sigma}_k(\varepsilon)$ and trajectories from the ε-neighborhood of $\tilde{\Sigma}_k(\varepsilon)$. On the solutions of the corrected system, the energy $E = T + \Pi$ of the conservative system changes according to the law* (9)*.*

Proof. The existence of the global family Σ_σ under the incommensurability of frequencies for the equilibrium follows from Theorems 1 and 2. The boundary value ε_0 is established by Lemma 1. Formula (10) is valid for k-frequency SOs, $1 \leqslant k \leqslant n$. Based on the above analysis of formula (10), there exists an isolated k-frequency oscillation ε-close to the oscillation of the conservative system with the energy level h^*. In system (7), the entire domain of initial points for solutions different from the equilibrium belongs to $\tilde{\Sigma}_\sigma$.

Formula (9) holds separately for E_φ and E_ε. The rate of change of E_φ coincides in sign with that of the energy E_ε: different kinetic energies are used. As a result,

$$\Delta E_\varphi(\varepsilon, h) \to \Delta E_\varphi(\varepsilon, h^*) = 0, \quad \Delta E_\varepsilon(\varepsilon, h) \to \Delta E_\varepsilon(\varepsilon, h^*) = 0$$

simultaneously as $h \to h^*$. The first limit means that in the controlled system (7), for points from $\tilde{\Sigma}_k(\varepsilon)$, all trajectories tend to the IO corresponding to the SO with the energy value h^* from Σ_k. According to the second limit, trajectories from the neighborhood of $\tilde{\Sigma}_k(\varepsilon)$ tend to $\tilde{\Sigma}_k(\varepsilon)$ with a zero limit value of the corresponding kinetic energy. Therefore, these trajectories also tend to the IO.

The number of k-frequency IOs coincides with C_n^k, the number of combinations of integral manifolds where k-frequency SOs are realized.

The proof of Theorem 4 is complete.

Remark 7. Theorem 4 concerns k-frequency SOs, $1 \leqslant k \leqslant n$. For the particular case $k = 1$, it was established in [9], with weaker conditions on the roots of the characteristic equation.

Example 1. Signal source recognition by extracting frequencies. Consider two linear oscillators with frequencies ω_x and ω_y. In the system, they possess families of symmetric two-frequency oscillations, degenerating into two families of single-frequency oscillations. To stabilize the IO of the controlled system, we apply the closed-loop system

$$\begin{aligned} &\dot{x} + \omega_x^2 x = \varepsilon(1 - K(h^*)\Pi)\dot{x}, \\ &\dot{y} + \omega_y^2 y = \varepsilon(1 - K(h^*)\Pi)\dot{y}, \quad \Pi = (\omega_x^2 x^2 + \omega_y^2 y^2)/2, \end{aligned} \tag{15}$$

where the coefficient $K(h^*)$ is computed from the energy value $h = h^*$ of the entire system. All IOs are stabilized according to a single scenario. System (15) contains two invariant manifolds where the individual oscillators are stabilized.

The signal is captured by energy. In system (15), the oscillation frequencies are extracted from the received signal, and the sources are recognized by the frequencies. The recognition capabilities grow when increasing the number of oscillators in the system.

The symmetric oscillation of a harmonic oscillator with a frequency ω is given by the formula $r = A\cos(\omega t)$, where $A^2 = h/2$. In the case of a single oscillator, the coefficient is $K(h) = 2/h$.

In (15), we have the frequency basis $\nu = (\omega_x, \omega_y)$, and the unified time is $\gamma = t$. Hence, the system of two oscillators behaves as a single harmonic oscillator with the frequency ω. The formula $K(h) = 2/h$ remains valid for system (15). Therefore, in system (15), we set

$$K(h^*) = 2/h^* = 1/(A_x^2\omega_x^2 + A_y^2\omega_x^2),$$

where A_x and A_y are the amplitudes of the oscillators with the energy levels h_x^* and h_y^*, respectively.

Example 2. Let the above system of two oscillators (Example (15)) be the linear approximation of the smooth system

$$\begin{aligned} &\dot{x} + \omega_x^2 x = X(x, y), \\ &\dot{y} + \omega_y^2 y = Y(x, y), \quad X(0,0) = Y(0,0) = 0. \end{aligned} \tag{16}$$

To study the neighborhood of zero in detail, we increase the observation scale for the system: $x = \varepsilon\xi$, $y = \varepsilon\eta$. The resulting quasilinear system has the form

$$\begin{aligned} &\ddot{\xi} + \omega_x^2 \xi = \varepsilon X(\varepsilon, \xi, \eta), \\ &\ddot{\eta} + \omega_y^2 \eta = \varepsilon Y(\varepsilon, \xi, \eta), \quad X(\varepsilon, 0, 0) = Y(\varepsilon, 0, 0) = 0. \end{aligned} \tag{17}$$

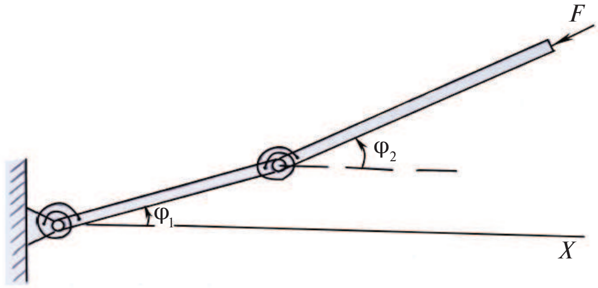

The model of an elastic rod under a follower force.

For $\varepsilon = 0$, system (17) admits single-frequency and two-frequency SOs: the latter have the basis (ω_x, ω_y). By Theorem 1, for $\varepsilon > 0$, the neighborhood of the equilibrium is filled with families of SOs with one and two frequencies. According to Theorem 2, each local SO family extends in system (16) to a global SO family and fills the oscillation domain in the system.

Example 3. The model of an elastic rod under a follower force [27].

The oscillations of beams, ropes, and cables are often studied based on adequate discrete rod models. Consider a particular case from [27]: the mechanical system consists of two identical rods of mass m and length l, connected by a hinge and a linear spring of stiffness c_2 (see the figure).

The first rod is attached by a hinge and a spring of stiffness c_1 to a fixed point O. A constant force F acts on the end of the second rod, directed along its axis. The system is located on a smooth horizontal plane. The deviations of the rods from the x-axis are described by the angles φ_1 and φ_2, respectively, measured from the straight line x; for the equilibrium, $\varphi_1 = \varphi_2 = 0$.

The kinetic energy T and the generalized forces Q_1 and Q_2 are

$$\begin{aligned} &T = \frac{ml^2}{6}[4\dot{\varphi}_1^2 + 3\dot{\varphi}_1\dot{\varphi}_2\cos(\varphi_2 - \varphi_1) + \dot{\varphi}_2^2], \\ &Q_1 = c_1\varphi_1 + c_2(\varphi_2 - \varphi_1) - Fl\sin(\varphi_2 - \varphi_1), \quad Q_2 = c_2(\varphi_2 - \varphi_1). \end{aligned} \tag{18}$$

We have a Lagrangian system with two degrees of freedom subjected to positional forces. For $F = 0$, the system is conservative.

In the equilibrium, the forces are $Q_1 = Q_2 = 0$: the system admits a unique (trivial) equilibrium. We compile the characteristic equation for the equilibrium:

$$7\lambda^4 + \frac{6a}{ml^2}\lambda^2 + \frac{36}{m^2l^4}c_1c_2 = 0, \quad a = 2c_1 + 16c_2 - 5Fl. \tag{19}$$

Under the condition $a^2 > 28c_1c_2$, the roots of this equation are pure imaginary, $\lambda = \pm\omega_{1,2}$, and the squared frequencies are given by

$$\omega_{1,2}^2 = \frac{3}{7ml^2}(a \pm \sqrt{a^2 - 28c_1c_2}).$$

The boundary value of the follower force F for the stability of the rectilinear rod configuration in the linear approximation is thus found. How will the oscillations of the rod respond to finite deviation angles?

According to Theorem 1, under incommensurable frequencies, the neighborhood of the equilibrium is filled with families of nondegenerate SOs with one and two frequencies; by Theorem 2, they extend to global families of nondegenerate SOs. Thus, only the oscillation domain filled with nondegenerate SOs is adjacent to the equilibrium. The equilibrium of the system is stable in the large.

Theorem 2 is applied to the system with a fixed parameter F that satisfies the frequency incommensurability condition. In Theorem 3, the nonlocal extension of a multifrequency oscillation in the parameter is carried out while preserving the basis. For $F > 0$, the numbers $\omega_{1,2}$ depend on F; the basis changes, so Theorem 3 is not applicable. The found nondegenerate SOs for countable values of the follower force F are not realized.

Note that for this model, the qualitative conclusions do not depend on the number of rods, and the oscillation amplitude is limited only by the spring stiffness.

For $F = 0$, symmetric oscillations exist; they are stabilized (Theorem 4) in the adaptive scheme (7).

8. CONCLUSIONS

A Lagrangian system subjected to positional forces is invariant with respect to the transformation $(q, \dot{q}, t) \to (q, -\dot{q}, -t)$ (i.e., belongs to the class of reversible mechanical systems). The phase space of the system is symmetric with respect to the set $M = \{q, \dot{q} : \dot{q} = 0\}$. An equilibrium admitting small oscillations with incommensurable frequencies is analyzed. The neighborhood of this equilibrium is filled with symmetric k-frequency oscillations (SOs), $1 \leqslant k \leqslant n$. (Here, n is the number of degrees of freedom of the system.) There are no other motions in the neighborhood. All SOs extend to global families of SOs and form an oscillation domain Ω adjacent to the equilibrium. The SO families globally extend in the system parameter. These results have been established in the paper and characterize the subject of the stabilization problem.

In an autonomous system, solutions form a family in the shift of the initial point along the trajectory. A distinction is made between the problems of stabilizing the entire family of solutions and an individual solution from the family. The second problem is solved using time-varying control. The family of solutions is stabilized by constructing a corrected system, i.e., a controlled system with an autonomous control law that acts with a small gain.

The results presented above are motivated by the problem of stabilizing multifrequency oscillations of a reversible mechanical system. This problem has not been posed previously. The subject of stabilization itself has been previously known only in the part related to Poincaré perturbation theory.

In this paper, we have described a global theory of symmetric multifrequency oscillations (symmetric conditionally periodic solutions, symmetric quasi-periodic motions, and symmetric conditionally periodic orbits) for the first time in the literature. The basic concepts have been introduced; necessary and sufficient conditions for the existence of a symmetric oscillation have been found; and local continuation properties of SOs have been established. Theorems on the birth of SOs and their extension to a global SO family, and a theorem on the global extension of SOs in the system parameter have been proved. Based on new original ideas, the theory has an accessible presentation without special knowledge requirements. Thus, a complete theory of symmetric multifrequency oscillations for a Lagrangian system subjected to positional forces has been elaborated.

This theory has been employed to pose and solve the stabilization problem (in the large) of multifrequency oscillations of a conservative system. The feedback control has been applied here; the idea was proposed by the author [9] and tested for single-frequency oscillations before. The control system (7) is independent of the number of frequencies in the SO. In the adaptive scheme, an isolated oscillation (IO) of the controlled system is stabilized. For the case of k frequencies, an IO is found close to the SO with the desired energy level h^*: the SO belongs to the global family Σ_k of k-frequency SOs. Stabilization is ensured by attracting trajectories to the IO.

The autonomous control used is universal: it applies to any Lagrangian system and stabilizes k-frequency oscillations, $1 \leqslant k \leqslant n$, where n is the number of degrees of freedom of the system. A corrected conservative system has been constructed, in which the current potential energy on the trajectory of the multifrequency SO is tracked via feedback.

REFERENCES

1. Bogolyubov, N.N., *O nekotorykh statisticheskikh metodakh v matematicheskoi fizike* (On Some Statistical Methods in Mathematical Physics), Kiev: Akad. Nauk Ukr. SSR, 1945.
2. Bogolyubov, N.N. and Mitropol'skii, Yu.A., *Asimptoticheskie metody v teorii nelineinykh kolebanii* (Asymptotic Methods in the Theory of Nonlinear Oscillations), Moscow: Nauka, 1974.
3. Arnold, V.I., Kozlov, V.V., and Neishtadt, A.I., *Matematicheskie aspekty klassicheskoi i nebesnoi mekhaniki* (Mathematical Aspects of Classical and Celestial Mechanics), Moscow: VINITI, 1985.
4. Samoilenko, A.M., *Elementy matematicheskoi teorii mnogochastotnykh kolebanii. Invariantnye tory* (Elements of the Mathematical Theory of Multifrequency Oscillations. Invariant Tori), Moscow: Nauka, 1987.
5. Pontryagin, L.S., On Dynamic Systems Close to Hamiltonian, *Zh. Eksp. Teor. Fiz.*, 1934, vol. 4, no. 9, pp. 883–885.
6. Van der Pol, B., Forced Oscillations in a Circuit with Non-linear Resistance (Reception with Reactive Triode), *The London, Edinburgh, and Dublin Philosophical Magazine and Journal of Science*, 1927, ser. VII, vol. 3, no. 13, pp. 65–80.
7. Poincaré, H., Sur les courbes définies par une équation différentielle, *Journal de mathématiques pures et appliquées*, 1882, vol. 8, no. III, pp. 251–296.
8. Andronov, A.A., Vitt, A.A., and Khaikin, S.E., *Teoriya kolebanii* (Oscillation Theory), 2nd ed., edited and supplemented by Zheleztsov, N.A., Moscow: Gos. Izd-vo Fiz. Mat. Lit., 1959.
9. Tkhai, V.N., Stabilization of Oscillations in an Autonomous Corrected Conservative System by Constructing an Attracting Cycle, *Autom. Remote Control*, 2025, vol. 86, no. 6, pp. 531–544.
10. Tkhai, V.N., An Adaptive Stabilization Scheme for Autonomous System Oscillations, *Autom. Remote Control*, 2024, vol. 85, no. 9, pp. 894–905.
11. Tkhai, V.N., Continuation of Periodic Motions of a Reversible System in Non-rough Cases with Application to the N-planet problem, *J. Appl. Math. Mech.*, 1998, vol. 62, no. 1, pp. 51–65.
12. Tkhai, V.N., Lyapunov Families of Periodic Motions in a Reversible System, *J. Appl. Math. Mech.*, 2000, vol. 64, no. 1, pp. 41–52.
13. Lyapunov, A.M., *The General Problem of the Stability of Motion*, London–Washington: Taylor & Francis, 1992.
14. Andronov, A.A. and Vitt, A.A., On Lyapunov Stability, *Zh. Eksp. Teor. Fiz.*, 1933, vol. 3, no. 5, pp. 373–374.
15. Boubaker, O., The Inverted Pendulum Benchmark in Nonlinear Control Theory: A Survey, *Int. J. Adv. Robot. Syst.*, 2013, vol. 10, no. 5, pp. 233–242. https://doi.org/10.5772/55058
16. Fradkov, A.L., Swinging Control of Nonlinear Oscillations, *Int. J. Control*, 1996, vol. 64, no. 6, pp. 1189–1202. https://doi.org/10.1080/00207179608921682
17. Åström, K.J. and Furuta, K., Swinging up a Pendulum by Energy Control, *Automatica*, 2000, vol. 36, no. 2, pp. 287–295. https://doi.org/10.1016/S0005-1098(99)00140-5
18. Shiriaev, A., Perram, J.W., and Canudas-de-Wit, C., Constructive Tool for Orbital Stabilization of Underactuated Nonlinear Systems: Virtual Constraints Approach, *IEEE T. Automat. Contr.*, 2005, vol. 50, no. 8, pp. 1164–1176. https://doi.org/10.1109/TAC.2005.852568
19. Kant, K., Mukherjee, R., and Khalil, H., Stabilization of Energy Level Sets of Underactuated Mechanical Systems Exploiting Impulsive Braking, *Nonlinear Dynam.*, 2021, vol. 106, pp. 279–293. https://doi.org/10.1007/s11071-021-06831-3
20. Guo, Yu., Hou, B., Xu, Sh., et al., Robust Stabilizing Control for Oscillatory Base Manipulators by Implicit Lyapunov Method, *Nonlinear Dynam.*, 2022, vol. 108, pp. 2245–2262. https://doi.org/10.1007/s11071-022-07321-w

21. Alexandrov, A.Yu. and Tikhonov, A.A., Electrodynamic Control with Distributed Delay for AES Stabilization in an Equatorial Orbit, *Cosmic Res.*, 2022, vol. 60, no. 5, pp. 366–374.

22. Rumyantsev, V.V., On the Stability of Motion with Respect to Part of Variables, *Vest. Mosk. Gos. Univ. Ser. Mat. Mekh. Astr. Fiz. Khim.*, 1957, no. 4, pp. 9–16.

23. Rouche, N., Habets, P., and Laloy, M., *Stability Theory by Liapunov's Direct Method*, New York: Springer, 1977.

24. Tkhai, V.N., A Family of Oscillations Connecting Stable and Unstable Permanent Rotations of a Heavy Solid with a Fixed Point, *Mech. Solids*, 2023, vol. 58, no. 6, pp. 2067–2079.

25. Bruno, A.D., *Local Methods in Nonlinear Differential Equations*, Berlin–New York: Springer-Verlag, 1989.

26. Pontryagin, L.S., *Ordinary Differential Equations*, Reading, MA: Addison-Wesley, 1962.

27. Merkin, D.R., *Introduction to the Theory of Stability*, New York–Berlin–Heidelberg: Springer, 1997.

This paper was recommended for publication by L.B. Rapoport, a member of the Editorial Board

ISSN 0005-1179 (print), ISSN 1608-3032 (online), Automation and Remote Control, 2026, Vol. 87, No. 8, pp. 713–729.

Prospects of Using Class D Amplifiers in Microgrid Systems with Nonlinear Loads

D. D. Vorontsov[*,**,a] **and N. A. Korgin**[***,b]

[*] *Moscow Institute of Physics and Technologies, Moscow, Russia*
[**] *"STC AKTOR" LLC, Moscow, Russia*
[***] *Trapeznikov Institute of Control Sciences, Russian Academy of Sciences, Moscow, Russia*
e-mail: [a] *vorontsov.da@phystech.edu,* [b] *nkorgin@ipu.ru*

Received June 27, 2025
Revised December 26, 2025
Accepted February 17, 2026

Abstract—Modern methods for mitigating nonlinear inverter voltage distortions in low-power microgrid systems are considered: proportional-resonant/multi-resonant controllers, virtual impedance and droop control, dual voltage inverters, and self-oscillating class D amplifiers. The study outlines the fundamental properties and the principle of parasitic harmonic mitigation. Special attention is paid to the number of controllers required to implement each of the methods, the effectiveness of nonlinear distortion mitigation through the study of the number of harmonics, and the reduction of the total harmonic distortion with and without the application of each method. The compatibility of each method with the output power controller is also analyzed. The benefits and drawbacks of existing methods are analyzed, as well as the prospects of using a self-oscillating class D amplifier for the control of nonlinear distortions in microgrid systems.

Keywords: microgrid, voltage source inverter, total harmonic distortion, power quality, nonlinear load

DOI: 10.7868/S1608303226080048

1. INTRODUCTION

Nowadays, research in the field of off-grid power systems and the additional storage and delivery of electrical energy (EE) to the AC grid is actively developing. A system consisting of an EE source and a converter, designed for parallel connection with another similar system or with a power grid, is called a microgrid system. AC systems are preferred for power distribution. At the core of an AC microgrid is a voltage-source inverter(VSI), which performs the conversion from direct current to alternating current (DC/AC conversion). In recent years, microgrid VSIs have developed significantly. Existing synchronization methods [1, 2] allow not only several inverters to operate parallel to each other but also to connect to a common power grid to supply electricity, as well as to control the output power using droop control technology [3]. However, in isolated systems consisting of several sources and inverters, as well as in low-power grids disconnected from large-scale power grids, the challenge of mitigating nonlinear distortion is critical. Connecting a load with a high nonlinearity index can lead to a severe distortion of the grid voltage. The nonlinearity index—total harmonic distortion (THD)—is regulated by GOST [4] and must be no more than 8%. Violation of this power quality indicator can lead to both the failure of connected electrical equipment and the incorrect operation of the phase-locked loop (PLL), resulting in the desynchronization of the VSI.

2. MODERN MICROGRID VSI

2.1. Isolated VSI

Before proceeding to the comparison of methods for mitigating nonlinear distortions, it is necessary to describe the system under study to which these methods are applied. A voltage source inverter, by definition [9], is a converter that transitions direct current to alternating current [10]. Modern DC/AC converters are based on full-bridge or half-bridge circuits [11]. Fundamentally, the control of full-bridge and half-bridge circuits has no significant differences. The main difference between these circuits is the number of power switches; transistors are most often used for this purpose. Due to this difference, restrictions are imposed on the inverter regarding the maximum DC voltage and current through each arm of the converter. In microgrid inverters, half-bridge circuits are more frequently used, requiring a higher input voltage, since working with alternative EE sources, such as wind or solar energy, often involves high DC voltages. Figure 1 shows a classic diagram of a half-bridge converter and a control loop. For the correct operation of this circuit, at least one current controller is required [11] to form the reference signal and pulse-width modulation (PWM) supplied to the gates of the switches. In the general case, the functions f, g can be arbitrary nonlinear functions of its variables. In the classical case, these functions describe a sinusoidal signal:

$$i_{ref}(t) = I \sin(\omega t + \varphi_0).$$

The compensator is most often a proportional-integral (PI) controller. In the case of synchronizing inverters with other similar inverters or with the grid, the description of the AC system cannot be set arbitrarily; the sinusoidal signal must be synchronized with respect to what is observed in the grid.

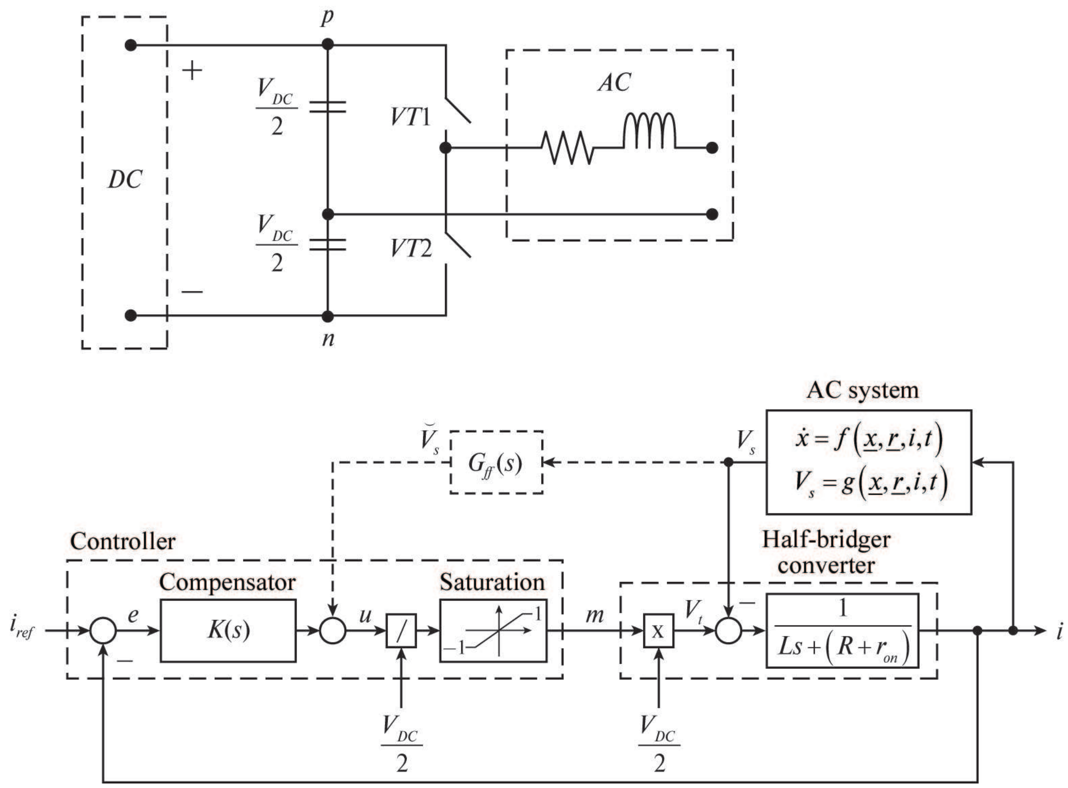

Fig. 1. Half-bridge converter.

2.2. Phase-Locked Loop Synchronization

The most widely used method for generating a reference signal from the available AC grid voltage is the phase-locked loop (PLL). The block diagram of the classic PLL method for a three-phase grid [1, 2] is shown in Fig. 2. It is important that the voltage is regulated in a rotating dq0 reference frame, the transition to which is carried out using Clarke and Park transformations [12]. The angle θ obtained as a result of the method's operation is the rotation angle of the grid's quadrature basis. Specifically, this angle is the phase angle of the first phase. For a single-phase grid, this method is also applicable; it is necessary to artificially create an orthogonal signal β lagging behind the original one by $\pi/2$ [6–8, 13]. One of the fastest methods is the SOGI (Second Order Generalized Integrator) PLL method [7], which uses a second-order integrator applied to the original signal. Thus, the phase angle obtained using the PLL method can be used for the inverse Park–Clarke transformation. Combined with the control method outlined in the previous section, the system provides the minimum required number of controllers for the parallel operation of a voltage source inverter and an arbitrary AC power grid; however, such a control method has a significant drawback. Despite the ability to control the output current of the inverter, the resulting control loop does not allow one to control the values of active and reactive output powers. To be able to accurately control the output power, a droop controller is added to the system.

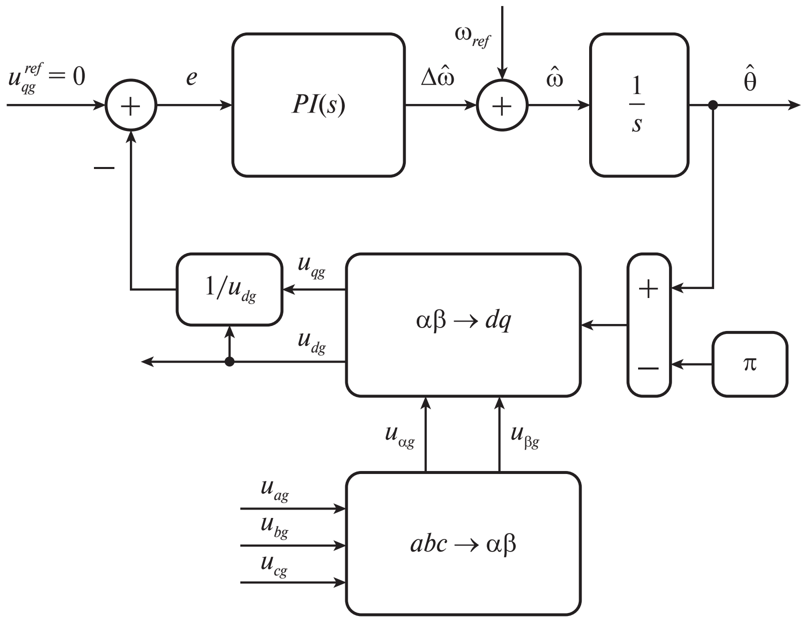

Fig. 2. PLL synchronization of a three-phase grid.

2.3. Droop Control

To control the active and reactive power, it is necessary to introduce at least two controllers that control the change in power. The classic droop control method can be written as follows:

$$f = f_0 - mP,$$
$$U = U_0 - nQ,$$

where f and U are the frequency and voltage values of the reference signal, respectively, and f_0 and U_0 are the voltage and frequency settings; in the case of a utility grid, $f_0 = 50$ Hz and $U_0 = 230$ V; m, n are the controller coefficients, and P, Q are the measured active and reactive

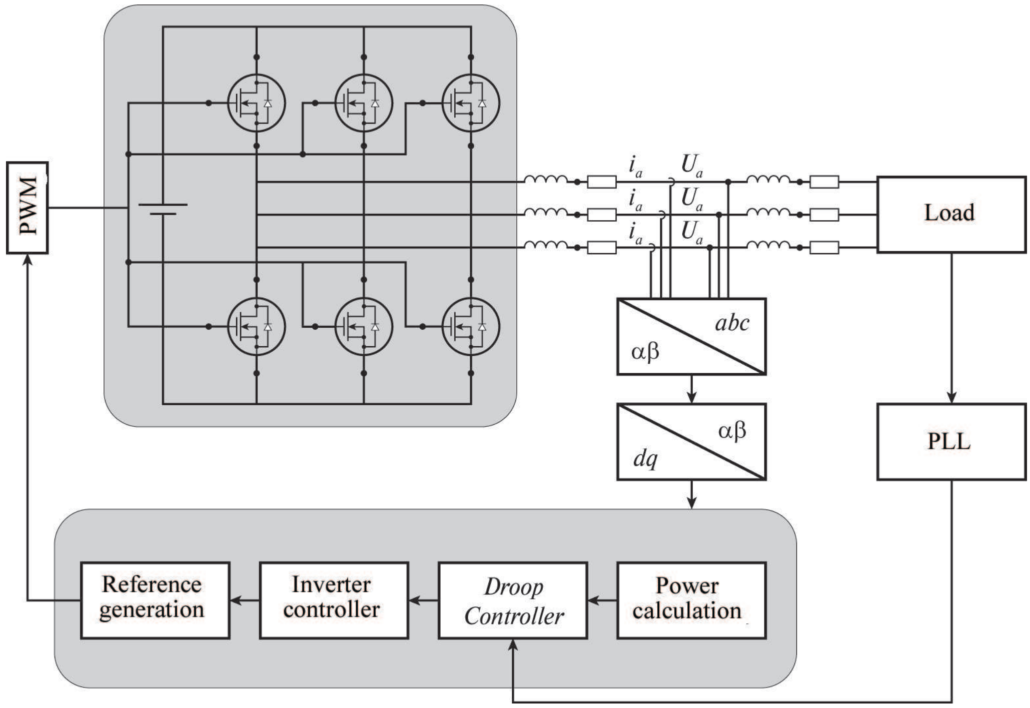

Fig. 3. Conventional control scheme of a microgrid voltage source inverter.

power. When operating in the $dq0$ basis, instantaneous power values are conveniently calculated using the equations:

$$P = V_d I_d + V_q I_q,$$
$$Q = V_q I_d - V_d I_q.$$

The block diagram for controlling the inverter using a PLL block and droop control is shown in Fig. 3. This control scheme has a total of at least four proportional or PI controllers. In [14–16], it is proposed to add or complicate droop controllers to improve transient characteristics and increase the accuracy of output power regulation. However, as part of the comparison of methods for mitigating nonlinear harmonics, additional droop controllers are omitted if the harmonic mitigation method does not suggest otherwise. Going forward, when comparing the number of controllers necessary to implement a particular method, the baseline will be the modified control scheme shown in Fig. 3.

3. METHODS FOR MITIGATING NONLINEAR DISTORTIONS

Before moving directly to the methods for mitigating nonlinear distortions in voltage source inverters, the following important definitions are introduced. A nonlinear load is any load whose current depends on the voltage nonlinearly. Parasitic or nonlinear harmonics are voltage components at frequencies different from the fundamental frequency; in the case of a utility grid, this means any voltage harmonics other than 50 Hz. To assess the level of nonlinear distortions, various metrics are used, such as: THD—the ratio of the root mean square (RMS) value of parasitic harmonics to the RMS of the fundamental; total rated current distortion (TRD)—calculated similarly to THD but for the load current; total demand distortion—the ratio of the RMS of parasitic current harmonics to the RMS value of the load current. These metrics are regulated by international standards IEEE 519 and IEEE 1547, as well as GOST 32144-2013 [4]. The voltage signal is the most sensitive regarding nonlinear distortions, as severe distortions can lead to incorrect PLL operation, which in turn can cause the inverter to fail.

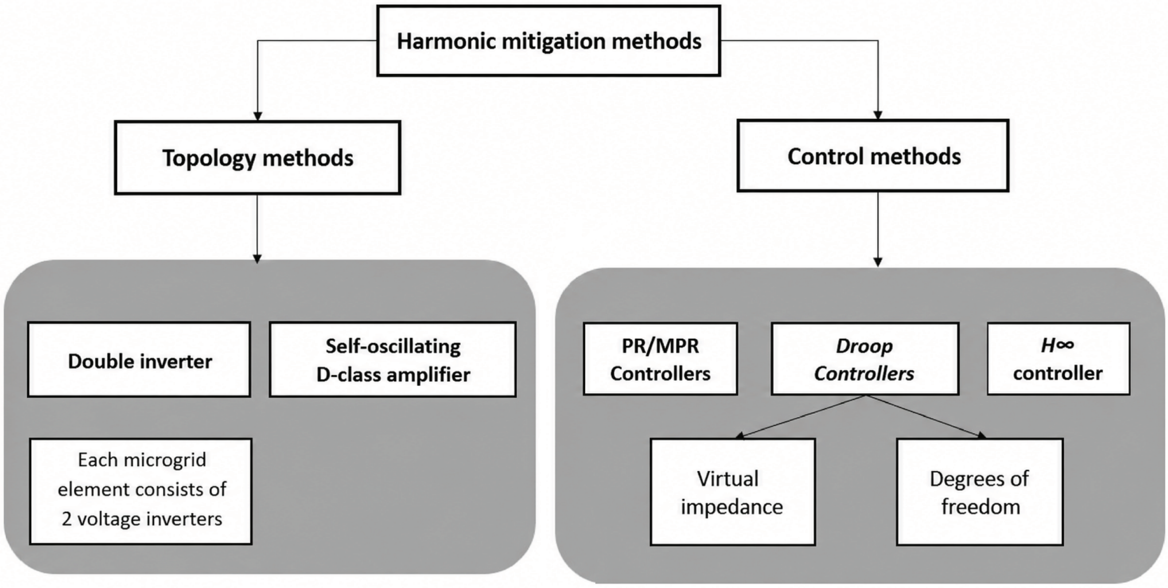

Fig. 4. Categorization of harmonic mitigation algorithms.

Methods for mitigating nonlinear harmonics can be roughly divided into two main categories: controller-based and topological. Controller-based methods include those based on changing the system's control loop, thereby mitigating voltage nonlinearities. These methods can be further divided into two main categories: methods using resonant controllers (introducing proportional resonant or multiresonant (PR or MPR) controllers into the control loop [17–21]), and methods modifying the droop controller (by introducing additional controllers and modifying the droop controller, an improvement in the voltage signal was achieved [14, 22–27]). Separately, it is worth mentioning the H∞ controller, which also allows mitigating nonlinear distortions, although currently, this controller is practically not used. Topological methods refer to modifying the inverter topology, moving away from the classical half-bridge circuit. Thus, in [28], a circuit with counter-connection of two inverters is used for harmonic mitigation. In [5, 29], a self-oscillating class D amplifier is used as an inverter; however, this method is poorly studied in the field of microgrids. A conditional breakdown of modern methods is presented in Fig. 4.

3.1. PR and MPR Controllers

One of the most common methods for improving power quality in microgrid inverters is the use of a PR controller instead of a classic PI current controller [17–19]. Such a controller has infinite gain when the input signal has a resonant frequency. In real systems, achieving such a transfer function is impossible; besides, in a real system, the signal frequency will slightly differ from the carrier frequency due to the inevitable presence of higher-order harmonics. To describe a real PR controller, a damping frequency $\omega_c \ll \omega_0$ is introduced, where ω_0 is the frequency limiting the gain near the resonant frequency. The transfer function of such a controller is written as follows:

$$W(s) = K_p + \frac{2K_r\omega_c s}{s^2 + \omega_0^2}.$$

In [18, 19, 21], the process of designing an inverter with a PR controller to improve power quality is described in detail. Figure 5 shows the block diagram for controlling such an inverter. In [30], a comparative analysis of the operation of an inverter with PI and PR controllers in three-phase systems with an unbalanced load was carried out, and the THD index was analyzed. An unbalanced

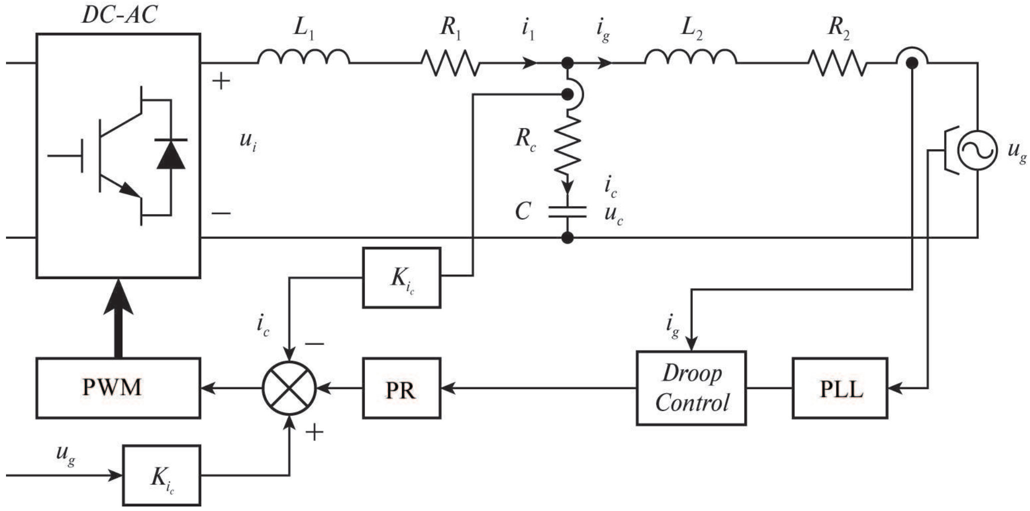

Fig. 5. Block diagram of inverter control with a PR controller.

load can introduce small nonlinear distortions into the voltage signal, which are well mitigated by a PR controller added to the control scheme. However, with a high degree of distortion, [31, 32] propose using a MPR controller. It proposes to add additional components operating at $n\omega_0$ to the transfer function of a simple PR controller, where n is the number of the harmonic introducing strong nonlinear distortions. Thus, the additional component of the controller has a higher gain the higher the amplitude of the nth harmonic. The transfer function of such a controller is described by the equation:

$$W(s) = K + \frac{2K_r\omega_c s}{s^2 + \omega_0^2} + \sum_n \frac{2K_{r,n}\omega_c s}{s^2 + 2\omega_c s + n\omega_0}.$$

The equation uses a sum over harmonics that are multiples of the carrier; in the general case, the frequency of the additional resonance can be an arbitrary frequency introducing distortions into the signal; however, in electrical systems, parasitic harmonics are multiples of the fundamental, which simplifies the application of the controller. The advantages and disadvantages of these controllers are evaluated below.

Advantages:

- PR controller mitigates small distortions without adding and tuning additional controllers.
- MPR controller allows for nonlinear harmonic mitigation even for severe distortions.
- Both controllers show good results when working with an unbalanced load.
- The methods are widely studied in various scientific papers; there are detailed guidelines for designing microgrid inverters using PR and MPR controllers.

Limitations:

- When mitigation is required, the number of resonant components increases significantly, each of which requires additional tuning. In [20, 22], a method for automatic tuning is proposed; however, tuning is still necessary.
- With a large number of resonant controller components, the computational complexity of the system increases significantly. In the case of using automatic coefficient tuning, the computational power required increases multiplicatively.

3.2. Droop Controller-Based Methods

The second large group of controller-based compensators can be considered methods for mitigating nonlinear harmonics based on the modification of the droop controller. They can be roughly divided into the virtual impedance modification method [24, 26] and the multiple degrees of freedom controller method [23].

The study examines methods using virtual impedance [26]. Initially, this method was used to improve the stability indicators of microgrid systems connecting reactive loads. The essence of the method is the artificial formation of impedance in the system and adding it to the result of the droop control module. This allows controlling the output power of the system more precisely, and according to [14], also increases system stability in the event of incorrect tuning of the droop coefficients. Figure 6 shows the basic scheme for constructing a virtual impedance. In [25], it is proposed to use two droop controllers (before and after the addition of virtual impedance), as well as additional controllers that monitor the magnitude of the generated virtual impedance. As a result of the system operating on a rectifier load with an RC circuit, the TRD indicator was reduced by 22.70%. In [26], a two-stage virtual impedance generation scheme is proposed, consisting of a classic virtual impedance shaper, to the input of which the load current is supplied. The second part of the shaper is an active impedance component shaper based on the inverter output current. The study also applied PR current and voltage controllers, as a result of which the system THD decreases by 12.5%. The fastest mitigation method is proposed in [27]. Current and voltage controllers, when using virtual impedance in this work, use a matrix of separated harmonics; each element of the proposed matrix carries information about a specific harmonic, as a function of the other harmonics of the signal and the amplitude of this harmonic. As a result of the experiments conducted in this study, the high response speed of such a system when connecting a nonlinear load was revealed. The THD index in this case decreases to 2%. The advantages and limitations of using these methods are summarized below.

Advantages:

- Allows mitigating strong nonlinear distortions; with certain tuning, it also allows controlling the THD value of the output voltage.
- Based on the droop control method, which guarantees the ability to control the inverter's output power.

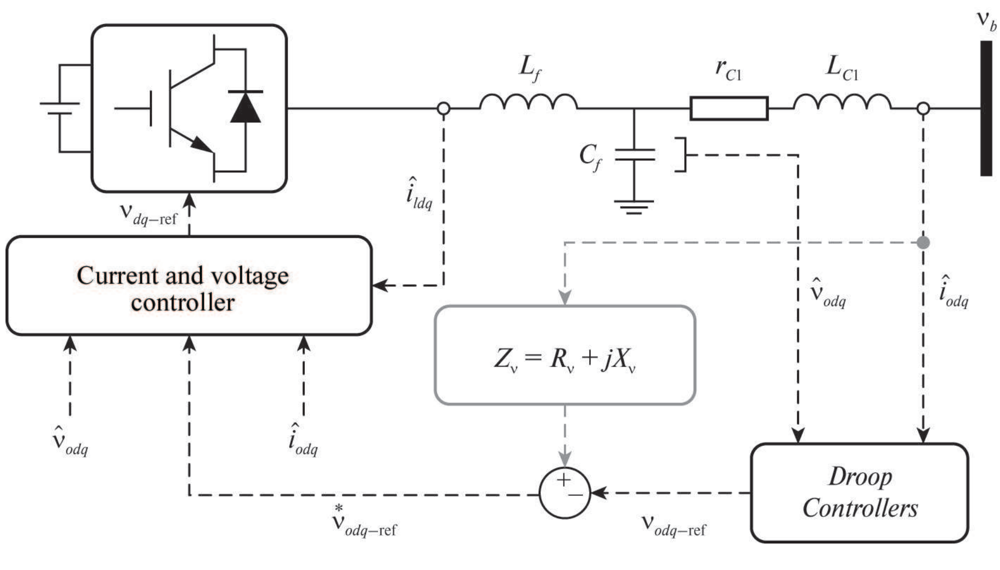

Fig. 6. Block diagram of virtual impedance controllers.

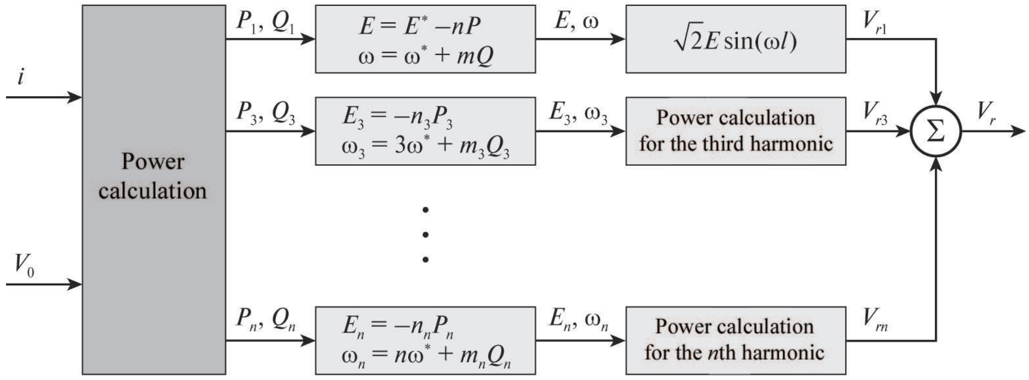

Fig. 7. Droop controller with multiple degrees of freedom.

- The methods are widely studied in various scientific papers.

Limitations:

- To use this method, it is necessary to introduce at least three additional controllers; applying modern methods based on virtual impedance control also requires the use of additional voltage control loops or droop controllers.
- The use of method [27] requires extremely complex computational operations, which significantly increases the need for computing power of the control processor.

The discussion now shifts to the droop controller method with multiple degrees of freedom [23]. The paper proposes dividing the classical method into several constituent parts, each of which will be responsible for a specific harmonic. The controller for each harmonic can be written as follows:

$$E_i = -n_i P_i,$$
$$\omega_i = n\omega - m_i Q_i,$$

where n_i, m_i are the controller coefficients for each harmonic, and P_i, Q_i are the power of the ith harmonic. The structural diagram of this method is presented in Fig. 7. In this case, to calculate the power of the ith harmonic, the method of separate power calculation [33] is used. The result of the controller's operation is the voltage setting of the inverter taking into account the mitigation of parasitic harmonics. The effectiveness of this method is shown when operating isolated microgrid systems; however, this method has both advantages and significant limitations.

Advantages:

- Allows mitigating arbitrary nonlinear distortions caused by various nonlinear loads.
- Allows mitigating individual harmonics by introducing only one additional calculation link.
- Based on the droop control method, which allows for highly accurate control of the inverter's output power.

Limitations:

- To mitigate a large number of parasitic harmonics, it requires additional tuning of the controllers for each harmonic, which significantly increases computing power requirements.
- Calculating active and reactive power for each individual harmonic requires large computing power.
- Complex tuning of controllers for each of the harmonics.
- The method is poorly researched, which can lead to difficulties in system design.

3.3. H∞ controller

In [34], an inverter control method based on the use of an H∞ current controller and an internal low-pass filter is proposed. The proposed strategy consists of a cascaded current, voltage controller and control loops that are created on H∞ controllers. Modeling of both isolated network operation and connection to a utility grid was carried out. The proposed methods have a number of advantages and limitations.

Advantages:

- The proposed method copes with small nonlinear grid distortions.
- The controller provides a smooth transition from autonomous operation to grid-connected operation.
- The controller does not require high computing power; tuning the controller boils down to a convex problem.

Limitations:

- The application of this method is poorly researched; works are based on mathematical modeling.
- The H∞ controller is difficult to implement in discrete systems.
- The possibility of connecting droop control in the proposed system has not been investigated.

3.4. Dual VSI

Dual voltage inverter The discussion now shifts to topological methods for parasitic harmonic control. Of special attention is the method proposed in [28]. The method is based on changing the inverter topology. Thus, rather than a classic half-bridge circuit, two voltage source inverters are used. The first main inverter provides the payload and is synchronized using the PLL method. The additional inverter operates in opposition to the main one and creates a signal that, when added

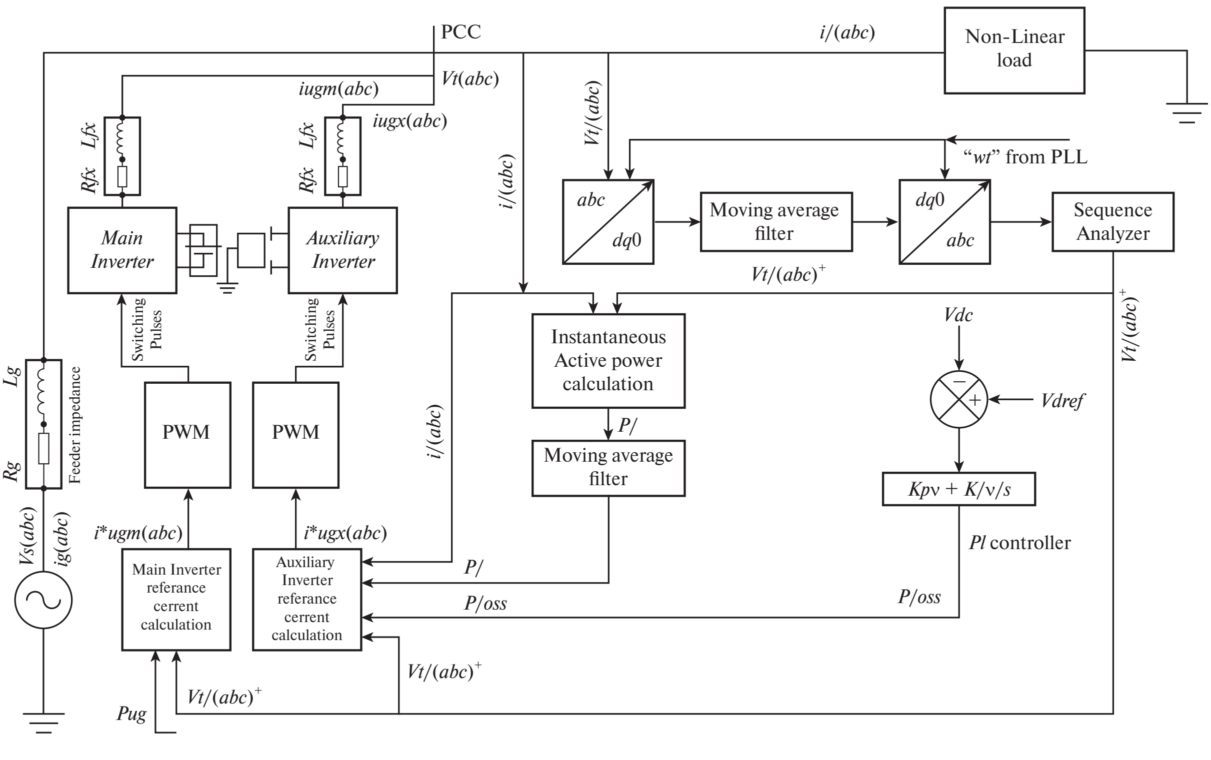

Fig. 8. Control loop of a dual voltage source inverter.

to the signal from the main inverter, provides a common output signal with minimized distortions. For the operation of the additional inverter, in addition to the usual control circuit setting the reference voltage and mitigating nonlinear distortions, it is required to account for ohmic losses at the inverter output; for this, an additional PI controller is introduced into the control loop, to the input of which the difference between the target inverter voltage and the constant DC bus voltage is fed. The complete control circuit for the proposed dual inverter is presented in Fig. 8. According to the experiments conducted in the work, the proposed microgrid inverter copes excellently with mitigating nonlinear harmonic components and provides a decrease in THD by more than 8 times. The advantages of such an inverter:

Advantages:

- High output voltage stability provided by the compensating additional inverter.
- Low need for computational load, since this inverter requires the introduction of an additional five controllers to control the additional inverter.
- The ability to mitigate arbitrary harmonics by setting a special reference signal for the additional inverter.

Limitations:

- The need to design an additional voltage inverter based on a half-bridge circuit, as well as an additional output filter.
- Increased power consumption caused by ohmic losses at the output of the additional inverter.
- High system cost due to the use of two inverters.

3.5. Self-Oscillating Class D Amplifier

One of the methods for mitigating nonlinear distortions at the inverter output is based on the use of a self-oscillating class D amplifier [9]. Such an amplifier circuit has not previously been used in microgrid systems. This amplifier performed well in acoustic systems. This topology copes excellently with suppressing interference when amplifying an acoustic signal [35]. In [29], a method for using such an inverter as a power microgrid inverter is proposed, and in [5], the operation of a class-D inverter as part of both an isolated and a grid connected microgrid system is modeled. An analysis of operation on a nonlinear rectifier load and a comparison with the classic inverter described in Section 2 of this article was carried out.

3.5.1. Amplifier Control

The control system of the self-oscillating class D amplifier is examined in greater detail below. Figure 9 presents the electrical and structural diagrams of the auto-generating class D amplifier in operational form. Here the operators W_1–W_8 are frequency response functions of the circuit consisting of passive elements, and $W_n(A)$ is the frequency response function of the series-connected comparator D_2 and half-bridge converter D_3, where A is the auto-generation voltage magnitude. In this system, the condition for self-oscillations is satisfying the harmonic balance equation for the frequency response functions of the power switch $W_n(A)$ and the linear part of the system $W_t(2\pi jf)$, i.e., the presence of a purely imaginary root of the linearized system:

$$W_n(A)W_t(2\pi jf) = -1. \tag{1}$$

As a result of solving equation (1), obtained in [29], the auto-generation condition is met at a frequency $f_0 = 92.5$ kHz. The transfer functions of the amplifier are expressed as follows:

$$W_{fb} = W_5W_6W_7W_n(-1), \tag{2}$$

$$W_d = \frac{W_{fb}W_4}{1 + W_{fb}W_8}. \tag{3}$$

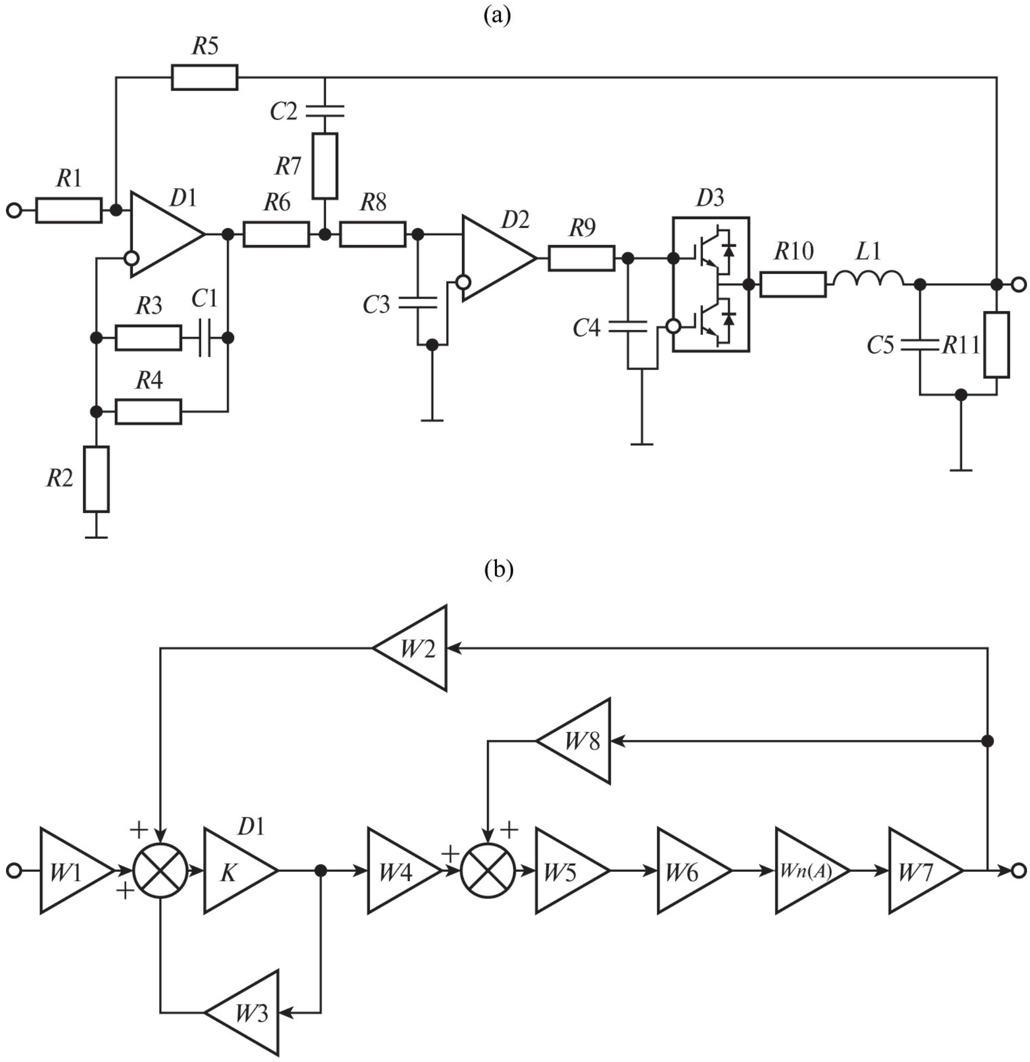

Fig. 9. (a) Electrical circuit, (b) block diagram of a self-oscillating class-D amplifier.

Here (2) is the open transfer function of the class D amplifier, and equation (3) is the frequency response function taking into account the negative feedback W_8 and the integrating link W_4. The system described in relation (3) has a significant drawback: the transmission coefficient of such an amplifier changes by more than 4 times, and the phase shift is from $\pi/2$ to π radians. The introduction of an additional feedback W_2 closed through an operational amplifier D_1 covered by its own feedback W_3 allows solving this problem. From the frequency response function of an ideal operational amplifier (gain $K \to \infty$) (4) and the transfer function of the amplifier, the system transfer function (5) is derived:

$$W_o = \frac{K}{1 + KW_3} \approx \frac{1}{W_3}, \tag{4}$$

$$W = \frac{W_d W_1}{W_3(1 + \frac{W_d}{W_3} W_2)}. \tag{5}$$

In [5, 29] it is demonstrated, through modeling, the high stability of the self-oscillating class D amplifier to nonlinear distortions introduced by a rectifier capacitive load; according to the simulation results, the THD index of the system decreased by more than 10 times. It is also noteworthy that

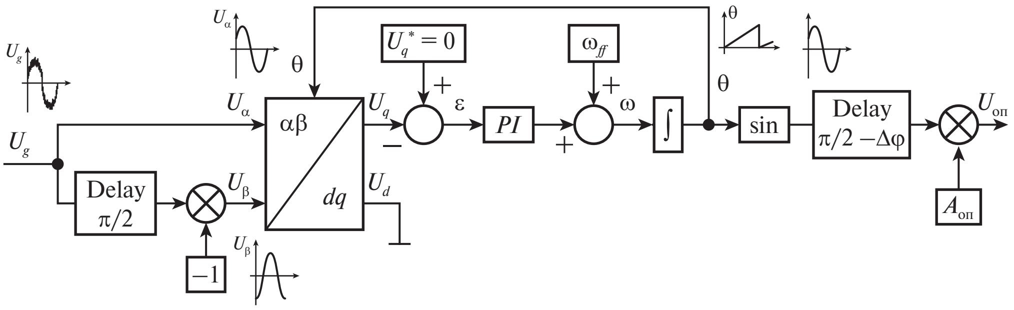

Fig. 10. PLL scheme for synchronization of a self-oscillating class D amplifier.

PWM generation and the current control loop in this inverter are implemented via analog means, and a small-amplitude sinusoidal signal is applied to the amplifier input.

3.5.2. Synchronisation Control

Attention is now directed toward the synchronization control method of the class D self–oscillating amplifier to form an isolated microgrid system. One of the main features of this inverter control method is the analog PWM circuit; because of this, unlike the aforementioned control methods, an analog sinusoidal signal of small amplitude is supplied to the input of the electrical system, which subsequently forms discrete signals on the gates of the power transistors. This feature allows significantly reducing the PLL loop processing frequency. When designing a PLL for this inverter, it is also necessary to take into account the presence of a constant DC offset of the output signal relative to the input by an angle $\Delta\varphi$. Figure 10 shows the structural diagram of PLL control for a self-oscillating class-D amplifier. It can be observed that the primary difference from the classic single-phase PLL is the presence of a phase shift at the output of the loop. In addition to accounting for the phase shift when working with analog PWM, it is also necessary to take into account the difference in the amplitude of the PLL input signal, measured directly at the inverter output (in the case of a utility grid, the amplitude of such a signal will be 310 V) and the amplifier input signal. Simulation data [5] and experiments show that this signal varies in the range of 3–5 V. Therefore, a multiplier is added to the output of the PLL loop, which allows forming the reference signal using the formula:

$$U_{ref} = A_{ref} \sin(\theta + 2\pi - \Delta\varphi),$$

where A is calculated when the converter is launched before turning on to the common microgrid network using the formula:

$$A_{ref} = \left.\frac{U_{in}}{U_{out}}\right|_{U_{out}=220\text{ V}}.$$

Consequently, to control the synchronization of the inverter based on a class D amplifier, a simple modification of the classic PLL control circuit with computationally simple modifications that take into account the features of the self-oscillating class D amplifier is used.

3.5.3. Benefits and Drawbacks of the Method

The advantages and limitations of this method for mitigating nonlinear distortions in a microgrid inverter are evaluated below.

Advantages:

- Nonlinear harmonic mitigation regardless of the connected load without the use of additional controllers.
- Analog implementation of current and voltage feedback and PWM generation, allowing to significantly reduce the computational load on the control processor.

- The ability to form a reference signal using the droop control method and virtual impedance.
- Mitigation of an arbitrary number of parasitic harmonics.

Limitations:

- More complex design of the inverter's electrical circuit.
- Insufficiently researched in the field of microgrid inverters.
- The need to generate an analog reference signal to control the inverter.

4. COMPARISON OF THE DESCRIBED METHODS

Several methods for mitigating nonlinear distortions in microgrid voltage source inverters have been described. Each of the listed methods presents a certain amount of both advantages and disadvantages. PR, MPR, and virtual impedance controllers are currently well studied and cope with mitigating nonlinear loads; however, the more distorted the voltage signal, the greater the computing power required for this. The H∞ controller performs excellently in transitioning from autonomous operation to grid-connected operation, and also copes with nonlinear distortion mitigation; however, the implementation of an H∞ controller in a discrete system requires additional study. Also, an inverter based on such a controller requires additional experimental research, since most modern studies in this area describe mathematical models of the system. The dual voltage inverter topology allows mitigating any nonlinear distortions without a significant increase in computational load, but requires designing two power inverters, which also increases system losses. The self-oscillating class-D amplifier has not previously been used in microgrid systems, but has performed well in isolated operation on nonlinear loads and, according to simulation results, is capable of operating as part of a microgrid without losing its properties. In addition, simple analog current control and PWM generation reduce the computational burden on the system. For further comparison of the proposed methods, we define the main parameters by which one can make a choice in favor of using one or another method for mitigating nonlinear harmonics.

(1) Number of controllers. This parameter reflects the computational load on the control processor, as well as the complexity of setting up the final system. A smaller number of controllers corresponds to a lower system need for computing power. For fair evaluation, Section 2 provides the minimum number of controllers for controlling each inverter; at the same time, the analog implementation of these controllers will not be taken into account in the total number of controllers, since it does not carry a computational load during the inverter operation.

(2) Mitigated harmonics. This parameter allows evaluating the complexity of the nonlinear load connected as part of the experiment. This parameter is especially critical for methods that use additional controllers to mitigate each voltage harmonic.

(3) Absolute THD decrease, %. Allows evaluating the overall usefulness of the method in mitigating nonlinear harmonics. The final THD indicator according to GOST [4] must strictly be less than 8% for the correct operation of the system.

(4) THD ratio. Calculated as the ratio of the THD indicator without using a particular method to the THD indicator using this method. Allows quantifying the effectiveness of each method in mitigating nonlinear distortions.

(5) Droop control compatibility. Potentially, each of the methods is compatible with the Droop control method; however, within the framework of modern research, this technology has not been applied to each of the described methods, which, in turn, can open the way to new research.

(6) Investigated nonlinear loads. Most studies describe the nonlinear load used. Understanding the load topology will significantly help in designing a distortion-resistant voltage source inverter. The most dangerous for inverter operation is a rectifier load with an RC cha in; inverters that handle such a load well are most resistant to nonlinear voltage distortions.

Comparison of the described methods for mitigating nonlinear distortions

Criterion	MPR	Virtual impedance	Dual inverter	H∞ controller	Multiple degrees of freedom	Class D inverter
Number of controllers	$^3N+3$	Min. 8, max. N^2+3	7	^{2}5	$N+3$	^{1}3
Harmonics mitigated	^{3}Up to 11	^{1}Up to 15	^{3}Up to 11	^{2}Up to 13	1, 5, 7, 11	^{1}Up to 15
THD decrease, %	5.28–2.806	29.85–6.37	28.37–3.22	5.31–2.00	N/A	11.75–1.16
THD ratio	1.88	^{3}4.69	^{2}8.81	2.655	N/A	^{1}10.13
Droop control compatibility	^{1}Compatible	Required	^{2}Not investigated	^{2}Not investigated	Required	^{2}Not investigated
Investigated load	^{2}DBR + *R*, *RL*, *RC*	^{1}DBR + *R*, *RL*, *RC*, *LC*	N/A	^{3}DBR + *RL*, *LC*	Unbalanced reactive load	^{2}DBR + *R*, *RL*, *RC*

Table provides a comparative characteristic of the proposed methods for mitigating nonlinear harmonics. The indices 1, 2, 3 in the table mark those cells whose method parameters are most effective for a given criterion; the smaller the index—the more effective the method. For methods that use controllers to mitigate each of the harmonics, the designation N is used in the first criterion—the number of harmonic controllers.

4.1. Prospects of using the class D amplifier

The primary advantages and prospects for using a self-oscillating class-D amplifier in microgrid systems are described below.

(1) Comparative characteristics provided in table, indicate that the self-oscillating class D amplifier requires the smallest number of controllers to ensure the operation of the control loop. Since each of the methods uses feedback controllers similar in their action, the computational load introduced by each of the controllers can be considered additive. In view of this, it can be stated that the self-oscillating class D amplifier requires the least computational cost to implement a control loop for a microgrid inverter with the ability to mitigate nonlinear harmonics.

(2) Based on the results of comparing the number of mitigated harmonics, as well as the decrease in the THD level, it is concluded that the use of a self-oscillating class D amplifier is more effective than many modern methods in the quality of nonlinear load mitigation, which indicates the possibility of use not only in microgrid systems with strict requirements for allowable computing power but also in systems with high requirements for the quality of supplied electricity.

(3) In view of the use of analog PWM generation for controlling the synchronization of a self-oscillating class D amplifier, calculating the pulse length of the discrete signal supplied to the gates of power transistors is not required. This factor also allows reducing the computational load on the controller unit, since a significant reduction in the frequency of the control loop operation is permissible.

Based on the aforementioned factors, the primary applications of a self-oscillating class D amplifier in microgrid systems are deducted: these are systems that require a stable sinusoidal signal under conditions of high nonlinearity of the connected load, for example, high-power chargers; these are microgrid systems that impose restrictions on computing power, for example, small-sized ones. The self-oscillating class-D amplifier ensures operation in microgrid systems with the described requirements.

5. CONCLUSION

Based on the results presented in table, it can be concluded that further research into self-oscillating class-D amplifiers within the framework of microgrid systems is necessary. Such a voltage source inverter requires less computational power, while excellently handling regulation under conditions of high load nonlinearity. Experimental validation of the results presented in [5] is the next research step. Additionally, it is necessary to conduct research into the compatibility of such an inverter with droop control technology. When designing low-power grid-connected microgrid systems, as well as isolated ones based solely on identical voltage source inverters, the property of system invariance with respect to the connected load is extremely important. The use of a self-oscillating class D amplifier at the core of such a system will allow this task to be handled effectively, requiring less computational power than when using other harmonic mitigation methods.

In addition to research on the self-oscillating class-D amplifier, attention should also be paid to research on the $h\infty$ controller. Experimental validation of the results presented in [34], as well as research into the droop control method as part of such an inverter, will potentially reveal the benefits of this method compared to the most frequently used ones.

THD mitigation indicator for the dual inverter method [28] also deserves special attention. With a small increase in computational power, the authors managed to achieve a better indicator than when using MPR and virtual impedance methods. Further research in this area may also reveal additional benefits of the proposed method.

Most of the proposed methods, according to [36], are potentially applicable to the issue of controlling circulating currents arising as a result of the parallel operation of several inverters. Research in this area is also currently extremely relevant, as the control and minimization of circulating currents will increase system operation efficiency and reduce ohmic losses.

REFERENCES

1. Kulkarni, S.V. and Gaonkar, D.N., An investigation of PLL synchronization techniques for distributed generation sources in the grid-connected mode of operation,*Electric Power Systems Research*, 2023, vol. 223, art. no. 109535.
2. Adzic, E., Porobovic, V., Dumnic, B., et al., PLL synchronization in grid-connected converters, *Proc. 15th International Power Electronics and Motion Control Conference (EPE/PEMC)*, 2012, Novi Sad, pp. 1–7.
3. Tayab, U.B., Roslan, M.A.B., Hwai, L.J., and Kashif, M., A review of droop control techniques for microgrid, *Renewable and Sustainable Energy Reviews*, 2017, vol. 76, pp. 717–727.
4. *GOST 32144-2013*, State Standard of the Russian Federation, Electrical energy, introduced July 1, 2014.
5. Vorontsov, D.A., Modeling of parallel operation of D-class amplifiers as a microgrid voltage inverter, *Upravlenie bol'shimi sistemami*, 2025, no. 118, pp. 300–324.
6. Karimi-Ghartemani, M., Ooi, B.-T., and Bakhshai, A., Application of enhanced phase-locked loop system to the computation of synchrophasors, *IEEE Transactions on Power Delivery*, 2011, vol. 26, no. 1, pp. 22–32.
7. Hackl, C.M. and Landerer, M., Modified second-order generalized integrators with modified frequency locked loop for fast harmonics estimation of distorted single-phase signals, *IEEE Transactions on Power Electronics*, 2020, vol. 35, no. 3, pp. 3298–3309.
8. Du, H., Sun, Q., Cheng, Q., et al., An adaptive frequency phase-locked loop based on a third-order generalized integrator, *Energies*, 2019, vol. 12, art. no. 309.
9. Potashov, R. and Kuznetsov, S., New class-D amplifiers based on UCD technology, *Novosti elektroniki*, 2007, no. 2, pp. 20–24.

10. Meleshin, V.I., *Tranzistornaya preobrazovatel'naya tekhnika* (Transistor converter technology), Moscow: Technosphera, 2005, pp. 374–390.

11. Yazdani, A. and Iravani, R., *Voltage-Sourced Converters in Power Systems: Modeling, Control, and Applications*, Hoboken, NJ: IEEE Press/Wiley, 2010, ch. 2, pp. 21–47.

12. Chattopadhyay, S., Mitra, M., and Sengupta, S., Clarke and Park transform, *Electric Power Quality*, 2011, pp. 89–96.

13. Ciobotaru, M., Teodorescu, R., and Blaabjerg, F., Improved PLL structures for single-phase grid inverters, *Proc. Power Electronics and Intelligent Control for Energy Conservation Conference (PELINCEC)*, 2005, pp. 1–6.

14. Keyvani-Boroujeni, B., Fani, B., Shahgholian, G., et al., Virtual impedance-based droop control scheme to avoid power quality and stability problems in VSI-dominated microgrids, *IEEE Access*, 2021, vol. 9, pp. 144999–145011.

15. Fan, B., Li, Q., Yao, G., et al., A novel droop control strategy of reactive power sharing based on adaptive virtual impedance in microgrids, *IEEE Transactions on Industrial Electronics*, 2022, vol. 69, no. 11, pp. 11335–11347.

16. AlSadat, M., Vlasov, Y., Vorobev, P., et al., Improving transients for droop-controlled inverters, *Proc. 2023 IEEE Applied Power Electronics Conference and Exposition (APEC)*, 2023, pp. 1003–1008.

17. Nowak, M., Binkowski, T., and Pirog, S., Proportional-resonant controller structure with finite gain for three-phase grid-tied converters, *Energies*, 2021, vol. 14, art. no. 6726.

18. Nazeri, A.A., Zacharias, P., Ibanez, F.M., and Somkun, S., Design of proportional-resonant controller with zero steady-state error for a single-phase grid-connected voltage source inverter with an LCL output filter, *Proc. 2019 IEEE Milan PowerTech*, 2019, pp. 1–6.

19. Cha, H., Vu, T.-K., and Kim, J.-E., Design and control of proportional-resonant controller based photovoltaic power conditioning system, *Proc. 2009 IEEE Energy Conversion Congress and Exposition*, 2009, pp. 2198–2205.

20. Hu, P., He, Z., Li, S., and Guerrero, J.M., Non-ideal proportional resonant control for modular multilevel converters under sub-module fault conditions, *IEEE Transactions on Energy Conversion*, 2019, vol. 34, no. 4, pp. 1741–1750.

21. Zhang, N., Tang, H., and Yao, C., A systematic method for designing a PR controller and active damping of the LCL filter for single-phase grid-connected PV inverters, *Energies*, 2014, vol. 7, pp. 3934–3954.

22. Buraimoh, E., Aluko, A.O., Oni, O.E., et al., Decentralized virtual impedance-conventional droop control for power sharing for inverter-based distributed energy resources of a microgrid, *Energies*, 2022, vol. 15, art. no. 4439.

23. Alghamdi, S., Sindi, H.F., Al-Durra, A., et al., Reduction in voltage harmonics of parallel inverters based on robust droop controller in islanded microgrid, *Mathematics*, 2023, vol. 11, art. no. 172.

24. Wang, L., Li, T., Cheng, Z., et al., Unified droop control of AC microgrids under different line impedances: revisiting droop control and virtual impedance method, *Frontiers in Energy Research*, 2023, vol. 11, art. no. 1168235.

25. Micallef, A., Apap, M., Spiteri-Staines, C., and Guerrero, J.M., Mitigation of harmonics in grid-connected and islanded microgrids via virtual admittances and impedances, *IEEE Transactions on Smart Grid*, 2017, vol. 8, no. 2, pp. 651–661.

26. Shan, P., Sun, Y., Song, Y., et al., Adaptive parameter tuning and virtual impedance injection control for coupled harmonic mitigation of photovoltaic converter, *IEEE Transactions on Power Electronics*, 2025, vol. 40, no. 1, pp. 162–175.

27. Li, Y., He, J., Liu, Y., et al., Decoupled mitigation control of series resonance and harmonic load current for HAPFs with a modified two-step virtual impedance shaping, *IEEE Transactions on Industrial Electronics*, 2023, vol. 70, no. 8, pp. 8064–8074.

28. Kshatri, A., Bhatta, A., Ksherti, B.T., and Poudel, A., THD analysis of microgrids using dual voltage source inverters strategy under nonlinear loads, *Authorea*, 2024, August 30.

29. Vorontsov, A.V., Self-maintained amplifier in a power inverter, *Elektronnye informatsionnye sistemy*, 2020, no. 2, pp. 50–61.

30. Gadde, P.H. and Brahma, S., Comparison of PR and PI controllers for inverter control in an unbalanced microgrid, *Proc. 2020 52nd North American Power Symposium (NAPS)*, 2021, pp. 1–6.

31. Veretennikov, I., Vlasov, Y., Ibanez, F.M., et al., Proportional multiresonant controller with automatic gains adjustment for grid-connected inverters, *Proc. 2023 IEEE Belgrade PowerTech*, 2023, pp. 1–6.

32. Moosavi, M., Farivar, G., Iman-Eini, H., and Shekarabi, S.M., A voltage balancing strategy with extended operating region for cascaded H-bridge converters, *IEEE Transactions on Power Electronics*, 2014, vol. 29, no. 9, pp. 5044–5053.

33. Ulinuha, A., Masoum, M.A.S., and Islam, S.M., Harmonic power flow calculations for a large power system with multiple nonlinear loads using decoupled approach, *Proc. 2007 Australasian Universities Power Engineering Conference*, 2007, pp. 1–6.

34. Hornik, T. and Zhong, Q.C., A current-control strategy for voltage-source inverters in microgrids based on H∞ and repetitive control, *IEEE Transactions on Power Electronics*, 2011, vol. 26, no. 3, pp. 943–952.

35. Joshi, S., Tripathi, R., Badoni, M., et al., Design and development of non-linearly controlled class-D audio amplifier, *Electronics*, 2022, vol. 11, art. no. 77.

36. Khan, I., Vijay, A.S., and Doolla, S., Nonlinear load harmonic mitigation strategies in microgrids: state of the art, *IEEE Systems Journal*, 2022, vol. 16, no. 3, pp. 4243–4255.

This paper was recommended for publication by S.A. Krasnova, a member of the Editorial Board

ISSN 0005-1179 (print), ISSN 1608-3032 (online), Automation and Remote Control, 2026, Vol. 87, No. 8, pp. 730–740.

CONTROL IN TECHNICAL SYSTEMS

Optimal Navigation in Regular Transport Networks with Minor Traffic Congestion

P. P. Bobrik

Solomenko Institute of Transport Problems, Russian Academy of Sciences, Moscow, Russia
e-mail: Bobrikpp@mail.ru

Received September 14, 2025
Revised February 5, 2026
Accepted February 16, 2026

Abstract—Questions of the organization of movement in transport networks are considered. The emphasis is placed on the most simple and cheap solutions. Optimal nodal navigation in a network with insignificant traffic jams is sought. It is proved that, for a square grid, the fastest movement to the origin of coordinates will be obtained when the route tends to the coordinate diagonals with subsequent winding on them.

Keywords: flows on a graph, Hippodamian system, nodal navigation, insignificant traffic jams, control with incomplete information, time-optimal problem, cost of control

DOI: 10.7868/S1608303226080058

1. INTRODUCTION

At present, when automobiles move in cities, the use of navigators has become practically universal. They solve several basic tasks at once: access to the city map, determination of the current location, obtaining in real time information about traffic jams and other characteristics of flows and their regulation, selection of the fastest route, and target indication to the driver in real time.

As a rule, such navigators are free for users, at least in their simplest tariffs, because of which questions of their cost are rarely raised. Nevertheless, substantial expenses constantly go to their functioning. These are street cameras, communication means, collection of information in real time, computing equipment, the staff of employees of various structures of traffic organization, taxes, etc. In other words, although final users do not see these costs, they exist and pass through the accounting departments of outside structures. And they are sometimes rather substantial in recalculation for each single movement. In such a situation the statement of the question of reducing such expenses is natural.

Although these problems are most clearly and sharply manifested in automobile flows of megacities, to one degree or another they are characteristic of all transport networks. In the most general case the question should be posed as follows: how to organize movement with the least accompanying costs when choosing a route and following it?

At present, questions of transport planning are so extensive and nontrivial that they have taken shape as a separate scientific discipline [1]. Although Dijkstra's algorithm for finding the shortest route in a graph is polynomial [2, 3], for large cities with millions of nodes this problem has become sufficiently cumbersome. Individual drivers without complex information-computing systems can no longer solve it well. As a result, flows become more and more chaotic and subject to the influence of outside information factors, and movements themselves around the city lose efficiency. Instead of choosing optimal solutions when forecasting flows, probabilistic approaches based on considerations of repetitions of past situations have more and more often begun to be used. At the same time, modeling of transport flows in real time is receiving ever greater spread in the world [4, 5].

The hopes of recent years for the use of modern neural networks, even embedded in basic mechanisms of deductive reasoning [6, 7], also can only partially help to cope with the complexity. Say, for them examples of features of architectural building are needed, which are not explicitly present in the initial data used for training the neural network.

All this involuntarily pushes to the thought that the problem is excessively complicated [8]. And it is necessary to try to simplify it as much as possible. As often happens, most transport problems are conditioned by nontransport reasons. For example, for cities traffic jams, as a rule, are conditioned by wrong architectural and planning decisions, which accumulate for centuries, when for free movement of the flow there is simply not enough corresponding volume of roads [9]. Correspondingly, in these conditions many transport solutions in fact are also nontransport. As an example, one can point to intercepting parking lots or fiscal restrictions on owners of transport means with the aim of reducing their number in cities.

One of the main approaches for organizing qualitative movements over a territory is the formation of corresponding urban development on the planning horizon of tens of years. And first of all, the creation of the correct topology of the street-road network. It can be shown that in many cases it is expedient to choose regular networks, i.e., networks with a repeating structure, as target ones [10]. They are optimal by many parameters, including nontransport ones. Their value is confirmed by the fact that they are widely used in practice from ancient times.

In this article the simplest square network will be considered. Although it is not the most effective among regular ones [11], it is the simplest by structure and therefore the most convenient for building. It can be considered as a target one for many territories, allowing one to achieve a high quality of movements.

As in any other network, traffic jams can also arise in a square network. Therefore, for it the task of movements under conditions of incomplete information is also actual. In the article a very simple variant of navigation through a square network without the use of navigators or any other devices is proposed. It is proved that it leads to the fastest movement.

2. PROBLEM STATEMENT

Consider some finite weighted graph $G(V, E, L)$, where $V = \{v_i\}$ is the set of its vertices; $E = \{e_i\}$ is the set of edges connecting its vertices; $L = \{l_i\}$, $l_i > 0$, are positive lengths of edges [2]. We shall consider that this graph describes some transport network: the street-road network of a megacity, a railway network, or even beds in a field. In the general case, the task is posed of finding such rules of choosing movement from some initial vertex $u \in V$ in order finally to get to some terminal vertex $v \in V$.

Consider at first the simplest square regular network, which consists of vertical and horizontal roads. We choose, without loss of generality, such units of length that the coordinates of the vertices of the graph describing it would have integer values, and the length of the edges between vertices would be equal to one. Then the roads are described by the lines:

$$x_i = \pm n, \quad y_j = \pm m, \quad n, m \in \mathbb{Z}. \tag{1}$$

The distances between roads are also equal to one.

Such a network has great practical significance in the design of real transport systems. For example, when it is chosen, classical city blocks arise. Such a network has even received in urbanistics a special name, Hippodamian, after the name of the Greek architect Hippodamus, who applied it in the restoration of Miletus destroyed in the course of the Greco-Persian wars [12]. In the design of transport corridors on the scale of regions and whole continents, the latitudinal-meridional principle is often used, which also leads to a square network. And even beds in fields appear as a variety of this approach.

One can move along the roads of the network. We choose such a unit of time that the speed of movement would be equal to one. Then the time of movement between adjacent nodes will also be unit.

Without loss of generality, we place the initial point of departure of the route $u(n, m)$ in the first coordinate octant, i.e., with positive coordinates, $n > 0$, $m > 0$. And in the origin of coordinates $v(0, 0)$ we place the terminal point of the route. For such a network it is required to determine rules of choosing the direction of movement in each node in order to get by the shortest way from some point $u \in V$ to the origin of coordinates. This, for example, can be done if in each node such an edge is chosen, movement along which leads to a decrease of the distance to the origin of coordinates [13].

Let us note several simplest properties of this network.

Statement 1. *In a Hippodamian network, for any pair of points not lying on one straight line of the network, there exist several shortest routes of equal length.*

Corollary 1. *Under violations of passage along any one section of the network, for vertices not lying on one straight line, its bypass with the same route length will be found.*

Thus, for the Hippodamian network the property of stability of traffic length under violations is characteristic, which turns out to be very important for practical applications.

Definition 1. The distance or length $l_{n,m} = n + m$ of the network node (n, m) will be called the extent of its shortest route to the origin of coordinates of the node in a square network.

3. THE CASE OF TRAFFIC JAMS WITH SMALL PROBABILITY

Let us now complicate the task. Let on some edges of the graph there arise obstacles of some kind to free movement, which further we shall call traffic jams. The locations of traffic jams are not known in advance. I.e., initially this is a task of control under conditions of incomplete information. But, coming to any node, we receive additional information both about the node itself and about traffic jams on edges adjacent to it: for example, simply by looking at the corresponding road; or at a traffic light, besides the color permitting or prohibiting passage, some number of the same color can be shown, which will characterize the intensity of the traffic jam; or in some other way. In other words, for the driver this is local information, accessible only at the point of presence.

In such a statement of the task, the information used for choosing the further direction of movement, as well as for orientation and position in the network, is much more simple and therefore cheaper than information about the whole graph G. At the same time, such sufficiently expensive tasks are automatically excluded as collecting information about the structure of the graph and the current location of traffic jams; the use of an onboard computing device is not required, nor providing it with communication with the information supplier; it is not necessary to determine the optimal route (in the case of a large graph with millions of vertices this is a separate long task) and to make sure of its existence, to organize following the route. From this point of view such control of movement is much more simple and cheap. Further it will be shown that under conditions of such scanty information such control exists. And it will even lead to optimal movements. But this becomes possible only due to the very simple and repeating structure of a regular network [14].

We shall suppose that for the event that a traffic jam will be found on an edge, there exists some probability p; further we shall consider it a small quantity.

In practice, traffic jams can be very diverse in their properties. In this work we shall consider that a traffic jam is always passable, i.e., having begun movement along an edge with a traffic jam, we shall necessarily get to an adjacent node. But the time of passing the edge in this case increases by some quantity $d < 1$.

Statement 2. *If there is no information about the presence of a traffic jam on an edge, then the mathematical expectation of the time of passing this edge will be equal to* $1 + pd$.

Proof. There are two variants. Either there will be a traffic jam on this road, or there will not. If there will be a traffic jam on it, then the time of movement will be $1 + d$; if there is no traffic jam, then it is 1. The probabilities of these events are respectively p and $1 - p$. Then the mathematical expectation of the time $M(e)$ of passing the edge will be equal to:

$$M(e) = p(1 + d) + (1 - p) \cdot 1 = 1 + pd. \tag{2}$$

Corollary 2. *The expected average time of passing an edge will exceed the time of passing a free edge by a quantity not more than of the first order of smallness.*

As was said earlier, by the condition of the task it is not known in advance where and when traffic jams will arise. In such a statement of the task one cannot bypass traffic jams in advance, since information (not all) about the state of the network comes only in the course of movement. Correspondingly, the task of choosing the further direction of movement is also forced to be solved in the course of movement.

Definition 2. Movement from point to point, when from time to time the direction of movement is chosen, will be called navigational.

A distinctive feature of navigation is that the route is not known in advance, even when movement has already begun, even already having begun movement [15, 16]. This will depend on information about traffic jams coming during movement, i.e., the task is a variety of adaptive control.

If the choice of direction occurs only in nodes of the network, then such navigation is called nodal. Nodal navigation is characteristic of many real networks: railway and automobile roads, routers in computer networks, electric networks, gas and oil pipelines, etc. It has great practical significance, which is why it makes sense to distinguish it by a separate name.

Definition 3. We shall call any algorithm of choosing in each node the next edge for movement the choice rules π.

In this article the choice rules do not necessarily have to be unambiguous. In the case of probabilistic rules, they will determine the probabilistic dynamics of flows on the network, as in Markov networks.

4. TIME-OPTIMAL PROBLEM

For movement under conditions of traffic jams the former quality criterion, the minimum length of a route, becomes not actual. Now one should consider the time-optimal problem. The task is posed to find such rules π of route choice in order to reach the origin of coordinates in minimum time. Further only such rules π will be considered which always lead to the terminal point of the route.

Definition 4. We shall denote by the expression $t_\pi(u) = t_\pi(n, m)$ the mathematical expectation of the time of reaching the origin of coordinates from the point $u(n, m)$ under the choice rules π. The index π will be omitted further if it is implied by the context. If the rules π are optimal, then $t(u) = t(n, m) = t_{n,m}$ is the mathematical expectation of the least possible time.

The least quantity $t_{n,m}$ will be called the time of the node, and differences of quantities of the type $t_{n,m} - t_{n-1,m}$ or $t_{n,m} - t_{n,m-1}$ will be called the times of the corresponding edges for movement from the point (n, m).

By the condition of the task, the occurrence of traffic jams on edges does not depend on each other in any way, which is really observed under rare traffic jams. Therefore, in accordance with the principle of dynamic programming, the very notion of the time of a node is correct.

In what follows the following will be very useful.

Lemma 1. *For each sufficiently small p around the origin of coordinates there exists a domain σ, in which for each node of the network the time is equal to $t_{n,m} = n + m + O(p) = l_{n,m} + O(p)$.*

Proof. The proof follows from the smallness of the quantity p and Statement 2.

In other words, the metric in a neighborhood of the origin of coordinates will differ insignificantly from the initial Hippodamian one for a square network. Correspondingly, the smaller p is, the larger the domain σ will be. For any two points u_1 and v_1 the following will be true.

Corollary 3. *In the domain σ, if $l(u) < l(v)$, then $t(u) < t(v)$.*

Further we shall consider only nodes of the network which are situated to the right and below the diagonal of the first octant, including its boundaries, i.e., nodes $u(n, m)$ whose coordinates will satisfy the relations $0 \leqslant m \leqslant n$. For nodes from the upper diagonal half the reasoning will be analogous.

Corollary 4. *If the penalty $d < 1$, then in the domain σ the fastest routes can leave nodes only along the left and lower edges.*

Proof. When moving upward or to the right, the length of the node increases by one. For returning to the same level of distances it is necessary to spend at least one more unit of length. Since in the domain σ the hierarchy of distances to the origin of coordinates is preserved, passing through a traffic jam will be faster than its possible bypass.

Let us note that, for preserving most conclusions, the restriction $d < 1$ from above by one can be considerably improved to quantities close to 2. But this will strongly complicate the exposition without obtaining new qualitative advantages. It will be necessary to investigate the sizes of the domain σ, the form of its boundaries, after which the formulations of the statements will become much more cumbersome.

Corollary 4 makes it possible to find optimal control in the form of rules for choosing directions of movement in nodes. Consider at first two special cases of nodes on the abscissa axis and on the diagonal of the first coordinate octant.

Example 1. Let us find the values $t_{n,0}$. Consider at first the node $(1, 0)$ on the abscissa axis to the right of the origin of coordinates. In view of the symmetry of the task with respect to the coordinate axes and their diagonals, analogous reasoning can be given for the points $(0, 1)$, $(0, -1)$, $(-1, 0)$. Only movement along the road to the left brings closer to the origin of coordinates, since movement downward increases the distance $l(u)$. In accordance with the statement above, the mathematical expectation of the time of movement along it is equal to $t(1, 0) = 1 + pd$.

For other points on the abscissa axis of the type $(n, 0)$, for optimal control it is required analogously to choose only the direction to the left in view of the nonoptimality of bypassing traffic jams in the domain σ. Then $t_{n,0} = n(1 + pd)$.

Corollary 5. *The times of edges on the coordinate axes are greater than the lengths of edges by a quantity of the first order of smallness.*

Example 2. Let us find the values of the time of the node $t_{1,1}$ on the diagonal of the coordinate octant. In accordance with the principle of dynamic programming, for finding the least time of movement from each point one should choose that direction which will give the best result taking into account already known optimal routes.

By Corollary 4, among the directions of further movement one should choose either along the edge downward or along the edge to the left. From Example 1 it is known that the least mathematical expectations of times for the points $(1, 0)$ and $(0, 1)$ are equal and are equal to $1 + pd$. At the point $(1, 1)$ the following four variants are possible. Both necessary directions will be with traffic jams. The lower edge will be with a traffic jam, and the left one free. On the left there will be a traffic jam, the lower one free. Both edges will be free from traffic jams. Correspondingly, the probabilities of these events will be equal to p^2, $p(1 - p)$, $(1 - p)p$, $(1 - p)^2$.

Let us formulate the rules of choosing the direction π, consisting in that we shall choose an edge without traffic jams always when this is possible. If both edges are free or both are with traffic jams, then we choose any one with equal probability. Under such a choice, in three of four cases a free edge will be chosen. Then the mathematical expectation of the time of the diagonal node will be equal to:

$$t_{1,1} = p^2(1 + d + t_{1,0}) + p(1 - p)(1 + t_{1,0}) + (1 - p)p(1 + t_{0,1}) + (1 - p)^2(1 + t_{0,1}). \tag{3}$$

Since $t_{1,0} = t_{0,1} = 1 + pd$, the expression is simplified to:

$$t_{1,1} = (1 + pd) + 1 + p^2 d = 2 + pd + p^2 d. \tag{4}$$

Since $t_{1,0} = 1 + pd$, the time of the vertical edge $t_{1,1} - t_{1,0}$ is equal to $1 + p^2 d$. And since the probability p is a small quantity, the times of the lower $t_{1,1} - t_{1,0}$ and left $t_{1,1} - t_{0,1}$ edges from the node $(1, 1)$ exceed their lengths by quantities not of the first, but already of the second order of smallness. In other words, they are faster than edges on the coordinate axes. Further it will be shown that a similar property can be ensured for all points outside the coordinate axes.

5. OPTIMAL NAVIGATION

Consider now the general case of an arbitrary node $u(n, m)$, whose coordinates will satisfy the relations $0 < m \leqslant n$, i.e., located in the half of the octant without the abscissa axis.

Definition 5. The rules of choosing the direction of movement π will be called diagonal if:

1) The choice is made only between the lower and left edges;
2) If the left edge is free, then it is chosen;
3) If there is a traffic jam on the left edge, and the lower one is free, then the lower one is chosen;
4) If there are traffic jams on both edges, then we choose the left one.

In other words, in the simultaneous presence of a pair consisting of a free edge and an edge with a traffic jam, the free edge is always chosen. In other cases the advantage always has the left edge. Under such rules the movement tends in the direction of the diagonal of the octant, whence its name was taken.

If in all nodes the diagonal choice rules are used, then in accordance with the principle of dynamic programming the times of nodes will be uniquely determined around the origin of coordinates. Consider some node (n, m). The time of the node to the left of it $(n-1, m)$, denote by $t_{left} = t_{n-1,m}$, and the time of the lower node $(n, m - 1)$ as $t_{down} = t_{n,m-1}$.

Statement 3. *For the diagonal rules π the recurrent relation is true*

$$t_{n,m} = t_{left} + 1 + (p - p^2)(t_{down} - t_{left}) + p^2 d. \tag{5}$$

Proof. The mathematical expectation of time for the diagonal rules is collected from the probabilities of all possible states of the edges:

$$t_{n,m} = p^2(t_{left} + 1 + d) + p(1-p)(t_{left} + 1) + (1-p)p(t_{down} + 1) + (1-p)^2(t_{left} + 1). \quad (6)$$

Opening the brackets and grouping the summands, we obtain the required expression.

According to Lemma 1, the times of the nodes t_{left} and t_{down} differ from their lengths by quantities of the first order of smallness. But the lengths of these nodes are equal. Therefore the difference of the times t_{down} and t_{left} will also be of the first order of smallness. And the summand $(p - p^2)(t_{down} - t_{left})$ will already be of the second order of smallness. Therefore the time of the left edge differs from unity by a quantity of the second order of smallness.

Recall that on the abscissa axis the times of edges were greater than lengths by quantities of the first order of smallness.

Corollary 6. *For the zero and first horizontal layers of nodes of the network it is true that* $t_{n-1,1} < t_{n,0}$.

Statement 4. *If* $t_{n-1,m} < t_{n,m-1}$, *then the diagonal rules* π *are optimal control of movement of the time-optimal problem in the node* (n, m), *where* $0 < m \leqslant n$.

Proof. For the node $(1, 1)$ above the optimal control and its time were directly found. For the node $(1, 1)$ it is directly checked that the diagonal choice rules also give optimal control. Consider an arbitrary node (n, m). The proof is based on a direct check of each combination of traffic jams on the lower and left edges. If both edges are free, then the left edge is chosen, since the time of the left vertex is less than that of the lower one, and the times of the edges are equal and equal to unity. If the left edge is free, and the lower one is with a traffic jam, then both the time of the left edge is less and the time of the left node is less. If the left one is with a traffic jam, and the lower one is free, then the lower one is chosen, since by the conditions of the task the value of the penalty d when passing along the left edge will be greater than the difference of the times of the left and lower nodes, since in the domain σ this difference has the first order of smallness. If there are traffic jams on both edges, then we choose the left one, since the times of the edges are equal, and the time of the left node is less.

Statement 4 is also true in the opposite direction.

Lemma 2. *Under the diagonal choice rules* π *in the domain* σ *the inequality* $t_{n-1,m} < t_{n,m-1}$ *will be fulfilled.*

Proof. We shall carry out the proof by induction. The base of induction. Consider the nodes $(2, 2)$ and $(3, 1)$. For them it is true:

$$t_{2,2} = (1-p)^2(1 + t_{1,2}) + (1-p)p(1 + t_{1,2}) + p(1-p)(1 + t_{2,1}) + p^2(1 + d + t_{2,1}), \quad (7)$$

$$t_{3,1} = (1-p)^2(1 + t_{2,1}) + (1-p)p(1 + t_{2,1}) + p(1-p)(1 + t_{3,0}) + p^2(1 + d + t_{2,1}). \quad (8)$$

As for nodes symmetric with respect to the diagonal, in view of the symmetry of the task it will be true that $t_{1,2} = t_{2,1}$. And $t_{3,1} < t_{4,0}$ by Corollary 6, since the latter node lies on the abscissa axis. Comparing the expressions by each summand, we obtain that $t_{2,2} < t_{3,1}$. Thus we obtain three consecutive nodes along an oblique diagonal with times $t_{2,2}$, $t_{3,1}$, $t_{4,0}$ in the order of nondecrease and growth for the last pair. Further we shall call such triples of nodes oblique. There are also two horizontal layers, where the times of nodes of the upper layer along an oblique diagonal are less than the times of nodes of the lower layer.

The induction step. Let for some triple of nodes it be true that $t_{n-2,m} \leqslant t_{n-1,m-1} < t_{n,m-2}$, and also for any positive i the inequality $t_{n-1+i,m-1} < t_{n+i,m-2}$ is fulfilled. Consider two nodes

$(n-1,m)$ and $(n,m-1)$ to the right and above this triple. Their times are determined by the recurrent formulas

$$\begin{aligned} t_{n-1,m} &= (1-p)^2(1+t_{n-2,m}) + (p-p^2)(1+t_{n-2,m}) \\ &\quad + (p-p^2)(1+t_{n-1,m-1}) + p^2(1+d+t_{n-2,m}), \end{aligned} \tag{9}$$

$$\begin{aligned} t_{n,m-1} &= (1-p)^2(1+t_{n-1,m-1}) + (p-p^2)(1+t_{n-1,m-1}) \\ &\quad + (p-p^2)(1+t_{n,m-2}) + p^2(1+d+t_{n-1,m-1}). \end{aligned} \tag{10}$$

Each of the summands of the upper expression will be greater than or equal to the analogous summand of the lower formula. Moreover, the equality sign can be only for nodes of the type $(k-1,k)$ and $(k,k-1)$ around the diagonal of the octant. Substituting these inequalities, we obtain the statement being proved. Therefore, if there is an oblique triple, then to the right of it there will also be an oblique triple. I.e., they are arranged in layers horizontally. On the other hand, if there are not less than two horizontal layers $y=k$ and $y=k-1$ where $t_{i,k} < t_{i+1,k-1}$, then there will always be found an oblique triple above them. This will be a triple of nodes of the type $(k+1,k+1)$, $(k+2,k)$, $(k+3,k-1)$, i.e., beginning from the coordinate diagonal. The proof is analogous by the formulas above, only it is necessary to take into account that in view of the symmetry of the task there is the strict equality $t_{k,k+1} = t_{k+1,k}$.

Theorem 1. *The diagonal choice rules are optimal control of movement for the domain σ without the coordinate axes.*

As is seen from the previous exposition, the times of all edges, except those lying on the coordinate axes, exceed their lengths by a quantity not more than quantities of the second order of smallness. In other words, for most cases the diagonal rules provide a very high quality of control, practically eliminating the influence of traffic jams during movement.

The very principle of the striving of a route to the domain where there exists the greatest number of variants of continuation of movement and, correspondingly, of bypassing traffic jams, has a fundamental character. Therefore it is very plausible that it can be used under much less severe restrictions. Consider some directions for generalizing the results.

6. FINITE VALUES OF THE PROBABILITY p

Although formally the probability of occurrence of a traffic jam in the given statement of the task is considered an infinitely small quantity, for practical applications cases with finite values are of interest. In particular, the question is of interest how far the domain σ can extend. Here the following will be useful.

Statement 5. *The time of any edge is more than* 1 *and not more than* $1+pd$.

This follows from Statement 2 with the remark that, when approaching any node, additional information becomes accessible, which can reduce the mathematical expectation of the time of movement along it.

According to Corollary 3, in the domain σ, if $l(u) < l(v)$, then $t(u) < t(v)$. This can be considered as an alternative definition of the domain of applicability of the diagonal choice rules. The very notion of the domain σ exists by definition only under the limiting transition with respect to the probability p, which does not allow one to calculate its boundaries at some finite p. On the contrary, the given property is sufficiently easy to check. This makes it possible to obtain quantitative estimates of the size and form of the domain where the proposed control of movement will be optimal.

One of the rough estimates of the extent of the domain σ can be the condition $t(u) < l(u)+1$, which makes bypasses ineffective. In accordance with Statement 5, for $d<1$ the domain will include all nodes with $l(u) < 1/p$. For example, when the probability of a traffic jam is equal to one hundredth, the diameter of such a domain in a city will be of the order of 200 blocks. Few megacities in the world are of such an extent. In other words, this is although a rough estimate, but already having practical sense.

At high values of the probability p another difficulty arises. A chain reaction of generation of other traffic jams by traffic jams can begin because of the reduction of the throughput capacity of the whole network. Then the simultaneous appearance of a traffic jam on the left and lower edges can begin to arise successively during movement, which will require taking into account not only the nearest edges, but also more distant ones. And this requires both more extensive information about the current state of the graph and a modification of the choice rules themselves. I.e., the very statement of the task changes. How strongly the parameter p can be increased remains an open question.

7. PENALTY FOR PASSING A TRAFFIC JAM

In the current statement of the task it was supposed that a traffic jam is always passable. And the undesirability of its passing was given by the quantity of the time penalty d, which was chosen less than unity. This was done in order that the bypass would be nonoptimal. Indeed, the diagonal rules lead to routes with a successive decrease of the lengths of the passed nodes. In them the principle of bypassing traffic jams on the horizon of observability is already laid. And any bypass outside diagonal directions leads to an overrun in length by 2 units.

Variants of statements of the task with large values of d are also possible. And they really arise in practice, which conditions interest in them. But under such quantities bypasses of traffic jams become optimal. And this requires additional assumptions to the initial statement of the task at the methodological level.

When choosing a bypass, it is extremely desirable to expand the zone of informing drivers about more distant edges, and not only adjacent ones. And this contradicts the aims of this article, where, on the contrary, the emphasis is placed on simplifying movement and reducing the cost of its accompaniment. At the same time, one can also inform in different ways. For example, one can give information about the state of edges removed from the current position through one vertex. Or one can give the whole current graph of the network. Depending on the chosen variant, a whole set of independent statements of tasks with their own features and domain of application arises.

It is necessary to distinguish the types of traffic jams. For example, they can be constant, and they can change after some interval of time. In the latter case it is necessary explicitly to indicate the law of occurrence and disappearance of congestions. This leads to new series of mathematical models. A separate case arises when movement through an edge is prohibited, for example because of the closure of a road section for repair or because of some other insurmountable reason. In this case there may generally not exist any route to the origin of coordinates, i.e., the task becomes incorrect.

Despite the indicated and other difficulties, cases of bypasses of traffic jams are very important for practice. But at present there does not exist a unified approach to solving such a task. In cities, navigators with display of the location of traffic jams and their intensities are most often used. At this it is necessary to remember that such information comes with a delay. Sometimes explicit indicators of bypasses help. In traffic control centers, expensive methods of modeling and forecasting are very often used. At the same time, probabilistic approaches and expert estimates based on knowledge about past analogous situations are used.

In the most neglected cases high values of p and d will lead to situations when in some parts of the network movement will generally stop. Then there arises already the task not of choosing movement, but generally of the existence of at least one possible route. For example, tasks of flow in a percolation cluster arise [17], which are very complex even for theoretical investigation.

The absence of a good cheap solution says that road networks with high values of the probability of occurrence of a traffic jam and high costs of penalties must be avoided in every possible way. Including the use of nontransport methods: architectural and planning decisions, traffic restrictions, stimulation of small sizes of automobiles, reduction of the number of automobile owners, compact cities, etc.

8. CONCLUSION

The diagonal rules generate optimal nodal navigation when moving in a square network with small traffic jams in some domain around the origin of coordinates.

The diagonal rules admit a very simple and convenient for practical use interpretation. It consists in the striving to the diagonals of the coordinate octant. Upon reaching the diagonal, the winding of the route onto the diagonal begins. This makes it possible to move through the network in an optimal way without the use of any additional computing or information devices. This becomes possible because under such choice rules the greatest number of variants of bypassing traffic jams is achieved.

The proposed control can be chosen as a target one when constructing real transport networks with regular topology in view of its simplicity, stability of traffic length, and cheapness. Such an approach is an alternative to the existing trends toward complication of the mechanisms of control and management of real transport flows, and correspondingly of the growth of costs for them.

FUNDING

The work was carried out within the framework of the state assignment of the Solomenko Institute of Transport Problems of the Russian Academy of Sciences for 2026, no. 075-00605-26-00.

REFERENCES

1. Yakimov, M.R., Nesterova, A.S., and Popov, Yu.A., *Transportnoe planirovanie: transport obshchego pol'zovaniya: monografiya* (Transport Planning: Public Transport: Monograph), Moscow: Agentstvo RADAR, 2024.

2. Emelichev, V.A., Melnikov, O.I., Sarvanov, V.I., et al., *Lektsii po teorii grafov* (Lectures on Graph Theory), Moscow: Nauka, Gl. red. fiz.-mat. lit., 1990.

3. Christofides, N., *Teoriya grafov. Algoritmicheskii podkhod* (Graph Theory: An Algorithmic Approach), Moscow: Mir, 1978.

4. Shvetsov, V.I., Algorithms for Traffic Flow Assignment, *Avtom. Telemekh.*, 2009, no. 10, pp. 148–157.

5. Gasnikov, A.V., Klenov, S.L., Nurminskii, E.A., et al., *Vvedenie v matematicheskoe modelirovanie transportnykh potokov* (Introduction to Mathematical Modeling of Traffic Flows), Gasnikov, A.V., Ed., Moscow: MCCME, 2013.

6. Betin, V.N., Ivashchenko, V.A., and Suprun, A.P., Use of regular features of partially defined functional neural networks in solution search, *Nauchno-tekhnicheskaya informatsiya. Seriya 2: Informatsionnye protsessy i sistemy*, 2024, no. 4, pp. 1–8.

7. Betin, V.N., Dem'yanov, A.E., Ivashchenko, V.A., et al., Some approaches to creating hybrid systems oriented toward work with knowledge by embedding artificial neural networks in them, *Informatizatsiya i svyaz'*, 2021, no. 6, pp. 20–26.

8. Evin, I.A., Introduction to the theory of complex networks, *Komp'yuternye issledovaniya i modelirovanie*, 2010, vol. 2, no. 2, pp. 121–141.

9. Tarkhov, *Evolyutsionnaya morfologiya transportnykh setei* (Evolutionary Morphology of Transport Networks), Smolensk–Moscow: Universum, 2005.

10. Bobrik, P.P., Comparison of the efficiency of triangular and square regular transport networks, *Transport: nauka, tekhnika, upravlenie*, 2000, no. 7, pp. 26–31.

11. Bobrik, P.P., On the advantage of triangular topology of a transport network over square topology, *Transport: nauka, tekhnika, upravlenie*, 2005, no. 3, pp. 32–34.

12. Glazychev, V.L., *Urbanistika* (Urban Studies), Moscow: Evropa, 2008.

13. Bobrik, P.P., Navigation in networks and its information support, *Informatizatsiya i svyaz'*, 2024, no. 2, pp. 7–13.

14. Bobrik, P.P., Navigation in regular transport networks, *Proc. 14th St. Petersburg Int. Conf. on Integrated Navigation Systems*, St. Petersburg: State Research Center of the Russian Federation, Concern CSRI Elektropribor, 2007.

15. Bobrik, P.P., A system of route-selection signs providing a minimum-cost flow in a transport network, *Transport Rossii; problemy i perspektivy – 2008. Proc. All-Russian Scientific and Practical Conf.*, Moscow: MIIT, 2008, pp. 44–45.

16. Bobrik, P.P., On one method of traffic flow control, *Program of the 4th Int. Conf. "System Identification and Control Problems" (SICPRO-07), January 29–February 1, 2007*, Moscow: Institute of Control Sciences, 2007, p. 25, report 4204.

17. Tarasevich, Yu.Yu., *Perkolyatsiya: teoriya, prilozheniya, algoritmy: uchebnoe posobie* (Percolation: Theory, Applications, Algorithms: A Textbook), Moscow: Editorial URSS, 2002.

This paper was recommended for publication by R.V. Meshcheryakov, a member of the Editorial Board

ISSN 0005-1179 (print), ISSN 1608-3032 (online), Automation and Remote Control, 2026, Vol. 87, No. 8, pp. 741–750.

Modeling the Impact of Chronic Disease Prevalence on COVID-19 Mortality

V. Y. Kisselevskaya-Babinina

M.V. Lomonosov Moscow State University, Moscow, Russia
e-mail: silvaze@yandex.ru

Received November 3, 2025
Revised January 26, 2026
Accepted January 29, 2026

Abstract—A model of the COVID-19 epidemic in a population heterogeneous by chronic non-communicable diseases is presented. A synthetic population is recreated, preserving the causal relationships between chronic diseases, sex, and age. Infection of individuals in the population is simulated, and the effect of the dependence of the course of COVID-19 on the presence and type of specific chronic diseases in infected individuals is modeled. The results of the epidemic modeling in the original population are compared with those in populations with reduced prevalence of chronic non-communicable diseases. Diseases whose reduced prevalence leads to the greatest reduction in COVID-19 mortality, the number of years of life lost, and the load on intensive care equipment are identified.

Keywords: Bayesian network, Markov model, synthetic population

DOI: 10.7868/S1608303226080068

1. INTRODUCTION

One of the indicators of a population's vulnerability to infectious diseases is the prevalence of chronic non-communicable diseases, which represent the body's decline and decreased resilience. The more chronic diseases a person has, the worse his prognosis for infectious diseases becomes [1, 2]. The distribution of chronic diseases in the population is one of the significant factors determining the differences in COVID-19 mortality rates among countries [3]. Effective control of chronic diseases and the development of policies aimed at reducing their prevalence can help lessen the negative consequences of an infectious disease epidemic.

The impact of chronic diseases on the COVID-19 epidemic was studied using mathematical models with a system of differential equations, or via agent-based modeling. In differential equations models the entire population is divided into groups of people with chronic diseases and those without chronic diseases [4–6]. The [5] proposed that the most cost-effective strategy for reducing COVID-19 burden on population is to lessen the incidence of infection in patients with chronic diseases due to their high vulnerability. Authors of agent-based models usually incorporate chronic diseases in individuals indirectly through age [7]. However in [8] it was shown that the conditional probability of hospitalization of an individual with COVID-19 is higher when taking into account both chronic diseases and age compared to taking into account age alone.

Mathematical models in general do not include the type and number of chronic diseases in individuals, while observational evidences show different increases in the risk of death for different diseases and the presence of a nonlinear cumulative effect [9]. A chronic disease that increases the risk of severe illness and hospitalization may not affect the risk of death [10]. Modeling multiple diseases simultaneously is complicated by the fact that chronic diseases form a causal network in which the development of one disease increases the probability of the development of a certain type of other diseases over time [11–13].

This paper presents a mathematical model which takes into account the complex interaction mechanisms between multiple chronic diseases and an infectious disease. The aim of the study is to determine how the prevalence of various chronic diseases in a population influences mortality from COVID-19. A series of computational experiments with reduced prevalence levels of various chronic diseases was conducted to determine their contribution to mortality and healthcare resource workload during the COVID-19 epidemic.

2. MODELED MECHANISMS

The model was designed to reproduce the COVID-19 epidemic in a megapolis. The reference was the COVID-19 epidemic in Moscow in 2020–2021. The process of COVID-19 infection in the population was considered random with a uniform probability distribution, and the population was considered uniformly mixed and heterogeneous in terms of sex, age, and chronic diseases.

The presence of various chronic diseases in individuals was considered a dependent random variable. The risk of developing a new chronic disease increases with age. The development of a particular type of chronic disease also depends on sex and the pre-existing chronic diseases. Research [12] has discovered clusters of diseases that occur together with a probability higher than that of a single disease. The sequence of chronic diseases development forms a network with distinct clusters. To reproduce these dependencies, a Bayesian network was created, and its parameters were estimated.

COVID-19 infection causes destruction of pulmonary epithelial cells, leading to respiratory failure and the need for hospitalization. Provided extensive lung damage, COVID-19 leads to the development of L-type pneumonia and, if the condition worsens, H-type pneumonia [14]. In case of L-type pneumonia, a respiratory support using non-invasive ventilation is recommended, while for H-type pneumonia, invasive mechanical ventilation (IMV) is recommended. These methods require monitoring in intensive care units. The average duration of COVID-19 treatment is 2 to 6 weeks [15]. According to these considerations, the course of COVID-19 in an infected patient was modeled as a series of transitions between severity states using a Markov model. The model included the patient's respiratory states (RS): spontaneous breathing, non-invasive ventilation and invasive mechanical ventilation.

The course of COVID-19 depends on the presence of chronic diseases. Moreover, the severity of COVID-19 depends on both the type and number of chronic diseases. For this model, a risk score for severe COVID-19 was created. The score value was calculated as the sum of the weights of an individual's diseases present; the higher the value, the worse the prognosis. A relative weight was assigned to each disease reflecting its contribution to the increased risk of death. To model the impact on the disease course, the transition probabilities of the Markov model were dependent on the risk score value.

3. MATHEMATICAL DESCRIPTION OF THE MODEL

This section successively describes the creation of a risk score for severe COVID-19, the creation of a Markov model of COVID-19 progression, the generation of a synthetic population using a Bayesian network, and the overall scheme of the computational experiment. This order is determined by the fact that the list of chronic diseases to be modeled in individuals was determined while creating the risk score, and the possible states of individuals at the initial point in time were determined while creating the Markov model. This information was thereafter used to construct a synthetic population. For creating a risk score, a Markov model and a Bayesian network, the data from patients treated with COVID-19 in the infectious diseases department of Moscow hospital from March 2020 to June 2021 were used [16].

3.1. Risk Score for Severe COVID-19

The CoRS-COVID score described in [17] was used as a risk score for severe COVID-19.

Consider $\boldsymbol{x} = (x_1, \dots, x_n),\ x_i \in \mathbb{R}$ as a list of individual characteristics. The risk of a person to severe course of the disease can be represented with function $\phi_\Pi = f(\boldsymbol{x}),\ \phi \in \mathbb{R}$, where $f(\boldsymbol{x})$ is the ranking function. If a person $\boldsymbol{x_1}$ has higher risk comparing to person $\boldsymbol{x_2}$, then the corresponding function values will be

$$\phi_{\Pi_1} = f(\boldsymbol{x_1}) > \phi_{\Pi_2} = f(\boldsymbol{x_2}).$$

The objective of developing a risk function is to allocate the characteristics $(x_1, \dots, x_n)$ that impact the infectious disease course and the type of function $f(\boldsymbol{x})$. In particular, the search for the function $f(\boldsymbol{x})$ can be among additive value functions that are composed of the sum of one-dimensional operators $[A]$ of each characteristic:

$$\varphi = f(\boldsymbol{x}) = A_1x_1 + A_2x_2 + \dots + A_nx_n.$$

Consider operators $\{A_i\}$ as

$$A_ix_i = k_ix_i, \quad k_i \in \mathbb{Z}.$$

We will use $x_i \in \{0, 1\}$, where 1 corresponds to chronic disease i's presence and 0 to chronic disease i's absence.

Then

$$\phi_\Pi = \sum_i k_ix_i. \tag{1}$$

We will call ϕ_Π a risk score for a severe disease course and k_i the relative weight of a chronic disease i. For the convenience of clinical use, k_i lies in the domain of integers.

Consider a logistic regression in which the dependent variable is the probability of the lethal outcome of the disease y and the independent variables are the characteristics $\boldsymbol{x}$

$$P(y|\boldsymbol{x}) = \frac{1}{1 + e^{-z(\boldsymbol{x})}}, \tag{2}$$

where

$$z(x) = \boldsymbol{w}^\intercal\boldsymbol{x} + b = w_1x_1 + w_2x_2 + \dots w_nx_n + b, \quad \boldsymbol{w}, b \in \mathbb{R},$$

$z(x)$ is a monotonic function of a linear combination. Thus,

$$\boldsymbol{w}^\intercal\boldsymbol{x_1} > \boldsymbol{w}^\intercal\boldsymbol{x_2} \Rightarrow P(y|\boldsymbol{x_1}) > P(y|\boldsymbol{x_2}).$$

Therefore operators $A_i = w_i$ can be considered as ranking function for health status. Because $w_i, b \in \mathbb{R}$ are real and $k_i \in \mathbb{Z}$ are integers, we shall round

$$k_i = [w_i]. \tag{3}$$

To develop ϕ_Π we selected characteristics $\boldsymbol{x}$ as chronic diseases that had odds ratio of a lethal outcome significantly higher than 1.2 or lower than 0.8. The logistic regression (equation (2)) using $\boldsymbol{x}$ was created; the parameters $\boldsymbol{w}$ and b were estimated with maximum likelihood method. The diseases' weights were obtained using equation (3). The final list $\boldsymbol{x}$ consists of 13 diseases (coronary heart disease, hypertension, arrhythmia, cerebrovascular disease, vascular thrombosis, anemia, chronic kidney disease stages 1–3, emphysema, fatty liver disease, metastatic cancer, and autoimmunity) with their weights ranging from −4 to 1.

3.2. Markov Model of COVID-19 Progression

The modeling of COVID-19 course was carried out using the Markov model of COVID-19 progression [18].

Let $\{S_t, t = 0, 1, 2, 3, \ldots\}$ be a homogeneous Markov chain defined in measurable space $(E, \mathfrak{F})$ with transition probabilities

$$\mathbb{P}(s, B) = \mathbb{P}(D = S_{t+1} \in B | S_t = s),\ s \in E,\ B \in \mathfrak{F},$$

and the initial probabilities distribution

$$\pi_0(B) = \mathbb{P}(S_0 \in B),\ B \in \mathfrak{F}. \tag{4}$$

We defined the state space E for the Markov model of COVID-19 progression as consisting of five states: hospital stay without respiratory support s_1, hospital stay on non-invasive ventilation s_2, hospital stay on invasive mechanical ventilation s_3, recovery s_4, and death in the hospital s_5. The transition probability matrix T is

$$T = \begin{pmatrix} p_{11} & p_{12} & p_{13} & p_{14} & p_{15} \\ p_{21} & p_{22} & p_{23} & p_{24} & p_{25} \\ p_{31} & p_{32} & p_{33} & p_{34} & p_{35} \\ 0 & 0 & 0 & 1 & 0 \\ 0 & 0 & 0 & 0 & 1 \end{pmatrix}, \quad \text{where } p_{ij} = \mathbb{P}(S_{t+1} = s_j | S_t = s_i).$$

The transition probabilities p_{ij} were estimated using the multinomial logistic regressions, that have the transition probabilities $P(S_t, B)$ from the current state as the dependent variable and the value of a risk score for severe COVID-19 ϕ_Π (equation (1)) as the independent variable:

$$\begin{aligned} p_{il}(\phi_\Pi) &= \mathbb{P}(S_{t+1} = s_l | S_t = s_i) = \frac{e^{-\beta^i_{0l} - \beta^i_l \phi_\Pi}}{1 + \sum_{k=1}^5 e^{-\beta^i_{0k} - \beta^i_k \phi_\Pi}}, \\ p_{i5}(\phi_\Pi) &= \mathbb{P}(S_{t+1} = s_5 | S_t = s_i) = \frac{1}{1 + \sum_{k=1}^5 e^{-\beta^i_{0k} - \beta^i_k \phi_\Pi}}, \end{aligned} \qquad l = 1, \ldots, 4, \forall i. \tag{5}$$

The prediction of COVID-19 course for one individual n within one day time step is

$$S_{t,n} = T^t(\phi_{\Pi,n}) S_{0,n}.$$

The parameters $\{\beta\}$ for transition probabilities p_{ij} were estimated using the maximum likelihood method based on data of patients treated in a hospital with COVID-19.

3.3. Synthetic Population

Consider a population $\mathcal{P}$ of individuals $\{a_n\}_{n=1}^N$. Each individual has the list V^n of random variables, denoting characteristics of individuals. The list of characteristics consisted of V_1^n as age group; V_2^n as sex; V_{3-16}^n as presence of chronic diseases, partially corresponding to the characteristics x_i of risk score equation (1); and $V_{17}^n = S_0^n$ as the type of respiratory status at the moment of hospitalization, which corresponds to the first state π_0 of the Markov model in equation (4).

A synthetic population was created using a Bayesian network [19]. The Bayesian network was a directed acyclic graph; its nodes were random variables V_i denoting the characteristics of individuals, and its edges r_i denoted the dependent relations between the random variables. At each root node, the probability distribution $\mathbb{P}(V_i)$ of the values of the corresponding random variable V_i was determined. At each child node, the conditional probability distributions of the values of the random variables were determined depending on the value of the parent node: $\mathbb{P}(V_i | parents(V_i))$.

The unconditional joint probability of all random variables in the network is expressed through the product of all probabilities of the parents and parents of the parents of the nodes:

$$\mathbb{P}(V_1, \ldots, V_n) = \prod_{i=1}^n \mathbb{P}(V_i | parents(V_i)). \tag{6}$$

This equation can be used to generate a list of individuals with given characteristics via a sequential calculation.

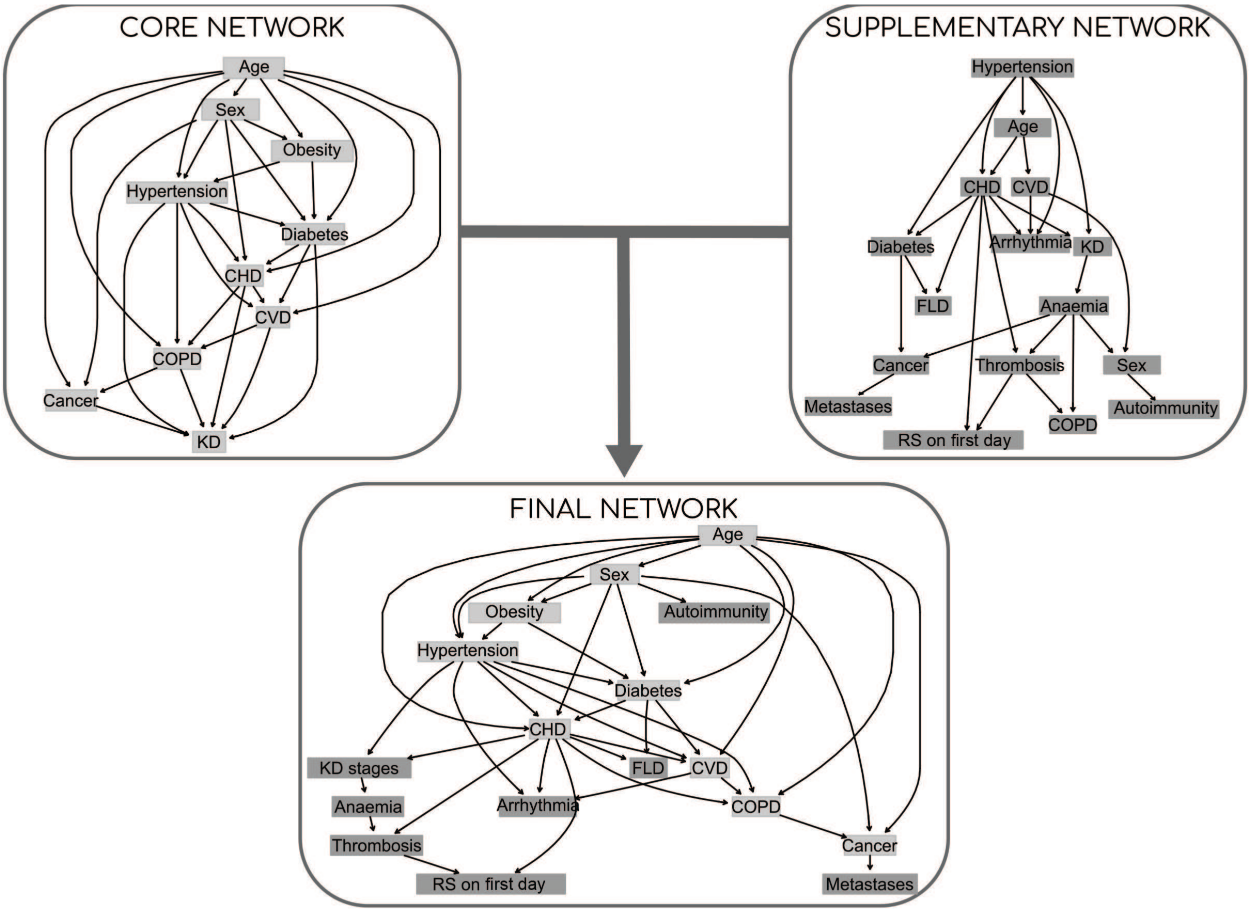

Fig. 1. A diagram of the merging of the Bayesian network graph based on the data of questionnaires (core network) and the Bayesian network graph based on the data of hospitalized patients (supplementary network). CHD—coronary heart disease, CVD—cerebrovascular disease, COPD—chronic obstructive pulmonary disease, KD—kidney disease, FLD—fatty liver disease, RS—respiratory support.

The Bayesian network for the considered synthetic population $\mathcal{P}$ was created in three stages. At the first stage, a core network was created using data from the 2021 Behavioral Risk Factor Surveillance System (BRFSS) collected by the US Centers for Disease Control and Prevention. The data represent the results of telephone surveys of 438 693 US residents on the presence of chronic diseases diagnosed by their physicians; their behavior; diet; living conditions; as well as information on state of residence, sex, age, survey date, and other information. We selected the responses on the following: sex, age group, presence of high blood pressure (hypertension), heart attack and coronary heart disease, stroke, cancer, chronic obstructive pulmonary disease, kidney disease, diabetes, and obesity using a BMI value. These characteristics formed the nodes of the core Bayesian network; the core network contained a total of 10 nodes. However, these data did not contain information on all the necessary chronic diseases included in the ϕ_Π index.

At the second stage, a supplementary network was created, for which data from patients treated with COVID-19 in the infectious diseases department of Moscow from March 2020 to June 2021 was used [16]. The data consist of the patient's sex, age, date of hospitalization, duration of treatment, type of respiratory support used for each day of treatment, treatment outcome and chronic diseases present. For the supplementary Bayesian network, we selected data on age, sex, diseases present in the BRFSS questionnaire (hypertension, coronary heart disease, stroke, kidney disease, diabetes, cancer, and chronic obstructive pulmonary disease); additional diseases included in the ϕ_Π index (arrhythmia, vascular thrombosis, anemia, fatty liver disease, metastases, and autoimmunity); and the patient's initial type of respiratory status s_0 at the time of hospitalization. The age of the patients was divided into groups corresponding to the BRFSS questionnaire categories. These characteristics formed 16 nodes of the supplementary network.

Optimization of both the core and supplementary networks was performed using the hill-climbing algorithm and maximization of the Bayesian Information Criterion

$$BIC(G|D) = \ln(P(D|G, \Theta)) - \frac{d}{2}\log m \xrightarrow[g,\Theta]{} \max,$$

where G is a graph structure, D is observation data, Θ are estimates of parameters given a structure, d is the number of free parameters, and m is the size of observation D.

At the third stage the two networks were merged together into one by adding the six absent nodes from the supplementary network to the core network, preserving parent edges and conditional probabilities (Fig. 1).

3.4. Computational Experiment Scheme

Figure 2 presents an overview of the experiment. Using the equation (6), a population of 100 000 individuals with randomly assigned characteristics was generated. For each individual, the risk score for severe COVID-19 was calculated by $\phi_{\Pi}^{n} = \sum_j k_j x_j^n$. The proportion p of the population was deemed infected with COVID-19, and the course of COVID-19 for all infected individuals was simulated using a Markov model. The probability of infection p was estimated as the ratio of the total number of detected COVID-19 cases as of January 2025 to the total number of Moscow residents in 2025 and amounted to 0.295. For each infected individual, transition probabilities in the model were calculated depending on the risk score value (equation (5)). Based on the transition

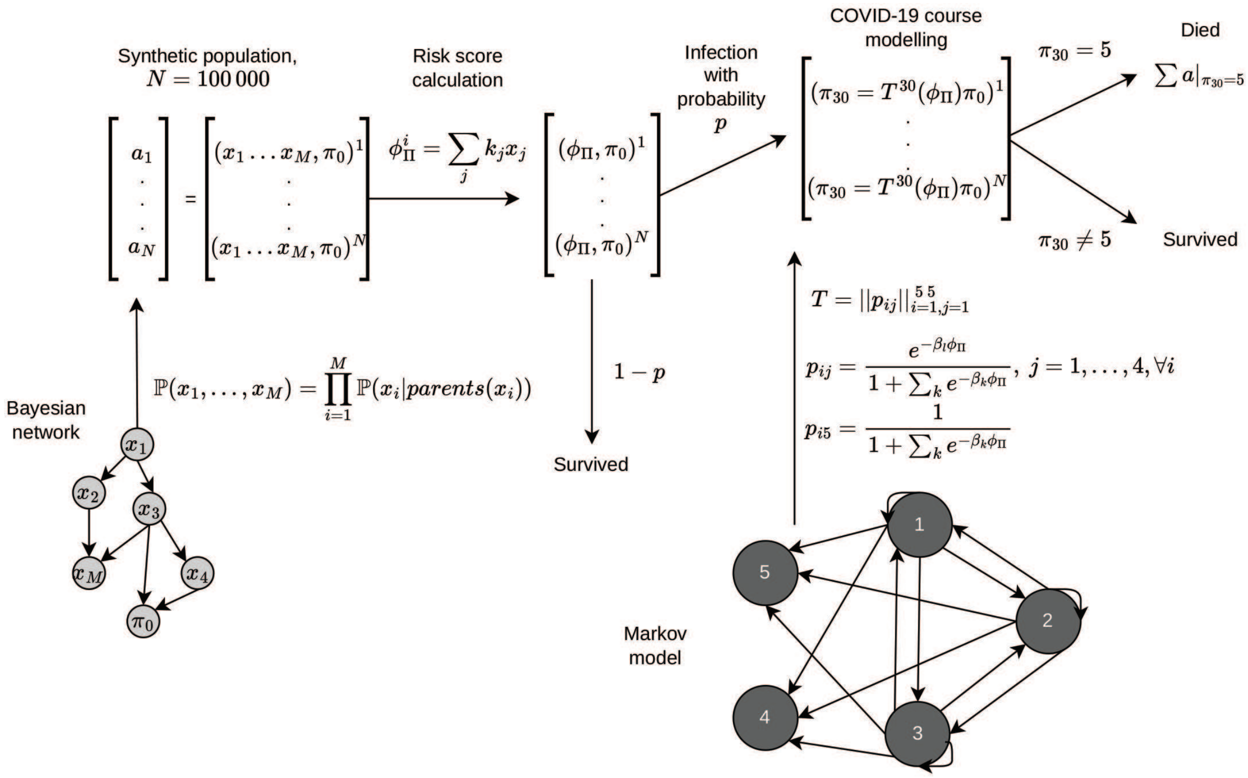

Fig. 2. An overview of the computational experiment: creating a population using a Bayesian network, calculating a risk score for each individual, randomly infecting the population, and simulating the course of COVID-19 in infected individuals using a Markov model.

probabilities, for each one-day time step the next state in the model was randomly chosen for each infected individual. The disease course for the infected was simulated for 30 days.

Estimates of the number of survivors and deceased, their sex, average age, and average length of stay were obtained. The prevalence of chronic diseases among deceased individuals and the relative risks of death for different diseases were calculated. For deceased individuals, estimates of years of life lost were obtained based on life expectancy in age groups calculated from data on mortality in Moscow for 2014 from the Human Mortality Database. To obtain reliable estimates, 100 random runs of the model were carried out, the results were averaged and confidence intervals were calculated.

A series of simulations of the COVID-19 epidemic were conducted in a population with a reduced prevalence of chronic diseases. In the original Bayesian network, the conditional probabilities $\mathbb{P}(V_i|parents(V_i))$ were lowered by 50% at one or more nodes V_i corresponding to chronic diseases, and a new synthetic population was generated. For individuals in the new population, infection with COVID-19 was randomly assigned, and a 30-day infection course was simulated; mortality, the sum of years of life lost, and the average length of stay were estimated. Epidemics in populations with a reduced prevalence of hypertension, obesity, diabetes, cancer, coronary heart disease, chronic obstructive pulmonary disease, and cerebrovascular disease were simulated. We also simulated a decrease in the prevalence of several diseases simultaneously, specifically hypertension and diabetes; hypertension and coronary heart disease and cerebrovascular disease; all cardiovascular diseases (hypertension, coronary heart disease, cerebrovascular disease, anemia, arrhythmia, and vascular thrombosis); and all diseases in the population. The obtained estimates were compared with the corresponding estimates from the original population.

4. RESULTS

Following 100 model runs, the average number of hospitalizations among 100 000 individuals was 29 470 people, and the number of deceased individuals amounted to 3682 people. Thus, the overall COVID-19 fatality rate in the synthetic population was 0.037, and the fatality rate among hospitalized was 0.125. The average age of the deceased was 57.6 years; the average age of deceased females was two years older than males. The number of years of life lost averaged to 23.61 years per person; the highest number of years of life lost was observed in the 60 to 69 age group.

The results of computational experiments in the original population and in populations with a 50% reduced prevalence of chronic diseases are given in the table. The greatest effect was observed for a reduction in the conditional probability of hypertension: a decrease in the number of individuals with hypertension from 39 018 people to 19 603 led to a decrease in the number of deaths from COVID-19 by 8.73% and the number of years of life lost by 6.9%. When comparing the effect relative to the number of individuals, the greatest effect was observed for a reduction in the conditional probability of coronary heart disease: a decrease in the number of individuals with coronary heart disease from 8096 to 4021 led to a decrease in the number of deaths from COVID-19 by 4.61% and the number of years of life lost by 2.9%; in addition, it caused the greatest effect on the decrease of the number of infected people requiring invasive mechanical ventilation on the first day of hospitalization—by 6%. Reductions in the prevalence of coronary artery disease and hypertension had the same effect on the number of days of invasive mechanical ventilation use—the decrease by 3.31%.

Diseases that do not directly influence COVID-19 severity contributed to mortality indirectly by being the causes of other diseases with a direct negative impact. For example, a reduction in the prevalence of obesity or diabetes, which were not included in the risk score for severe COVID-19, led to a decrease in COVID-19 mortality due to their relationships with other diseases in the Bayesian network.

Relative changes in epidemic parameters caused by a 50% decrease in the prevalence of chronic diseases in a synthetic population. CHD—coronary heart disease, COPD—chronic obstructive pulmonary disease, CVD—cerebrovascular disease, IMV—invasive mechanical ventilation

The disease with reduced prevalence	Change in number of deaths	Change in number of patients on IMV at the admission	Change in number of IMV usage days	Change in number of total years of life lost
Hypertension	−8.73%	−2.57%	−3.31%	−6.9%
Obesity	−1.38%	−0.47%	−0.49%	−1.3%
Diabetes	−0.51%	−0.82%	−0.37%	−0.3%
Cancer	−0.52%	=	−0.26%	−0.4%
CHD	−4.61%	−5.87%	−3.31%	−2.9%
COPD	−1.96%	=	−1.02%	−1.5%
CVD	−1.25%	=	−0.59%	−0.9%
Hypertension and diabetes	−9.06%	−3.20%	−3.58%	−7.1%
Hypertension, CVD, CHD	−12.97%	−7.45%	−6.31%	−9.6%
All cardiovascular diseases	−22.31%	−20.74%	−12.95%	−19.5%
All diseases	−23.1%	−21.24%	−12.35%	−19.7%

Reduction in the prevalence of several diseases simultaneously has a smaller effect than the sum of the effects of individual disease prevalence reductions. A 50% reduction in the prevalence of all diseases led to a 23% decrease in the number of deaths, a 12% decrease in the number of IMV days, and a 20% decrease in years of life lost. Thus, a 1% reduction in the quantity of people with chronic diseases leads to a 0.4% decrease in the number of COVID-19 deaths. Moreover, up to 96% of mortality was attributable to the high prevalence of cardiovascular diseases.

Model results showed that the high prevalence of chronic diseases in the population leads to a significant increase in mortality from infectious disease. In addition, chronic diseases increase the workload on healthcare resources, as illustrated by the prolonged usage of artificial lung ventilation and intensive care equipment due to the increased likelihood of high severity of the condition upon hospitalization. The relative decrease in years of life lost was smaller than that of the number of deaths. This is due to the fact that the decrease in the number of deaths mainly occurs in older age groups.

5. CONCLUSION

A model of the COVID-19 epidemic in a population heterogeneous in terms of chronic diseases was developed. According to the model's findings, a high prevalence of chronic non-communicable diseases is a major risk factor for increased mortality from infectious diseases in the population.

The model helped identify the diseases that have the greatest impact on mortality: hypertension and coronary heart disease. It was noted that a reduction in the prevalence of obesity and diabetes, which do not directly influence the course of COVID-19, also leads to a decrease in COVID-19 mortality in the population.

The ratio of the reduction in the prevalence of chronic diseases to the consequential decrease in the number of COVID-19 deaths was estimated to be 1% to 0.4%. Moreover, up to 96% of mortality was attributable to cardiovascular diseases.

This work is one of the first to study the relationship between infection parameters in a population and the prevalence of chronic diseases. This analysis can be applied when developing policies to reduce the burden of chronic diseases in the population. The proposed approach can be broadened and applied in the study of the influence of chronic diseases on the course and outcomes of other infectious diseases, such as influenza, rhinovirus, and hepatitis C.

FUNDING

This work was carried out with the financial support of the Moscow Center for Fundamental and Applied Mathematics in the Institute of Numerical Mathematics of the Russian Academy of Sciences (project with Ministry of Education and Science of Russia no. 075-15-2025-347).

REFERENCES

1. Vertkin, A.L., Rumyantsev, M.A., and Skotnikov, A.S., Comorbidity, *Clinical medicine*, 2012, vol. 90, no. 10, pp. 4–11.

2. Glezen, W.P, Impact of Respiratory Virus Infections on Persons With Chronic Underlying Conditions, *JAMA*, 2000, vol. 283, no. 4, pp. 499–505.

3. Corrao, G., Rea, F., and Blangiardo, G.C, Lessons from COVID-19 Mortality Data across Countries, *Journal of Hypertension*, 2021, vol. 39, no. 5, pp. 856–860.

4. Das, P., Upadhyay, R.K., Misra, A.K., et al., Mathematical Model of COVID-19 with Comorbidity and Controlling Using Non-Pharmaceutical Interventions and Vaccination, *Nonlinear Dyn.*, 2021, vol. 106, no. 2, pp. 1213–1227.

5. Omame, A., Sene, N., Nometa, I., et al., Analysis of COVID-19 and Comorbidity Co-infection Model with Optimal Control, *Optim. Control Appl. Methods*, 2021, vol. 42, no. 6, pp. 1568–1590.

6. Ssebuliba, J., Nakakawa, J.N., Ssematimba, A., et al., Mathematical Modelling of COVID-19 Transmission Dynamics in a Partially Comorbid Community, *Partial Differential Equations in Applied Mathematics*, 2022, vol. 5, pp. 100212.

7. Kerr, C.C., Stuart, R.M., Mistry, D., et al., Covasim: An agent-based model of COVID-19 dynamics and interventions, *PLoS Comput Biol*, 2021, vol. 17, no. 7, pp. e1009149.

8. Hadley, E., Rhea, S., Jones, K., et al., Enhancing the prediction of hospitalization from a COVID-19 agent-based model: A Bayesian method for model parameter estimation, *PLoS ONE*, 2022, vol. 17, no. 3, pp. e0264704.

9. Guan, W., Liang, W., Zhao, Y., et al., Comorbidity and Its Impact on 1590 Patients with COVID-19 in China: A Nationwide Analysis, *Eur. Respir. J.*, 2020, vol. 55, no. 5, pp. 2000547.

10. Terada, M., Ohtsu, H., Saito, S., et al., Risk Factors for Severity on Admission and the Disease Progression during Hospitalisation in a Large Cohort of Patients with COVID-19 in Japan, *BMJ Open*, 2021, vol. 11, no. 6, pp. e047007.

11. Jones, P.J., Ma, R., and McNally, R.J, Bridge Centrality: A Network Approach to Understanding Comorbidity, *Multivariate Behavioral Research*, 2021, vol. 56, no. 2, pp. 353–367.

12. Lappenschaar, M., Hommersom, A., Lucas, P.J.F., et al., Multilevel Temporal Bayesian Networks Can Model Longitudinal Change in Multimorbidity, *Journal of Clinical Epidemiology*, 2013, vol. 66, no. 12, pp. 1405–1416.

13. Aguado, A., Moratalla-Navarro, F., López-Simarro, F., et al., MorbiNet: Multimorbidity Networks in Adult General Population. Analysis of Type 2 Diabetes Mellitus Comorbidity, *Sci. Rep.*, 2020, vol. 10, no. 1, pp. 2416.

14. Gattinoni, L., Chiumello, D., Caironi, P., et al., COVID-19 Pneumonia: Different Respiratory Treatments for Different Phenotypes?, *Intensive Care Med.*, 2020, vol. 46, no. 6, pp. 1099–1102.

15. Bar-On, Y.M., Flamholz, A., Phillips, R., et al., SARS-CoV-2 (COVID-19) by the Numbers, *eLife*, 2021, vol. 9, pp. e57309.

16. Kiselevskaya-Babinina, V.Ya., Popugaev, K.A., Molodov, V.A., et al., The Use of Infectious Diseases Hospital Resources During the COVID-19 Epidemic Depending on Patient Characteristics, *Russian Sklifosovsky Journal "Emergency Medical Care"*, 2023, vol. 12, no. 3, pp. 481–488.

17. Kisselevskaya-Babinina, V.Y. and Sannikova, T.E., Razrabotka indeksa komorbidnosti CoRS-COVID i ego validaciya pri pomoshchi markovskoj modeli, *Upravlenie razvitiem krupnomasshtabnyh sistem (MLSD'2023): trudy SHestnadcatoj mezhdunarodnoj konferencii*, 2023, no. 1, pp. 1544–1552.

18. Kisselevskaya-Babinina, V.Ya., Romanyukha, A.A., and Sannikova, T.E., Mathematical Model of COVID-19 Progression: Prediction of Severity and Outcome, *Math. Models Comput. Simul.*, 2023, vol. 15, no. 6, pp. 987–998.

19. Sun, L. and Erath, A., A Bayesian network approach for population synthesis, *Transportation Research Part C: Emerging Technologies*, 2015, vol. 61, pp. 49–62.

This paper was recommended for publication by A.I. Mikhal'skii, a member of the Editorial Board

ISSN 0005-1179 (print), ISSN 1608-3032 (online), Automation and Remote Control, 2026, Vol. 87, No. 8, pp. 751–760.

Multi-Criteria Problems with Groups of Criteria Ordered by Importance (II). Decision Rules

A. P. Nelyubin[*,a] **and V. V. Podinovski**[**,b]

[*]*Mechanical Engineering Research Institute, Russian Academy of Sciences, Moscow, Russia*
[**]*National Research University Higher School of Economics, Moscow, Russia*
e-mail: [a]*nelubin@gmail.com*, [b]*podinovski@mail.ru*

Received December 8, 2025
Revised January 27, 2026
Accepted February 2, 2026

Abstract—For multi-criteria decision-making problems, by analogy with qualitative probability, the concepts of complete and partial qualitative importance are introduced as binary relations satisfying certain postulated properties. A new definition of a non-strict preference relation on the set of decision alternatives, generated by qualitative importance, is proposed, and its properties are examined. Analytical rules for pairwise comparison of alternatives in terms of preference are provided. The new preference relations are compared with those developed earlier for problems in which only individual criteria are initially ordered by importance. It is shown that when all criteria are completely ordered by importance, the two preference relations coincide.

Keywords: multi-criteria decision-making problems, ordering criteria by importance, criteria importance theory

DOI: 10.7868/S1608303226080078

1. INTRODUCTION

This article is a continuation of the authors' work [1], which provided a survey of the literature on criteria importance theory (CIT) for problems in which groups of criteria are ordered by importance, demonstrated the relevance of the theory, and outlined directions for further research. Based on recent results obtained for single-criterion decision-making problems under uncertainty with qualitative probability and ordinal utility [2], extended preference and indifference relations are introduced in this article for multi-criteria problems with ordinal criteria on the set of vector outcomes (and thus on the set of decision alternatives). The properties of these relations are examined, and simple decision rules for pairwise comparison of alternatives in terms of preference are provided. The relationship between the new non-strict preference relations and the relations previously used for problems in which only individual criteria are ordered by importance is studied in detail.

2. MATHEMATICAL MODEL AND BASIC DEFINITIONS FROM THE CRITERIA IMPORTANCE THEORY

Consider the following mathematical model of the decision-making situation [1]:

$$\langle X, f, Z_0, R \rangle ,$$

here X is the set of solution options; $f = (f_1, \ldots, f_m)$ is a vector criterion consisting of $m \geqslant 2$ individual criteria f_i; $Z_0 \subseteq (-\infty, +\infty)$ is the range of criteria values (the "criteria scale"); R is the decision makers (DM) non-strict preference. Each criterion f_i is a function defined on X

and taking values from Z_0. Each option x from the set X is characterized by its vector estimate $y(x) = f(x) = (f_1(x), \dots, f_m(x))$. The set of all vector estimates is $Z = Z_0^m$. Further, it is assumed that the criteria scale is ordinal: it is only known that preferences increase along their scale: the higher the estimate $z \in Z_0$, the more preferable it is.

The DM's preferences are modeled on Z using a non-strict preference relation R (yRz means that the vector estimate y is no less preferable than z). The relation R is a (partial) quasi-order, i.e., it is reflexive and transitive, and generates an indifference relation I and a (strict) preference relation P as follows: $yIz \Leftrightarrow yRz \wedge zRy$; $yPz \Leftrightarrow yRz \wedge \neg zRy$ (i.e., zRy is not true). The relation R is unknown and must be reconstructed based on information about the DM's preferences. In the absence of such information, only the strict preference relation $P^{\varnothing}$ (the Pareto relation) can be defined on the set of vector estimates Z: $yP^{\varnothing}z \Leftrightarrow (y_i \geqslant z_i, i = 1, \dots, m, y \neq z)$. Let $R^{\varnothing}$ be the union of $P^{\varnothing}$ and the vector equality relation.

To extend the relation $P^{\varnothing}$, additional information Ω about the DM's preferences is required, namely, information about the importance of criteria, for example, a message like "One group of criteria is more important than another". Let us provide basic definitions of equality and superiority in importance for disjoint groups of criteria. For simplicity, we will further denote criteria by their numbers, i.e., for example, the criterion f_i will be denoted as i, and the group (set) of criteria with numbers $i_1, \dots, i_q$ will be denoted as $A = \{i_1, \dots, i_q\}$.

Let A and B be disjoint nonempty groups of criteria, and in a vector estimate y all components y_i with numbers from A are equal to each other and all components y_i with numbers from B are equal to each other (i.e., $y_i = y_j$ for $i, j \in A$ and for $i, j \in B$). Denote y^{AB} vector estimates with such a structure. Denote $y^{A\leftrightarrow B}$ the vector estimate obtained from y^{AB} by replacing each component y_j, $j \in B$, with (any) component y_i, $i \in A$, and replacing each component y_i, $i \in A$, with (any) component y_j, $j \in B$.

Definition 1. Criteria groups A and B are equally important ($A \sim B$) when all vector estimates y^{AB} and $y^{A\leftrightarrow B}$ are equal in preference (indifferent).

Definition 2. A group of criteria A is more important than a group of criteria B ($A \succ B$) when any vector estimate y^{AB} such that $y_i > y_j$ for $i \in A$ and $j \in B$ is preferable to $y^{A\leftrightarrow B}$.

According to these definitions, the messages $A \sim B$ and $A \succ B$ define on the set Z the indifference relation $I^{A\sim B}$ and preference relation $P^{A\succ B}$, respectively:

$$\begin{aligned} yI^{A\sim B}z &\Leftrightarrow y = y^{AB}, \quad z = y^{A\leftrightarrow B}, \quad y_i \neq y_j, \quad i \in A, \quad j \in B; \\ yP^{A\succ B}z &\Leftrightarrow y = y^{AB}, \quad z = y^{A\leftrightarrow B}, \quad y_i > y_j, \quad i \in A, \quad j \in B. \end{aligned} \tag{1}$$

On the other hand, information Ω defines on the set 2^M of all subsets of the set of criteria (numbers) $M = \{1, \dots, m\}$ the importance relation $\succsim^{\Omega}$:

If $A \sim B \in \Omega$ or $B \sim A \in \Omega$ then $A \sim^{\Omega} B$; if $A \succ B \in \Omega$ then $A \succ^{\Omega} B$.

Each importance statement $A \sim^{\Omega} B$ and $A \succ^{\Omega} B$ generates on the set of vector estimates Z according to (1) a corresponding relation R^{ω}, namely the preference relation P^{ω} or indifference relation I^{ω}. Based on this information, the non-strict preference relation R^{Ω} (a reflexive and transitive relation) is defined on the set Z as the transitive closure of the union of all relations R^{ω} and the relation $R^{\varnothing}$:

$$R^{\Omega} = \mathrm{T}\left[\left(\bigcup_{\omega\in\Omega} R^{\omega}\right) \bigcup R^{\varnothing}\right], \tag{2}$$

where T is the symbol of the transitive closure operation of a binary relation. According to (2) the relation $yR^{\Omega}z$ is true if and only if there exists a chain of the form

$$yR^{\omega_1}u^1, u^1R^{\omega_2}u^2, \dots, u^{r-1}R^{\omega_r}z, \tag{3}$$

where u^k are vector estimates, and ω_k are messages from Ω (so that R^{ω_k} is P^{ω_k} or I^{ω_k} depending on the meaning of ω_k) or the symbol $\varnothing$. The relation of non-strict preference R^{Ω} generates the relations of preference P^{Ω} and indifference I^{Ω} in the manner indicated above.

3. QUALITATIVE IMPORTANCE OF CRITERIA

Qualitative importance is a binary relation $\succsim$ on the set 2^M of all subsets of the set of criteria (numbers) $M = \{1, \ldots, m\}$: the notation $A \succsim B$ means that the group of criteria A is no less important than the group of criteria B. This relation gives rise to the relations of strict superiority in importance $\succ$ and equal importance $\sim$. Qualitative importance is called *complete*, if it has the following properties (they are postulated as axioms):

C1. *Comparability*: $A \succsim B$ or $B \succsim A$ is true for any A and B.

C2. *Transitivity*: from $A \succsim B$ and $B \succsim C$ it follows $A \succsim C$.

C3. *Nontriviality*: $A \succ \varnothing$ for any $A \neq \varnothing$.

C4. *Additivity*: if $A \cap C = B \cap C = \varnothing$, then the relations $A \succsim B$ and $A \cup C \succsim B \cup C$ are either true or not true simultaneously.

Note that the validity of properties C1–C4 implies the validity of property

C5. *Reflexivity*: $A \succsim A$ for any A.

Qualitative importance is called *partial*, if it has properties C2–C5.

It should be noted that the postulated properties of qualitative importance are similar to the axioms of qualitative probability. (A detailed discussion of the properties of qualitative probability which are often unusual and far from obvious can be found in [3].) The difference lies only in the formulation of the axiom of nontriviality: qualitative probability requires only non-strict superiority for each event A, and therefore $A \sim \varnothing$ is allowed for $A \neq \varnothing$. This is explained by the fact that the axiom of nontriviality for probability covers cases of im-possible elementary events encountered in practice. For qualitative importance, statement $A \sim \varnothing$ means taking into account a criterion that has no significance at all. But if a set of criteria is formed in compliance with known requirements, which include non-redundancy and minimal dimension, then such a result should be considered as a violation of the specified requirements. This would mean adjusting the mathematical model of the problem situation by removing the corresponding criterion from the vector criterion. Therefore, for qualitative importance, it is natural to accept the requirement that $A \succ \varnothing$ for each $A \neq \varnothing$ (i.e., for every criterion).

Positive numbers $\beta_1, \ldots, \beta_m$ are called *qualitative (additive) importance values of criteria*, consistent with the qualitative importance $\succsim$, if they have the following property:

$$A \sim B \Rightarrow \sum_{i \in A} \beta_i = \sum_{i \in B} \beta_i; \qquad A \succ B \Rightarrow \sum_{i \in A} \beta_i > \sum_{i \in B} \beta_i.$$

If the importance values of criteria are normalized, i.e., equal to 1 in total, then they are called *qualitative importance coefficients of criteria* and are designated $\alpha_1, \ldots, \alpha_m$. The theory of qualitative probability indicates that for $m > 4$ qualitative importance values (and, of course, coefficients) may not exist [2, 3].

The complete or partial importance of criteria can be assessed by carrying out (with varying degrees of completeness) a procedure of pairwise comparisons of non-empty disjoint groups of criteria A and B, comparing by preference the corresponding vector estimates of the form y^{AB} and $y^{A \leftrightarrow B}$ and using the same considerations and procedure as when obtaining information on the qualitative importance of individual criteria. The procedure is described in detail in [3]. Having received a sufficient amount of information Ω, it is necessary to check it for consistency and, if necessary, correct it [1]. And, finally, construct $\succsim$ as an additive-transitive closure of the importance relation $\succsim^{\Omega}$, for example, using the matrix method specified in [1].

4. PREFERENCE AND INDIFFERENCE RELATIONS

Let us first extend the definitions of equality and superiority in importance to the general case where criteria groups A and B may intersect or be empty. Consider a vector estimate $y \in Z$ such that $y_i = a$ for $i \in A \cup B$, i.e., all of its components with numbers from A and B are equal to $a \in Z_0$. Let $b \in Z_0$ and $y' = (y \parallel y_i = b, i \in A) \in Z$ be the vector estimate obtained from y by replacing all of its components with numbers from A with b, and $y'' = (y \parallel y_j = b, j \in B) \in Z$ be the vector estimate obtained from y by replacing all of its components with numbers from B with b.

Definition 3. Criteria groups A and B are equally important ($A \sim B$), when all vector estimates y' and y'' are equally preferable.

Definition 4. A non-empty group of criteria A is more important than a group of criteria B ($A \succ B$), when any vector estimate y' with $b > a$ is preferable to a vector estimate y''.

Note that according to Definition 3, $A \sim A$ is true, and according to Definition 4, if $A \supset B$, then $A \succ B$; in particular, if $A \neq \varnothing$, then $A \succ \varnothing$.

We will introduce the definition of the relations $R^{\succsim}$, and thus the relations $P^{\succsim}$ and $I^{\succsim}$ on the set of vector estimates $Z = Z_0^m$ based on a given qualitative importance $\succsim$ (complete or only partial) axiomatically, i.e., we will specify a system of axioms that these relations must satisfy. First outline the class of binary relations.

Axiom 1. The relation $R^{\succsim}$ is reflexive.

Axiom 2. The relation $R^{\succsim}$ is transitive.

If these axioms are satisfied for $R^{\succsim}$, then the relation $P^{\succsim}$ is strict partial order, and the relation $I^{\succsim}$ is equivalence.

Axiom 3 (Pareto axiom). If the first vector estimate is not less than the second vector estimate component-wise, and at least one component of the first is greater than the corresponding component of the second, then the first vector estimate is preferable to the second: if $y_i \geqslant z_i$, $i = 1, \ldots, m$, $y \neq z$, then $yP^{\succsim}z$.

Consider two groups of criteria A, B and two vector estimates $y, z \in Z$ such that $y_i = z_j = a$, $i \in A$, $j \in B$, i.e., all their components with numbers from A and B are equal to $a \in Z_0$. Let $b \in Z_0$ and $y' = (y \parallel y_i = b, i \in A) \in Z$ and $z' = (z \parallel z_j = b, j \in B) \in Z$. We will say that vector estimates y and z *are changed (respectively improved, worsened) in the same way* according to groups of criteria A and B if they are replaced by y' and z' for arbitrary b and a (respectively for $b > a$, for $b < a$).

Axiom 4 (preference conservation). Let two vector estimates be improved in the same way according to two equally important groups of criteria A and B; if these vector estimates are of equal preference, then they will remain so; if the first vector es-timate is preferable to the second, then it will remain preferable to the second: for $A \sim B$ and $a < b$, if $yI^{\succsim}z$ then $y'I^{\succsim}z'$, and if $yP^{\succsim}z$ then $y'P^{\succsim}z'$.

Axiom 5 (preference strengthening). If two vector estimates, the first of which is no less preferable than the second, are improved in the same way according to two groups of criteria, the first of which is more important than the second, then the first of the obtained vector estimates will be preferable to the second: for $A \succ B$ and $a < b$, if $yR^{\succsim}z$ then $y'P^{\succ}z'$.

Axioms 4 and 5 express the following simple idea, which is most clearly formulated for the case of two criteria. Suppose it is possible to change the preference of each of the two vector estimates by changing the initial identical values of only one of the two criteria by the same amount. If the criteria are equally important, then it makes no difference which criterion is changed. If the first criterion is more important than the second, then it is preferable to improve the value of the more important criterion and worsen the value of the less important criterion. In an even more general form, the idea is well known: if two problems are being solved (for example, the assault of two strongholds) and the completeness of their solutions is equal, then it is reasonable to devote additional indivisible resources (reserves) to solving the more important problem. If the problems are equally important, then both methods of using resources are equally preferable.

The system of Axioms 1–5 provides a recursive (inductive) definition of relations $R^{\succsim}$, $P^{\succsim}$, $I^{\succsim}$, starting with relations $yI^{\succsim}y$, which are true for any $y \in Z$.

Example 1. Assume that $Z_0 = \{1, 2, 3, 4\}$ and the following consistent information about the importance of $m = 3$ criteria is provided: $1 \succ 2$, $2 \sim 3$, $\{2, 3\} \succ 1$. Using the additive-transitive closure of these relations the following complete qualitative importance is obtained:

$$\{1, 2, 3\} \succ \{1, 2\} \sim \{1, 3\} \succ \{2, 3\} \succ 1 \succ 2 \sim 3 \succ \varnothing.$$

Start with $y = (2, 2, 2)$. Since $\{2, 3\} \succ 1$, then $(2, 3, 3)P^{\succsim}(3, 2, 2)$ according to Axiom 5. And since $1 \succ 2$, then $(4, 3, 3)P^{\succsim}(3, 4, 2)$. It is convenient to represent these conclusions as a double chain (the arrows are drawn from the more preferable vector estimates to the less preferable ones), because it is necessary to change the vector estimates in each pair in the same way:

$$\begin{array}{ccccc} (2,2,2) \leftarrow & (2,3,3) & \leftarrow & (4,3,3) \\ & \downarrow_{23\succ 1} & & \downarrow_{1\succ 2} \\ (2,2,2) \leftarrow & (3,2,2) & \leftarrow & (3,4,2)\,. \end{array}$$

Therefore $(4, 3, 3)P^{\succsim}(3, 4, 2)$. *Double chains* like the one presented can be called *explanatory*: they clearly show why one of the vector estimates is preferable to the other (or why they are indifferent).

If the groups A and B are not empty and do not intersect, then for the vector estimates involved in the formulations of Axioms 4 and 5, $z' = y'^{A\leftrightarrow B}$ is satisfied in case $y = z$. Consequently, in the general case, the relation$R^{\succsim}$ includes the relation R^{Ω} (see (2)).

Remark. The deterioration of vector estimates can also be taken into account in the following analogs of Axioms 4 and 5:

Axiom 4*: for $A \sim B$ and $a > b$, if $yI^{\succsim}z$ then $y'I^{\succsim}z'$, and if $yP^{\succsim}z$ then $y'P^{\succsim}z'$.

Axiom 5*: for $A \prec B$ and $a > b$, if $yR^{\succsim}z$ then $y'P^{\succsim}z'$.

It can be shown that the system of Axioms 1, 2, 3, 4*, 5* is equivalent to the system of Axioms 1–5 in the sense that it defines the same relations $R^{\succsim}$, $P^{\succsim}$, $I^{\succsim}$. Double chains using Axioms 4* and 5* are *decreasing*. Thus, Axioms 4* and 5* can be used instead of Axioms 4 and 5. The combined use of Axioms 4, 5, 4*, and 5* does not extend the relations $R^{\succsim}$, $P^{\succsim}$, $I^{\succsim}$.

The decision rules presented below are based on the development of ideas from the theory of qualitative importance of criteria in multi-criteria decision-making problems [1]. Introduce the set of components of vector estimates y and z, ordered in non-decreasing order:

$$W(y, z) = \{y_1\} \cup \cdots \cup \{y_m\} \cup \{z_1\} \cup \cdots \cup \{z_m\} = \{w_1, \ldots, w_q\},$$

where $q \leqslant 2m$ and depend on y and z, $w_1 < \cdots < w_q$. Define $2(q - 1)$ sets of component numbers:

$$M_k(y) = \{i \in M \mid y_i \geqslant w_k\}, \quad M_k(z) = \{i \in M \mid z_i \geqslant w_k\}, \quad k = 2, 3, \ldots, q.$$
$$L_k(y) = \{i \in M \mid y_i \leqslant w_k\}, \quad L_k(z) = \{i \in M \mid z_i \leqslant w_k\}, \quad k = q-1, q-2, \ldots, 1.$$

The following two theorems are reformulations of the corresponding theorems from [2] as applied to multicriteria problems.

Theorem 1. *The relation $yR^{\succsim}z$ is true if and only if all of the following relations are true*

$$M_k(y) \succsim M_k(z), \quad k = 2, 3, \ldots, q. \tag{4}$$

Furthermore, if in (4) *all* $\succsim$ *are* $\sim$, *then* $yI^{\succsim}z$; *otherwise* (*when* (4) *contains* $\succ$) $yP^{\succsim}z$ *is true.*

Theorem 2. *The relation $yR^{\succsim}z$ is true if and only if all of the following relations are true*

$$L_k(y) \precsim L_k(z), \quad k = q-1, q-2, \ldots, 1. \tag{5}$$

Furthermore, if in (5) *all* $\precsim$ *are* $\sim$, *then* $yI^{\succsim}z$; *otherwise* (*when* (5) *contains* $\prec$) $yP^{\succsim}z$ *is true.*

Note that if we have a set $Z_0 = \{1, \ldots, q\}$, then it can be used in the role of $W(y, z)$.

Example 2. Under the conditions of Example 1 compare the vector estimates $y = (4, 3, 3)$ and $z = (3, 4, 2)$ by preference using Theorem 1. We have $W(y, z) = \{2, 3, 4\}$, $q = 3$ and

$$k = 2, \;\; w_2 = 3, \;\; M_2(y) = \{1, 2, 3\} \succ \{1, 2\} = M_2(z);$$
$$k = 3, \;\; w_3 = 4, \;\; M_3(y) = \{1\} \succ \{2\} = M_3(z).$$

Therefore $yP^{\succsim}z$ is true. Now compare the vector estimates $u = (1, 2, 3)$ and $v = (3, 1, 1)$ using Theorem 2. We have $W(u, v) = \{1, 2, 3\}$, $q = 3$ and

$$k = 2, \;\; w_2 = 2, \;\; L_2(u) = \{1, 2\} \succ \{2, 3\} = L_2(v);$$
$$k = 1, \;\; w_1 = 1, \;\; L_1(u) = \{1\} \prec \{2, 3\} = L_1(v).$$

Therefore, the vector estimates u and v are not comparable in preference.

Let the criteria $f_1, \ldots, f_m$ have a quantitative "physical" scale, which is interval [4] or of a higher level (for example, monetary income), and $\alpha_1, \ldots, \alpha_m$ are qualitative importance coefficients consistent with the qualitative importance $\succsim$. Construct a weighted sum

$$\sum_{i=1}^{m} \alpha_i \varphi(f_i(x)) = \sum_{i=1}^{m} \alpha_i \varphi(y_i),$$

where φ is an increasing function (in generalized criteria it is called a normalizing function). The value of the weighted sum is briefly denoted as $y(\alpha)$.

Theorem 3. *If $yR^{\succsim}z$ then $y(\alpha) \geqslant z(\alpha)$. Furthermore, if $yP^{\succsim}z$ then $y(\alpha) > z(\alpha)$, and if $yI^{\succsim}z$ then $y(\alpha) = z(\alpha)$.*

The proofs of this and the following theorems are given in the Appendix. Theorem 3 shows the possibility of using, if necessary, additive value functions (in particular, generalized criteria) for further analysis of a multi-criteria problem solved using the CIT.

5. PROBLEMS WITH INDIVIDUAL CRITERIA ORDERED BY IMPORTANCE

Consider problems in which only individual criteria are comparable in importance, i.e., the set Ω contain only messages of the form $i \succ j$ and $i \sim j$. A binary relation $\dot{\succsim}$ on the set of criteria (numbers) M that satisfies the axioms of reflexivity and transitivity is referred to as *ordinal importance*. If all criteria are ordered, then the importance is complete; otherwise, it is partial.

Assume that $A, B \in M$, in the formulation of the Axioms 1–5. Then the system of Axioms 1–5 on the basis of a given ordinal importance $\dot{\succsim}$ (complete or only partial) defines the relation $R^{\dot{\succsim}}$ on the set of vector estimates Z. It turns out that this relation coincides with $R^{\succsim}$ in the case when the information Ω concerns the importance of only individual criteria, i.e., when the qualitative importance $\succsim$ is an extension (continuation) of the ordinal importance $\dot{\succsim}$ on 2^M.

Theorem 4. $R^{\succsim} = R^{\dot{\succsim}}$ *in the case of ordinal importance.*

The following example shows that the relations $R^{\succsim}$ and $R^{\dot{\succsim}}$ for the qualitative importance $\succsim$ and ordinal importance $\dot{\succsim}$ generated by information Ω can be wider than the relation R^{Ω}.

Example 3. Let $m = 4, Z_0 = \{1, 2, 3, 4\}$ and $\Omega = \{1 \succ 3, 2 \succ 3, 2 \succ 4\}$. It is easy to verify, that transitive closure does not change the relation $\succsim^{\Omega}$. We will not write out the partial relation of qualitative importance $\succsim$: the validity of the relations that arise during the analysis for the pairs of sets under consideration (taking into account the properties of C2 and C4) will be obvious. For $y = (3, 4, 1, 2)$ and $z = (2, 1, 4, 3)$ we have $W(y, z) = Z_0,\ q = 4$. Taking into account Theorem 1, we obtain:

$$k = 2,\ \ w_2 = 2:\ M_2(y) = \{1, 2, 4\} \succ \{1, 3, 4\} = M_2(z);$$
$$k = 3,\ \ w_3 = 3:\ M_3(y) = \{1, 2\} \succ \{3, 4\} = M_3(z);$$
$$k = 4,\ \ w_4 = 4:\ M_4(y) = \{2\} \succ \{3\} = M_4(z),$$

so $yP^{\succsim}z$ is true. According to Theorem 4, $yP^{\dot{\succsim}}z$ is also true. However, it is impossible to construct an explanatory chain (3), so y and z are not comparable with respect to R^{Ω}.

It turns out, however, that in the case where information Ω concerns the importance of only individual criteria and on its basis all criteria can be ordered by importance, the relations $R^{\succsim}$ and R^{Ω} coincide.

Theorem 5. *$R^{\succsim} = R^{\Omega}$ in the case of complete ordinal importance.*

Example 4. Assume that additional information $4 \succ 1$ became known in Example 3. Then all criteria are ordered by importance: $2 \succ 4 \succ 1 \succ 3$. Now the explanatory chain (3) appears:

$$y = (3, 4, 1, 2)P^{1\succ 3}(1, 4, 3, 2)P^{2\succ 3}(1, 3, 4, 2)P^{2\succ 4}(1, 2, 4, 3)P^{2\succ 1}(2, 1, 4, 3) = z,$$

so $yP^{\Omega}z$ is true. The same result is obtained by adding the statement $4 \sim 1$ to Ω, which also allows us to completely non-strictly order all criteria by importance: $2 \succ 4 \sim 1 \succ 3$.

Thus, Theorem 5 shows that in the case of complete ordinal importance, the non-strict preference relation introduced earlier in the CIT is not extended, and therefore any suitable previously developed decision rules from this theory can be used.

6. CONCLUSION

This article introduces the concepts of complete and partial qualitative importance and axiomatically defines the non-strict preference relation on a set of decision options based on these concepts. In general, this relation is broader than a similar relation previously introduced in the criteria importance theory (CIT).

The presented fairly simple decision rules allow us to analyze multi-criteria problems with the information on the relative importance of not only individual criteria, but also groups of criteria with an ordinal scale.

It is shown that in the case of a complete ordering of individual criteria by importance, the non-strict preference relation introduced earlier in the CIT is not expanded, and any suitable previously developed decision rules from this theory can be used.

The obtained results form the basis for further development of the CIT for problems with groups of criteria ordered by importance, having more sophisticated scales than the ordinal one.

The presented results are useful for the initial analysis of political, social, and other decision-making problems in which preference information (criteria importance and their scales) is initially qualitative (non-numerical).

FUNDING

The study was implemented in the framework of the Basic Research Program at the National Research University Higher School of Economics (HSE University) and the state assignment of Ministry of Science and Higher Education of the Russian Federation for MERI RAS (FFGU-2024-0016).

APPENDIX

A.1. PROOF OF THEOREM 3

If $yR^{\succsim}z$ is true, then there exists a double chain in which the first node consists of two equal vector estimates $y^0 = z^0$, and the last node consists of y and z.

Consider two arbitrarily chosen adjacent nodes of this double chain, where the vector estimates s and t are involved in the first node, and the relation $A \succsim B$ is used to obtain vector estimates u and v in the second node. So, we have $\sum_{i\in A}\alpha_i \geqslant \sum_{i\in B}\alpha_i$ or $\sum_{i\in A\setminus B}\alpha_i - \sum_{i\in B\setminus A}\alpha_i \geqslant 0$, where the inequalities are strict in case $A \succ B$, and become equalities when $A \sim B$. The components of the vector estimates u and v with numbers from A and B are represented by some same number c, so that:

$$u_i = \begin{cases} c+l, & i \in A, \\ c, & i \in B \setminus A, \\ s_i, & i \notin A \cup B; \end{cases} \qquad v_i = \begin{cases} c+l, & i \in B, \\ c, & i \in A \setminus B, \\ t_i, & i \notin A \cup B. \end{cases}$$

The following equalities are true (note that if the summation is performed over empty set of indices, then it is equal to zero by definition):

$$\begin{aligned}
&[u(\alpha) - v(\alpha)] - [s(\alpha) - t(\alpha)] = \left[\sum_{i\in M}\alpha_i\varphi(u_i) - \sum_{i\in M}\alpha_i\varphi(v_i)\right] - \left[\sum_{i\in M}\alpha_i\varphi(s_i) - \sum_{i\in M}\alpha_i\varphi(t_i)\right] \\
&= \Bigg[\left(\sum_{i\in A\setminus B}\alpha_i\varphi(c+l) + \sum_{i\in A\cap B}\alpha_i\varphi(c+l) + \sum_{i\in B\setminus A}\alpha_i\varphi(c) + \sum_{i\in M\setminus(A\cup B)}\alpha_i\varphi(s_i)\right) \\
&\quad - \left(\sum_{i\in B\setminus A}\alpha_i\varphi(c+l) + \sum_{i\in A\cap B}\alpha_i\varphi(c+l) + \sum_{i\in A\setminus B}\alpha_i\varphi(c) + \sum_{i\in M\setminus(A\cup B)}\alpha_i\varphi(t_i)\right)\Bigg] \\
&\quad - \Bigg[\left(\sum_{i\in A\setminus B}\alpha_i\varphi(c) + \sum_{i\in A\cap B}\alpha_i\varphi(c) + \sum_{i\in B\setminus A}\alpha_i\varphi(c) + \sum_{i\in M\setminus(A\cup B)}\alpha_i\varphi(s_i)\right) \\
&\quad - \left(\sum_{i\in B\setminus A}\alpha_i\varphi(c) + \sum_{i\in A\cap B}\alpha_i\varphi(c) + \sum_{i\in A\setminus B}\alpha_i\varphi(c) + \sum_{i\in M\setminus(A\cup B)}\alpha_i\varphi(t_i)\right)\Bigg] \\
&= \sum_{i\in A\setminus B}\alpha_i\varphi(c+l) + \sum_{i\in B\setminus A}\alpha_i\varphi(c) - \sum_{i\in B\setminus A}\alpha_i\varphi(c+l) - \sum_{i\in A\setminus B}\alpha_i\varphi(c) \\
&= (\varphi(c+l) - \varphi(c))\left(\sum_{i\in A\setminus B}\alpha_i - \sum_{i\in B\setminus A}\alpha_i\right) = \delta \geqslant 0,
\end{aligned}$$

therefore

$$u(\alpha) - v(\alpha) \geqslant s(\alpha) - t(\alpha) + \delta.$$

Since $y^0(\alpha) - z^0(\alpha) = 0$ in the first node of the double chain, then the difference $u(\alpha) - v(\alpha)$ does not decrease and remains non-negative when moving along the chain to the right. Therefore $y(\alpha) \geqslant z(\alpha)$. Furthermore, if $yP^{\succsim}z$, then a relation of the form $A \succ B$ will be encountered at least once in the chain and therefore $y(\alpha) > z(\alpha)$ will be true; otherwise, if $yI^{\succsim}z$, then all relations will be of the type $A \sim B$ and the equality $y(\alpha) = z(\alpha)$ will be true. Theorem 3 is proved.

To prove Theorems 4 and 5, we will need one auxiliary statement that characterizes the structure of pairs of criteria groups related by qualitative importance in the case of ordinal importance under consideration.

Lemma 1. *If the qualitative importance $\succsim$ is obtained by extending the ordinal importance $\dot{\succsim}$ on 2^M, then the groups of criteria A and B in any relation $A \succsim B$ can be divided into separate criteria as follows:*

$$\begin{aligned} A &= i_1 \cup i_2 \cup \dots \cup i_{n_A},\ i_p \neq i_r \textit{ for } p \neq r; \\ B &= j_1 \cup j_2 \cup \dots \cup j_{n_B},\ j_p \neq j_r \textit{ for } p \neq r; \\ n_A &\geqslant n_B; \quad i_p \dot{\succsim} j_p, \quad p = 1, \dots, n_B. \end{aligned} \tag{A.1}$$

A.2. PROOF OF LEMMA 1

We will use the mathematical induction method. At the first step of constructing the relation $\succsim$ it contains all pairs $(i, j) \in \dot{\succsim}$ and $(i, \varnothing)$, $i \in M$, for which the conditions of Lemma 1 are satisfied. At each subsequent step we will add one new relation to the obtained relation, applying the rules of additivity or transitivity to the existing relations.

Suppose that conditions of Lemma 1 are satisfied for all pairs $A \succsim B$ at the step k of constructing the relation $\succsim$. Let the following additivity rule be applied at the step $(k+1)$: if $A \succsim B$ and $A \cap C = B \cap C = \varnothing$ then $A \cup C \succsim B \cup C$. Partition (A.1) for the relation $A \cup C \succsim B \cup C$ can be obtained from the existing partition (A.1) for the relation $A \succsim B$ by simply adding pairs $i_p \dot{\succsim} i_p$ for all $i_p \in C$.

Now let the following additivity rule be applied at the step $(k+1)$: if $A \succsim B$ and $A \supseteq C$, $B \supseteq C$ then $A \backslash C \succsim B \backslash C$. Partition (A.1) for the relation $A \backslash C \succsim B \backslash C$ can be obtained from the existing partition (A.1) for the relation $A \succsim B$ by first transforming it so that it contains pairs $i_p \dot{\succsim} i_p$ for all $i_p \in C$, and then excluding all these pairs. Such a transformation can always be carried out. Suppose that there are two pairs $i \dot{\succsim} j$ and $t \dot{\succsim} i$ for some $i \in C$ in the partition (A.1) for $A \succsim B$. Then, taking into account the transitivity of $\dot{\succsim}$, they can be replaced by the pairs $i \dot{\succsim} i$ and $t \dot{\succsim} j$. And this should be done with each number $i \in C$.

Let the transitivity rule be applied at the step $(k+1)$: if $A \succsim B$ and $B \succsim C$ then $A \succsim C$. Partition (A.1) for the relation $A \succsim C$ can be obtained from the existing partitions (A.1) for the relations $A \succsim B$ and $B \succsim C$. We have:

$$\begin{aligned} A &= i_1 \cup i_2 \cup \dots \cup i_{n_A},\ i_p \neq i_r \text{ for } p \neq r; \\ B &= j_1 \cup j_2 \cup \dots \cup j_{n_B},\ j_p \neq j_r \text{ for } p \neq r; \\ C &= t_1 \cup t_2 \cup \dots \cup t_{n_C},\ t_p \neq t_r \text{ for } p \neq r; \end{aligned}$$
$$n_A \geqslant n_B \geqslant n_C; \quad i_p \dot{\succsim} j_p, \quad p = 1, \dots, n_B; \quad j_p \dot{\succsim} t_p, \quad p = 1, \dots, n_C.$$

Using the transitivity of the relation $\dot{\succsim}$ the required partition (A.1) for the relation $A \succsim C$ is obtained: $i_p \dot{\succsim} t_p$, $p = 1, \dots, n_C$. Lemma 1 is proved.

A.3. PROOF OF THEOREM 4

Since $\dot{\succsim} \subseteq \succsim$ on 2^M, we have $R^{\dot{\succsim}} \subseteq R^{\succsim}$. Therefore, it suffices to prove that $R^{\dot{\succsim}} \supseteq R^{\succsim}$. Let $yR^{\succsim}z$ be true for some vector estimates $y, z \in Z$. Then according to Theorem 1 the relations (4) are satisfied. Introduce vector estimates y^k and $z^k, k = 1, \dots, q-1$:

$$y_i^k = \begin{cases} y_i, & y_i \leqslant w_k, \\ w_k, & y_i > w_k; \end{cases} \qquad z_i^k = \begin{cases} z_i, & z_i \leqslant w_k, \\ w_k, & z_i > w_k. \end{cases}$$

Construct a double chain starting with vector estimates $y^1 = z^1 = (w_1, \dots, w_1)$ and using only statements $i \dot{\succsim} j$. According to Lemma 1 there exists a partition (A.1) for the relation $M_2(y) \succsim M_2(z)$ from (4). Denote $n = |M_2(z)|$ for convenience. Let $u^1 = y^1$, $v^1 = z^1$. Improve the vector estimates u^p and v^p, $p = 1, \dots, n$ in the same way from $a = w_1$ to $b = w_2$ according to criteria i_p and j_p for each pair $i_p \dot{\succsim} j_p$, $p = 1, \dots, n$, from (A.1) one by one. According to Axioms 4 and 5 for each such improvement we obtain $u^{p+1} R^{\dot{\succsim}} v^{p+1}$, $p = 1, \ldots, n$. Note that $y^2 R^{\varnothing} u^{n+1}$ and $z^2 = v^{n+1}$. According to Axiom 2 (transitivity), we obtain $y^2 R^{\dot{\succsim}} z^2$.

Next, similarly use the relation $M_3(y) \succsim M_3(z)$ from (4) to construct a double chain starting with vector estimates y^2 and z^2. Since $M_2(y) \supseteq M_3(y)$ and $M_2(z) \supseteq M_3(z)$ the improvements of the vector estimates in the same way from $a = w_2$ to $b = w_3$ according to the criteria from $M_3(y)$ and $M_3(z)$ are possible in this case. As a result, we similarly obtain $y^3 R^{\dot{\succsim}} z^3$. Continue the described procedure until at step $k = q$, using the relation $M_q(y) \succsim M_q(z)$ from (4), we obtain $y^q R^{\dot{\succsim}} z^q$, which means $y R^{\dot{\succsim}} z$. Theorem 4 is proved.

A.4. PROOF OF THEOREM 5

In the general case $R^{\succsim} \supseteq R^{\Omega}$, therefore it is sufficient to prove that $R^{\succsim} \subseteq R^{\Omega}$ in the case of complete ordinal importance. We will use the well-known analytical decision rule to check $y R^{\Omega} z$in the case of complete ordinal importance. In this case, there exist ordinal coefficients of the criteria importance—positive numbers $\alpha_1^o, \ldots, \alpha_m^o$, equal in sum to one, for which the following conditions are satisfied $i \dot{\sim} j \Rightarrow \alpha_i^o = \alpha_j^o$, $i \dot{\succ} j \Rightarrow \alpha_i^o > \alpha_j^o$. Introduce the numbers

$$\alpha_{ik} = \begin{cases} \alpha_i^o, & y_i \geqslant w_k \\ 0, & y_i < w_k \end{cases}, \qquad i \in M, \ k = 2, \ldots, q.$$

Arrange all components of the vector $\alpha^k(y) = (\alpha_{1k}, \alpha_{2k}, \ldots, \alpha_{mk})$ in non-increasing order, and denote the resulting vector as $\alpha_{\searrow}^k(y)$. The following decision rule holds [3]:

$$y R^{\Omega} z \Leftrightarrow \alpha_{\searrow}^k(y) \geqq \alpha_{\searrow}^k(z), \quad k = 2, \ldots, q, \tag{A.2}$$

here $\geqq$ is the sign of vector non-strict inequality for n-dimensional vectors ($n \geqslant 2$): $a \geqq b \Leftrightarrow a_i \geqslant b_i$, $i = 1, \ldots, n$.

Let $y R^{\succsim} z$ be true for some vector estimates $y, z \in Z$. According to Theorem 1 the relations (4) are satisfied. For arbitrary $k = 2, \ldots, q$ we will prove that the relation $M_k(y) \succsim M_k(z)$ implies $\alpha_{\searrow}^k(y) \geqq \alpha_{\searrow}^k(z)$. Note that the numbers $\alpha_{ik}(y)$ are not equal to zero for $i \in M_k(y)$. Therefore, the vector $\alpha^k(y)$ consists of nonzero components with indices from $M_k(y)$. According to Lemma 1 the relation $M_k(y) \succsim M_k(z)$ has a partition A.1. Therefore, there also exists a corresponding pairwise partition of the components of the vectors $\alpha^k(y)$ and $\alpha^k(z)$:

$$\alpha_{i_1 k}(y) \geqslant \alpha_{j_1 k}(z), \ \alpha_{i_2 k}(y) \geqslant \alpha_{j_2 k}(z), \ \ldots, \ \alpha_{i_m k}(y) \geqslant \alpha_{j_m k}(z).$$

So, we obtain $\alpha_{\searrow}^k(y) \geqq \alpha_{\searrow}^k(z)$. Then, according to (A.2) $y R^{\Omega} z$ is true. Theorem 5 is proved.

REFERENCES

1. Nelyubin, A.P. and Podinovski, V.V., Multicriteria problems with importance-ordered criteria groups, *Autom. Remote Control*, 2022, no. 7, pp. 1108–1122.

2. Nelyubin, A.P. and Podinovski, V.V., Theoretical Basis and Methods of Decision Analysis under Uncertainty with Qualitative Estimates of Probabilities and Preferences, *Autom. Remote Control*, 2026, no. 7, pp. 657–667.

3. Podinovski, V.V., *Mnogokriterial'nye zadachi prinyatiya reshenii: teoriya i metody analiza: uchebnik dlya vuzov* (Multicriteria Decision-Making Problems: Theory and Methods of Analysis: A Textbook for Universities), Moscow: Urait, 2025.

4. Pfanzagl, J., *Theory of measurement*, Wiley, 1968.

This paper was recommended for publication by $\boxed{\text{A.I. Kibzun}}$, a member of the Editorial Board

ISSN 0005-1179 (print), ISSN 1608-3032 (online), Automation and Remote Control, 2026, Vol. 87, No. 8, pp. 761–762.

OBITUARY

ANDREI IVANOVICH KIBZUN

31.07.1951—06.05.2026

Laureate of the Government Prize of the Russian Federation in the field of science and technology, Doctor of Physical and Mathematical Sciences, Professor

On May 6, 2026, at the age of 75, Professor Andrei Ivanovich Kibzun passed away. He was an outstanding Russian scientist in probability theory, stochastic system optimization, probabilistic methods of systems analysis, stochastic programming, and the optimization of probabilistic and quantile performance criteria. He was also a talented educator, a remarkable colleague, and a kind friend.

Andrei Ivanovich Kibzun was born on July 31, 1951, in Khabarovsk. In 1968, he graduated from the Physics and Mathematics Boarding School No. 18 at Moscow State University, under the guidance of Academician A.N. Kolmogorov. In 1974, he graduated with honors from the Faculty of Aircraft Engineering of the Moscow Aviation Institute, and in 1975, he also graduated with honors from the Faculty of Mechanics and Mathematics of Lomonosov Moscow State University. This combination of strong engineering and mathematical training allowed him to begin active research at the Moscow Aviation Institute, where he defended his Candidate's dissertation in 1978 and his Doctoral dissertation in 1987. In 1989, A.I. Kibzun was awarded the academic title of Professor. It is important to note that already in his Candidate's dissertation, Andrei Ivanovich laid the foundations of a new scientific direction, which were further developed in his Doctoral dissertation and later in the work of his students. In 1990, Professor A.I. Kibzun worthily took the baton from the founder of the Department of Probability Theory and Mathematical Statistics, Academician V.S. Pugachev, the founder of the Soviet school of statistical control theory. Professor A.I. Kibzun preserved the traditions of this school and enriched them by attracting first-class scientists in stochastic systems, control theory, statistical estimation, and optimization to the department. In recent years, the main achievements of this school and of Andrei Ivanovich personally have been new algorithms for solving one-stage and two-stage probabilistic and quantile optimization problems, based on reduction to deterministic mixed-integer programming problems, as well as the analysis of these approximations in terms of accuracy and convergence. Under the supervision of A.I. Kibzun, 10 Doctoral and 20 Candidate's dissertations in physical and mathematical sciences have been defended. The efforts of his research team have been supported by more than 20 various international and Russian grants, including from the Russian Foundation for Basic Research, the Russian Science Foundation, and the Ministry of Education and Science of the Russian Federation.

The main scientific results of A.I. Kibzun are presented in three monographs on stochastic programming with probabilistic criteria and in more than 100 scientific articles. A.I. Kibzun and his students developed a set of methods for solving stochastic programming problems with probabilistic and quantile criteria, including the confidence method, the deterministic equivalent method, stochastic quasi-gradient methods, the sample approximation method, and others.

A.I. Kibzun paid great attention to methodological work and to teaching students. A textbook on probability theory and mathematical statistics, written jointly with colleagues, reflects the methodology developed by the department for teaching this discipline to engineering and economics students. For many years, A.I. Kibzun taught a special course, "Applied Stochastic Programming," for students of the Department of Probability Theory, in which he presented both the achievements of world science in this field and the results obtained by the department's scientific school.

Professor A.I. Kibzun served for many years as a member of the editorial board of the journal "Avtomatika i Telemekhanika" (Automation and Remote Control), where he prepared 12 thematic issues on contemporary optimization problems (in 1998, 2003, 2004, 2007, 2011, 2012, and 2017). He actively worked on the editorial boards of the journals "Vestnik komp'yuternykh i informatsionnykh tekhnologii" (Herald of Computer and Information Technologies) and "Applied Stochastic Models in Business and Industry", and was a member of the Scientific and Methodological Council for Mathematics and Mechanics of the Ministry of Education and Science of the Russian Federation.

Professor A.I. Kibzun actively participated in scientific and expert activities for 20 years, serving as a member of the Expert Council on Management, Computer Engineering, and Informatics of the Higher Attestation Commission under the Ministry of Education and Science of Russia. He shaped the policy for the certification of highly qualified scientific personnel, prepared the passports for scientific specialties in systems analysis, information processing, and mathematical modeling. He was a demanding yet supportive opponent, setting an example for young scientists in the rigor of mathematical formulations, conscientiousness, and devotion to science.

The merits of Andrei Ivanovich were highly appreciated by the Russian government: as part of a team of authors, he was awarded the Prize of the Government of the Russian Federation in the Field of Science and Technology in 1999 for the development and implementation of a methodology for the high-precision separation of spacecraft of various purposes, and he was awarded the title "Laureate of the Government Prize of the Russian Federation".

The entire life of Andrei Ivanovich Kibzun, his high professionalism, his dedication to his work, his attitude toward people, his love of life, optimism, diligence, and care for his loved ones will remain a fine example for us. His wise and kind advice helped colleagues, friends, and students. His constant readiness to listen and support created an atmosphere of genuine respect and trust around him.

The bright memory of the outstanding scientist and wonderful educator Andrei Ivanovich Kibzun will forever remain in the hearts of his family, colleagues, students, and friends.

Editorial Board of the journal "Automation and Remote Control," colleagues and friends